UCRL-11649

University of California

Ernest O. Lawrence Radiation Laboratory

TWO-WEEK LOAN COPY

This is a Library Circulating Copy which may be borrowed for two weeks. For a personal retention copy, call Tech. Info. Division, Ext. 5545

TEMPERATURE DEPENDENCE OF FLUORINE MAGNETIC RESONANCE SPECTRA

Berkeley, California

DISCLAIMER

This document was prepared as an account of work sponsored by the United States Government. While this document is believed to contain correct information, neither the United States Government nor any agency thereof, nor the Regents of the University of California, nor any of their employees, makes any warranty, express or implied, or assumes any legal responsibility for the accuracy, completeness, or usefulness of any information, apparatus, product, or process disclosed, or represents that its use would not infringe privately owned rights. Reference herein to any specific commercial product, process, or service by its trade name, trademark, manufacturer, or otherwise, does not necessarily constitute or imply its endorsement, recommendation, or favoring by the United States Government or any agency thereof, or the Regents of the University of California. The views and opinions of authors expressed herein do not necessarily state or reflect those of the United States Government or any agency thereof or the Regents of the University of California.

Research and Development

UCRL-11649

UNIVERSITY OF CALIFORNIA
Lawrence Radiation Laboratory
Berkeley, California

AEC Contract W-7405-eng-48

TEMPERATURE DEPENDENCE OF FLUORINE MAGNETIC RESONANCE SPECTRA

Richard Newmark

(Ph.D. Thesis)

November 1964

TEMPERATURE DEPENDENCE OF FLUORINE MAGNETIC RESONANCE SPECTRA

Contents

Abstract v

I. Introduction 1

II. Theory 4

A. Modified Bloch Equations 4

B. Density Matrix Treatment 6

C. Application to Three Spin Problems. 22

III. Kinetics 28

A. Population of the Rotamers 28

B. Averaged Coupling Constants and Chemical Shifts. 29

C. Rates of Exchange 31

IV. Experimental 42

V. Results and Discussion 45

A. $CFCl_2$-$CFCl_2$ 45

B. CF_2Br-CCl_2Br 51

C. CF_2Br-$CFBr_2$ 60

D. CFClBr-CFClBr 72

E. CF_2Br-CFBrCl 75

F. CF_2Br-CHBrCl 81

VI. Conclusions 89

A. Chemical Shifts 89

B. Barriers 91

Acknowledgements 95a

Appendices

A. The Solution to the Modified Bloch Equations 96

B. ABXIR Computer Program 98

C. Interpretation of ABXIR Computer Program 119

D. ABCIR and MCO Computer Programs 126

Bibliography 132

Figure Captions 135

TEMPERATURE DEPENDENCE OF FLUORINE MAGNETIC RESONANCE SPECTRA

Richard Newmark

Inorganic Materials Research Division,
Lawrence Radiation Laboratory,
Department of Chemistry,
University of California, Berkeley, California

November 1964

ABSTRACT

The theory of Kaplan for exchange in nuclear magnetic resonance (NMR) systems has been modified for exchange between three species with any number of nuclei of spin $\frac{1}{2}$, in which all the nuclei in each species are exchanged by the interconversion. A set of explicit equations for the density matrix elements in this case is written down. Computer programs have been written to solve the equations in the two and three spin cases. The results enable the calculation of NMR spectra of highly coupled nuclei undergoing exchange. Absolute reaction rate theory has been used to express the rates of exchange in terms of activation energies. This has been combined with the Kaplan theory to determine the free energies of activation for the internal rotation of several halogenated ethanes, $CFCl_2$-$CFCl_2$, CF_2Br-CCl_2Br, CF_2Br-$CFBr_2$, CF_2Br-CFBrCl, CFClBr-CFClBr, and CF_2Br-CHBrCl. Spectra were calculated assuming the limiting values for the transmission coefficient, $\kappa \ll 1$, $\kappa = 1$. In the first case free rotation occurs when the rotamer has sufficient energy to exceed the barriers. Alternatively, the second case implies that deactivation occurs almost immediately after rotation occurs. The experimental results on CF_2Br-CCl_2Br can only be explained by the second possibility.

The barriers are discussed in terms of the distortion necessary to form the activated complex in which the substituents are eclipsed.

The low temperature spectrum of the three rotamers of CF_2Br-CHBrCl shows two larger vicinal HF coupling constants (18 cps) and four small ones (less than 3 cps). The assignment of the rotamers made assuming that the low barrier observed between two of the rotamers does not involve eclipsing two large halogens indicates that the large coupling constants are trans and the four others are gauche coupling constants.

I. INTRODUCTION

Nuclear magnetic resonance (NMR) spectra as a function of temperature can provide considerable information about the rate of exchange between chemical species. Nuclei in different magnetic environments in a molecule resonate at different frequencies, resulting in chemical shifts. If the exchange rate between nuclei in two environments is much less than the chemical shift, then the spectra of the individual species are seen. If, on the other hand, the exchange rate is much higher than the chemical shift, only the 'time-averaged' spectrum is observed. At intermediate rates, a spectrum is obtained which is a function of the exchange rate.

NMR chemical shifts are of the order of 10 to 10,000 radians/second, and at reasonably accessible temperatures (-150°C to 200°C), it is possible to obtain barriers to interconversion of 7 to 30 kcal/mole. Gutowsky et al.[1,2] first observed the results of a system of exchanging molecules on an NMR spectrum, and calculated the rate of exchange. Since then NMR has been used extensively to obtain rates of chemical reactions.

Drysdale and Phillips[3] were the first to apply NMR to study hindered rotation in substituted ethanes. There are three rotamers corresponding to the three possible staggered configurations. These are depicted in Fig. 1 for CF_2Br-CHBrCl. Nair and Roberts[4] pointed out that an ABX spectrum is observed for the spin system in a molecule such as CF_2P-CHPQ when rapid exchange between the rotamers is occurring. The fluorines are non-equivalent even after averaging over the three rotamers, because the three rotamers have unequal populations. This thesis will describe the temperature dependence of the NMR spectra of substituted ethanes at sufficiently low temperatures to obtain the barriers to internal rotation.

The barrier is the increase in energy necessary to rotate from one staggered configuration through the eclipsed form to another staggered configuration.

The Bloch equations, as modified by McConnell,[5] are used to calculate spectra in which the coupling constants may be neglected. In many cases these equations provide suitable results, even for reasonably large coupling constants, but as soon as the coupling constant is about 50% of the corresponding chemical shift, the errors are considerable. Kaplan[6] and Alexander[7] have developed theories based on the self-consistent averaged density matrix of the spin system to describe NMR spectra as a function of the rate of exchange. The density matrix describes the system completely, including the coupling constants and chemical shift of each species undergoing exchange. Kurland and Wise[8] and Heidberg et al.[9] have used the theory of Alexander to study hindered internal rotation between identical systems for two spin systems, and the theory has been extended by Johnson[10] to electron transfer reactions. We have extended Kaplan's theory to calculate spectra of three species undergoing exchange. The method is explained in detail below, and applied to obtain the barriers in molecules described by AB and ABX spectra.

Much work has been done to measure the barriers to internal rotation of substituted ethanes. Wilson has written the most recent reviews of the subject.[11] From microwave spectra, extensive studies of substituted ethanes containing a methyl group indicate the barrier is approximately 3 kcal/mole in all of these compounds. Infrared and electron diffraction measurements have yielded larger barriers in the symmetrical molecules hexafluoroethane[12] and hexachloroethane[13] of 4.2 and 10.8 kcal/mole, respectively. Intermediate barriers have been reported for several

molecules containing a CF_3 group on one end from infrared and Raman spectral studies.[14,15] To obtain the barrier from the microwave or infrared data for an asymmetric top on an asymmetric framework is very difficult. For many halogenated ethanes containing fluorine the barrier is sufficiently large to be studied by NMR. This extends the type of molecules which can be conveniently studied to totally asymmetric cases. The barriers in CF_2Br-CCl_2Br, CF_2Br-$CFBr_2$, CF_2Br-CFBrCl, and $CFCl_2$-$CFCl_2$ have been analyzed in this work and are reported below. The barriers in the two isomers of CFClBr-CFClBr, previously reported,[16] have been recalculated using Kaplan's theory.

II. THEORY

A. Modified Bloch Equations

The modification of the Bloch equations to describe a system of exchanging nuclei of spin $\frac{1}{2}$ is most readily obtained by the following approach, first introduced by McConnell.[5] In the coordinate system rotating at the frequency of the radiofrequency field H_1, the Bloch equations for u and v, the components of the magnetization which are in-phase and out-of-phase with the rotating field, are

$$\frac{du}{dt} + \frac{u}{T_2} + (\omega_o - \omega)\, v = 0 \qquad (1)$$

$$\frac{dv}{dt} + \frac{v}{T_2} - (\omega_o - \omega)\, u = -\gamma H_1 M_z, \qquad (2)$$

where T_2 is the transverse relaxation time. If we assume M_z, the magnetic moment in the z direction, is not appreciably perturbed from M_o, the equilibrium magnetic moment, then we can replace M_z by M_o in Eq. (2).

Define $G = u + iv$, and add Eqs. (1) and (2); then the equation describing the complex magnetization for a nucleus in a magnetic field H_o is

$$\frac{dG}{dt} + [\frac{1}{T_2} - i(\omega_o - \omega)]\, G = -i\gamma H_1 M_o. \qquad (3)$$

If three nonequivalent nuclei are present, then we must write Eq. (3) for each different nucleus, since each one will be in a slightly different magnetic field H_o. If no exchange is occurring, there are three separate equations of the form

$$\frac{dG_A}{dt} + \alpha_A G_A = -i\gamma H_1 M_{oA}, \qquad \alpha_A = \frac{1}{T_{2A}} - i(\omega_{oA} - \omega),$$

$$M_{oA} = P_A M_o, \qquad (4)$$

where P_A is the population of species A. To modify Eq. (4) for exchange, we assume the nucleus is in one position A and then makes an instantaneous jump to some other configuration B. The probability that a change from A to B occurs is given by k_{AB}, and the probability for an A to C jump is k_{AC}. The mean lifetime of a nucleus in configuration A is given by

$$\frac{1}{\tau_A} = k_{AB} + k_{AC} = \frac{1}{\tau_{AB}} + \frac{1}{\tau_{AC}}, \tag{5}$$

where A, B, and C are all different subscripts representing the three species. The principle of detailed balance requires that

$$\frac{P_i}{\tau_{ij}} = \frac{P_j}{\tau_{ji}}. \tag{6}$$

The system is in thermal equilibrium and the exchange between rotamers does not affect this equilibrium.

In Eq. (4) we add terms due to the increase in magnetization of one species, and decrease for the other, due to exchange. The equations, modified for exchange are

$$\frac{dG_A}{dt} + \alpha_A G_A = -i\gamma H_1 P_A M_O + \tau_{BA}^{-1} G_B + \tau_{CA}^{-1} G_C - \tau_A^{-1} G_A, \tag{7}$$

$$\frac{dG_B}{dt} + \alpha_B G_B = -i\gamma H_1 P_B M_O + \tau_{AB}^{-1} G_A + \tau_{CB}^{-1} G_C - \tau_B^{-1} G_B, \tag{8}$$

$$\frac{dG_C}{dt} + \alpha_C G_C = -i\gamma H_1 P_C M_O + \tau_{AC}^{-1} G_A + \tau_{BC}^{-1} G_B - \tau_C^{-1} G_C. \tag{9}$$

For example, in Eq. (7) we add $\tau_{BA}^{-1} G_B + \tau_{CA}^{-1} G_C$ for the increase in magnetization when species B or C rotate to A. If A rotates to B or C, then there is a loss of magnetization, and we subtract

$$\tau_{AB}^{-1}G_A + \tau_{AC}^{-1}G_A = \tau_A^{-1}G_A.$$

The modified Bloch equations are readily solved in the slow-passage limit, which allows setting all the time derivatives equal to zero. The imaginary part of the total complex moment, $G = G_A + G_B + G_C$, is directly proportional to the absorption. The solution is outlined in Appendix A.

A Fortran II computer program was written for the SDS (Scientific Data Systems) 910 computer to calculate spectra, using the equation in Appendix A. The results will be discussed in detail in the sections on $CFCl_2$-$CFCl_2$ and CFClBr-CFClBr below.

The Bloch equation approach is completely classical. If the coupling constant is much less than the chemical shift, quantum mechanical coupling between nuclei can be introduced simply by including additional equations, similar to Eq. (4), for each possible resonance.[1] However, the theory developed by Solomen and Bloembergen[17] for exchange in HF (Eq. (A10) of their paper) gives a broadening twice that predicted from the solution of the modified Bloch equations in the fast exchange limit.

B. Density Matrix Treatment

Kaplan[6] has presented a general theory for exchange in which a density matrix represents each spin system. For the particularly simple example of exchange between a two proton species and a relatively infinite concentration of a one proton species, and for the coupling constant less than the chemical shift, he explicitly proves that the Solomen-Bloembergen result is correct for fast exchange whereas the modified Bloch equations give the correct result for slow exchange. The disadvantage of Kaplan's theory is that it requires the solution of a large number of simultaneous equations to obtain the absorption at each point. However, in most of

the compounds studied the coupling constant was the same order of magnitude as the chemical shift and it was necessary to apply Kaplan's theory to calculate the spectra.

The set of equations developed by Kaplan for the time-averaged density matrix has been modified to the case of internal rotation between three nonidentical species (or rotamers). The theory is considered in detail below. The simpler problem of internal rotation between identical species is treated in detail in Appendix I of Kaplan, and by Alexander.[7] The theory developed will be applicable to any system of three exchanging molecules in which one species interconverts to some other species. It can be easily extended to larger systems.

The procedure may be briefly described as follows. The density matrix of the two species undergoing exchange is obtained as the direct product of the individual density matrices. This is transformed by a unitary operation which effects the interconversion of the two species. An individual species is obtained after exchange by taking the trace over the other species. The time development of the species after exchange is weighted by its mean lifetime (the correlation time) and integrated over all time to give the average value. Since the spin system is at equilibrium, the result is set equal to the original density matrix before exchange. This defines a set of matrix equations for the self-consistent time-averaged density matrix. This approach is similar to the one first used by Gutowsky, McCall, and Slichter[1] to modify the Bloch equations for exchange. Finally, the absorption is obtained directly from the density matrix as the expectation value of the angular momentum in the x direction. The properties of the density matrix, used throughout this section, are described by Fano.[18]

The average density matrix for species A in the rotating coordinate system of the applied rf field, H_1, is defined as ρ_{oA}. The matrix elements of ρ_{oA} are obtained in the representation in which the spin Hamiltonian with the rf field equal to zero is diagonal. At thermal equilibrium, in the absence of H_1, the density matrix is diagonal with elements which are the Boltzmann populations of the energy levels,

$$\rho_{jj} = \frac{1}{N}\left[1 - \frac{\hbar F_z \omega_o}{kT}\right], \tag{10}$$

where k is Boltzmann's constant, $\hbar$ Planck's constant over 2π, T the absolute temperature, and F_z the value of the magnetization in state j, given by $F_z = \sum_k I_z^k$. In the case of a weak rf field, off-diagonal elements proportional to H_1 appear, and the diagonal elements are unchanged, to first order. The approximation that H_1 is small, and does not appreciably perturb the Boltzmann equilibrium, was also used in the derivation of the modified Bloch equations in order to replace M_z by M_o.

The density matrix for the joint state of two interacting systems is given by the direct product of the density matrix for the individual species. The interconversion between the two species is effected by a transformation of this direct product density matrix. It is assumed in the theory that species A and B interchange identities. In an equilibrium process in which the average effect is studied, this is indistinguishable from the actual physical process in which A transforms (or rotates) to B while, to preserve equilibrium, some other species (or rotamer) B transforms to A.

An element of the direct product density matrix is given by

$$(\rho_{oA} \times \rho_{oB})_{nm,uv} = (\rho_{oA})_{n,u} \times (\rho_{oB})_{m,v}. \tag{11}$$

In the direct product matrix the first pair of subscripts denote the row and the second pair the column. Since the off-diagonal elements of the density matrix are first order in H_1, the product of two off-diagonal elements can be neglected, and we only keep the terms diagonal in one of the density matrices,

$$(\rho_{oA} \times \rho_{oB})_{nm,uv} = \rho^A_{su}\, \rho^B_{tv}\, \delta_{su} + \rho^A_{su}\, \rho^B_{tv}\, \delta_{tv} + \rho^A_{su}\, \rho^B_{tv}\, \delta_{su}\, \delta_{tv}\,, \qquad (12)$$

where δ_{ij} is 1 if the subscripts are equal and zero otherwise. In Eq. (12) it is convenient to explicitly write down the third term, which will be treated separately from the first two, and note that we exclude the possibility that t=v in the first term, or s=u in the second. Further, the first order correction to a diagonal element will be neglected when it is multiplied by an off-diagonal element.

Exchange can occur only between a pair of species, so three unitary matrices, R^{AB}, R^{AC}, and R^{BC} must be formulated. Since the wave functions for the third species (or rotamer) are completely unaffected by the AB exchange, the exchange modified product density matrix is given by $R^{AB}(\rho_{oA} \times \rho_{oB})(R^{-1})^{AB}$.

It is easiest to describe the transformation by considering the particular example. Suppose that fluorines (or other nuclei of spin $\frac{1}{2}$) i and j of species A exchange with fluorines q and r of species B. The wave function before exchange is given by

$$\psi^{AB}_{LM} = \psi^A_L\,(\gamma_i\gamma_j)\;\psi^B_M\,(\gamma_q\gamma_r), \qquad (13)$$

where γ_i is the spin of the fluorine. After exchange, the labeling of γ_i and γ_q, and γ_j and γ_n is interchanged. The result is then expanded in the complete set of product wave functions, ψ^{AB}_{IJ}, the coefficients of

which are defined as the elements in the row LM in the exchange matrix R^{AB}. It is most convenient to take ψ^{AB}_{LM} as eigenfunctions of the Hamiltonian, so that the expansion of the exchanged wave function is nontrivial, although straightforward. This choice of basis is necessary for the density matrix to be diagonal to first order. To make the example more specific, let $\psi^A_1 = \alpha_1\ \alpha_2$ and $\psi^B_2 = p_B\alpha_3\beta_4 + r_B\beta_3\alpha_4$, where α is spin up $(+\frac{1}{2}\hbar)$, β spin down $(-\frac{1}{2}\hbar)$, and p_B and r_B are the normalized coefficients of the expansion of the eigenfunctions into basic product functions. The operation of exchange, defined by E, is then

$$\begin{aligned} E\ \psi^{AB}_{12} &= E\ \alpha_1\alpha_2\ (p_B\alpha_3\beta_4 + r_B\beta_3\alpha_4) \\ &= p_B\ \alpha_1\beta_2\alpha_3\alpha_4 + r_B\beta_1\alpha_2\alpha_3\alpha_4 \\ &= (p_Ap_B + r_Ar_B)\ \psi^A_2\ \psi^B_1 + (r_Ap_B - p_Ar_B)\psi^A_3\ \psi^B_1, \end{aligned} \tag{14}$$

where $\psi^A_2 = p_A\alpha_1\beta_2 + r_A\beta_1\alpha_2$, $\psi^A_3 = r_a\alpha_1\beta_2 - p_A\beta_1\alpha_2$, and $\psi^B_1 = \alpha_3\alpha_4$. The elements of the 12th row of the R^{AB} matrix are obtained directly from Eq. (14).

We consider first the explicit evaluation of R^{AB} for any number of spins on the two rotamers. The φ^A_i are defined as the complete set of basic product wave functions for rotamer A. In the above example, the four basic product functions are $\varphi^A_1 = \alpha_1\alpha_2$, $\varphi^A_2 = \alpha_1\beta_2$, $\varphi^A_3 = \beta_1\alpha_2$, and $\varphi^A_4 = \beta_1\beta_2$. The φ^B_i are the same as the φ^A_i, but for species B. This similarity is necessary so that if $\varphi^{AB}_{14} = \varphi^A_1\ \varphi^B_4$, then after exchange the wave function is given by $E\varphi^{AB}_{14} = \varphi^A_B\ \varphi^B_1$. It is at this point that we have required all the spins of molecule (or

species) A interconvert to spins of molecule B.

In the coordinate system rotating at the frequency of the applied H_1 field, ν, the Hamiltonian is given for each rotamer L by

$$\mathcal{H}_o^L = \sum_i I_{z,i}^L (\nu_i^L - \nu) + \sum_{i>j} J_{ij}^L \vec{I}_i^L \cdot \vec{I}_j^L, \qquad (15)$$

where $\nu_i^L = \gamma_i H_o/2\pi$ is the resonance frequency for nucleus i in rotamer L in cycles/second, J_{ij} the coupling constant, and $\vec{I}$ the angular momentum.

The linear combination of the φ_i which are eigenfunctions of the Hamiltonian are given by

$$\psi_i^A = \sum_i a_{ij} \varphi_j^A, \qquad (16)$$

and for rotamers B and C,

$$\psi_i^B = \sum_i b_{ij} \varphi_j^B, \quad \text{and} \quad \psi_i^C = \sum_i c_{ij} \varphi_j^C. \qquad (17)$$

Since the rotamers normally have different chemical shifts and coupling constants, the a and b matrices are unrelated. The matrices, a, b, and c are unitary and may be obtained by the usual methods for diagonalizing the Hamiltonian.

The combined wave function for species A and B is

$$\psi_{ik}^{AB} = \sum_{j,l} a_{ij} b_{kl} \varphi_j^A \varphi_l^B. \qquad (18)$$

Since the φ_j^A and φ_l^B form complete orthonormal sets, the ψ_{ik}^{AB} also form an orthonormal set. The expansion of the $\varphi_j^A \varphi_l^B$ is given by Eq. (19), where the coefficients are the transpose of those in Eq. (18),

$$\varphi_j^A \varphi_l^B = \sum_{q,r} a_{qj}\, b_{rl}\, \psi_{qr}^{AB} \tag{19}$$

Recalling that $E\varphi_j^A \varphi_l^B = \varphi_l^A \varphi_j^B$, we can obtain the result of the exchange on an eigenfunction from Eqs. (18) and (19),

$$\begin{aligned} E\, \psi_{ik}^{AB} &= \sum_{j,l} a_{ij} b_{kl} \varphi_l^A \varphi_j^B \\ &= \sum_{j,l} a_{ij} b_{kl} \sum_{q,r} a_{ql} b_{rj}\, \psi_{qr}^{AB} \\ &= \sum_{q,r} R_{ik,qr}^{AB}\, \psi_{qr}^{AB} \quad . \end{aligned} \tag{20}$$

Equation (20) gives the elements of the R^{AB} matrix, where the first pair of subscripts (as in the direct product density matrix) denote the row and the second pair the column. R can be written as the product of two unitary matrices, as

$$R_{ik,qr}^{AB} = (\sum_j a_{ij} b_{rj})(\sum_l a_{ql} b_{kl}) = T_{ir} T_{qk}. \tag{21}$$

Equation (21) defines the T matrix for the AB interchange. It will be convenient to describe the AC and BC interchanges by U and V, respectively, defined in analogy to T as

$$U_{ij} = \sum_k a_{ik} c_{jk}, \qquad V_{ij} = \sum_k b_{ik} c_{jk}. \tag{22}$$

From the orthogonality of the a and b matrices, it can be shown that T and R^{AB} are unitary. Furthermore, from Eq. (21) it is clear that R is symmetric — $R_{ik,qr}^{AB} = R_{qr,ik}^{AB}$.

The elements of the exchange-modified product density matrix are given by

$$Q_{ij,kl} = \sum_{s,t,u,v} R^{AB}_{ij,st} \, (\rho_{oA} \times \rho_{oB})_{st,uv} (R^{AB}_{uv,kl})^{-1} \, . \tag{23}$$

Since R is orthogonal and symmetric,

$$(R^{-1})^{AB}_{uv,kl} = R^{AB}_{uv,kl} \, . \tag{24}$$

Substituting Eqs. (12) and (21) gives

$$Q_{ij,kl} = \sum_{s,t,u,v} T_{it} T_{sj} \, (\rho^A_{su} \rho^B_{tv} \delta_{su} + \rho^A_{su} \rho^B_{tv} \delta_{tv}$$

$$+ \rho^A_{su} \, \rho^B_{tv} \delta_{su} \delta_{tv}) \, T_{ul} T_{kv} \, . \tag{25}$$

Considering only the first term of Eq. (25), the Kronecker delta makes the summation over s trivial,

$$Q_{ij,kl} = \sum_{t,u,v} T_{it} T_{uj} \, \rho^A_{uu} \, \rho^B_{tv} \, T_{ul} T_{kv} \, . \tag{26}$$

The ρ^B_{tv} factor makes the term first order. Therefore it is possible to substitute 1/N from Eq. (10) as the zeroth order approximation to ρ^A_{uu}. The sum over u then gives δ_{jl} from the orthogonality of the T matrix. The second term is treated in a similar manner.

In the third term of Eq. (25) the summation over s and t yields

$$\sum_{u,v} T_{iv} T_{uj} \, \rho^A_{uu} \rho^B_{vv} T_{ul} T_{kv} \, . \tag{27}$$

The first order approximation in Eq. (27) is that the diagonal density matrix elements are constants and may be removed from the summation. The sum over u and v then gives $\delta_{ik}\delta_{jl}$. However the diagonal elements cannot be replaced by 1/N because there remains the first order contribution from Eq. (10), and we will be interested in the differences between the diagonal elements. The result for the third term is then

$$\rho^A_{ik}\,\rho^B_{jl}\,\delta_{ik}\delta_{jl}. \tag{28}$$

Combining the above results yields Eq. (29) as the first order contribution to the elements of $Q_{ij,kl}$,

$$Q_{ij,kl} = \frac{1}{N}\left[\sum_{t,v} T_{it}T_{kv}\,\rho^B_{tv}\,\delta_{jl} + \sum_{s,u} T_{sj}T_{ul}\,\rho^A_{su}\,\delta_{ik}\right] + \rho^A_{ik}\rho^B_{jl}\,\delta_{ik}\delta_{jl}\,. \tag{29}$$

To separate the species after the exchange, we sum over the diagonal elements of species B, defined as Tr_B, in the exchange modified product density matrix to obtain species A. Thus, species A is given by

$$\sigma^A_o = X_{AB}Tr_B\left[R^{AB}(\rho_{oA} \times \rho_{oB})\,R^{AB}\right] + X_{AC}\,Tr_C\left[R^{AC}\,(\rho_{oA} \times \rho_{oC})\,R^{AC}\right]. \tag{30}$$

In Eq. (30) the second term allows for the AC exchange. The coefficients, X_{AB} and X_{AC}, are proportional to the relative probabilities of AB and AC interconversions, or k_{AB} and k_{AC}, respectively, where the rate constants were defined above, prior to Eq. (5). Normalizing, and substituting the correlation times for the rates, gives τ_A/τ_{AB} and τ_A/τ_{AC} for X_{AB} and X_{AC}, respectively. (Since the density matrices are normalized it is unnecessary to include an additional normalizing factor).

To evaluate the first term of Eq. (30), the $Tr_B Q_{ij,kl}$ sums the B diagonal elements of Q,

$$Tr_B Q_{ij,kl} = \sum_j Q_{ij,kj}. \tag{31}$$

Substituting from Eq. (29), we note that only the first and third terms contribute to the trace over the B elements. The second term in T only contributes, to first order, when s=u, which is forbidden (see Eq. (11)),

$$\mathrm{Tr}_B Q_{ij,kl} = \sum_{j,t,v} \frac{1}{N} T_{it} T_{kv} \rho^B_{tv} + \sum_j \rho^A_{ik} \rho^B_{jj} \delta_{ik}$$

$$= \sum_{t,v} T_{it} T_{kv} \rho^B_{tv} + \rho^A_{ik} \delta_{ik}. \qquad (32)$$

Note that the first term in Eq. (32) is independent of j. The summation over j thus gives N identical terms. In the second term the sum is over the diagonal elements of ρ_{oB}, which is unity. Including the analogous results from the second term in Eq. (30) and multiplying by the normalizing factors X_{AB} and X_{AC},

$$\sigma^{A_o}_{ik} = \sum_{t,v} \left[\frac{\tau_A}{\tau_{AB}} T_{it} T_{kv} \rho^B_{tv} + \frac{\tau_A}{\tau_{AC}} U_{it} U_{kv} \rho^C_{tv} \right] + \rho^A_{ik} \delta_{ik}. \qquad (33)$$

The contribution to species B after exchange is given by

$$\sigma^{B_o} = \frac{\tau_B}{\tau_{BA}} \mathrm{Tr}_A \left[R^{AB} (\rho_{oA} \times \rho_{oB}) R^{AB} \right] + \frac{\tau_B}{\tau_{BC}} \mathrm{Tr}_C \left[R^{BC} (\rho_{oB} \times \rho_{oC}) R^{BC} \right]. \qquad (34)$$

This is evaluated in exactly the same manner as Eq. (30) to yield

$$\sigma^{B_o}_{ik} = \sum_{s,u} \frac{\tau_B}{\tau_{BA}} T_{si} T_{uk} \rho^A_{su} + \sum_{t,v} \frac{\tau_B}{\tau_{BC}} V_{it} V_{kv} \rho^C_{tv} + \rho^B_{ik} \delta_{ik} \quad . \qquad (35)$$

The time development of the density matrix after exchange is given by

$$\rho(t) = e^{i\mathcal{H}t} \rho_o e^{-i\mathcal{H}t} = S(t) \rho_o S^{-1}(t) , \qquad (36)$$

where ρ_o is the value of the density matrix at t = 0, and $\mathcal{H} = \mathcal{H}_o + \mathcal{H}_1$

is the Hamiltonian in the coordinate system rotating at the frequency of the applied rf field. The perturbation due to the rf field adds a term $\mathcal{H}_1 = \sum_i I^L_{x,i} H_1$ to the Hamiltonian given in Eq. (15), where I_x is the angular momentum in the x direction. (H_1 is assumed to be in cps). Expanding $S(t)^A = e^{i(\mathcal{H}^A_o + \mathcal{H}^A_1)t}$ in powers of H_1, and keeping only first order terms, gives

$$S^A_{mn}(t) = e^{iE^A_m t}\delta_{mn} + \frac{(e^{iE^A_m t} - e^{iE^A_n t})I^A_{x,mn}H_1}{E^A_m - E^A_n}, \qquad (37)$$

where $E^A_m = \mathcal{H}^A_{o,mm}$ is the eigenvalue of the Hamiltonian in the absence of the perturbation.

At a time t after the exchange the density matrix for species A is obtained by substituting the value $\sigma^{A_o}_{ij}$ and the first order expressions for $S^A_{mn}(t)$ into Eq. (36). Note that the first two terms in Eq. (33) are of order H_1 so that only the diagonal term of Eq. (37) enters. The result is

$$\begin{aligned}\sigma^A_{ij}(t) &= \sum_{k,l} S^A_{ik}(t)\, \sigma^{A_o}_{kl} (S^{-1})^A_{ij}(t) \\ &= \sum_{t,v}\left[\frac{\tau_A}{\tau_{AB}} T_{it}T_{jv}\rho^B_{tv} + \frac{\tau_A}{\tau_{AC}} U_{it}U_{jv}\rho^C_{tv}\right] \\ &\quad + \frac{H_1 I^A_{x,ij}}{E_i - E_j}\left[1 - e^{i(E_i - E_j)t}\right]\left(\rho^A_{ii} - \rho^A_{jj}\right) \\ &\quad + \rho^A_{ij}\,\delta_{ij}. \qquad (38)\end{aligned}$$

In Eq. (38) the last term only contributes to diagonal elements of σ^A. It can be neglected since, as shown below, it is only necessary to obtain the off-diagonal elements. In the third term, $I_{x,qr}$, the angular

momentum in the x direction, vanishes unless i and j refer to states whose equilibrium magnetization differ by $F_z = \pm 1$. This difference between two diagonal elements is proportional to M_o, the equilibrium magnetization.

The density matrix for nucleus A after exchange is averaged by integrating from t=0 to infinity, weighted by the probability,

$$\frac{1}{\tau_A} e^{-t/\tau_A}$$

of existing for a time t after the exchange. The result is set equal to ρ_{oA} to define a self-consistent averaged density matrix. This requires that the system be in equilibrium. Thus

$$\rho_{oA} = \int_0^\infty \frac{e^{-t/\tau_A}}{\tau_A} \sigma^A(t)\, dt, \qquad (39)$$

where $\sigma^A(t)$ is given by Eq. (38) as a function of ρ_{oA}, ρ_{oB}, and ρ_{oC}. Similar equations for the B and C species define a complete set of equations for the self-consistent density matrix elements. Performing the integration and rearranging terms yields the complete set of simultaneous equations for the off-diagonal density matrix elements,

$$(1 + \alpha'^A_{ij}\tau_A)\,\rho^A_{ij} - \sum_{t,v}\left[\frac{\tau_A}{\tau_{AB}} T_{it}T_{jv}\,\rho^B_{tv} + \frac{\tau_A}{\tau_{AC}} U_{it}U_{jv}\,\rho^C_{tv}\right] = H_1 I^A_{x,ij} M_o \tau_A, \qquad (40)$$

$$(1 + \alpha'^B_{ij}\tau_B)\,\rho^B_{ij} - \sum_{t,v}\left[\frac{\tau_B}{\tau_{BA}} T_{ti}T_{vj}\,\rho^A_{tv} + \frac{\tau_B}{\tau_{BC}} V_{it}V_{jv}\,\rho^C_{tv}\right] = H_1 I^B_{x,ij} M_o \tau_B, \qquad (41)$$

$$(1 + \alpha'^C_{ij}\tau_C)\,\rho^C_{ij} - \sum_{t,v}\left[\frac{\tau_C}{\tau_{CA}} U_{ti}U_{vj}\,\rho^A_{tv} + \frac{\tau_C}{\tau_{CB}} V_{ti}V_{vj}\,\rho^B_{tv}\right] = H_1 I^C_{x,ij} M_o \tau_C, \qquad (42)$$

where $\alpha'^L_{ij} = i(E^L_i - E^L_j)$.

In NMR experiments, the expectation value of the magnetic moment in the x direction in the laboratory coordinate system is obtained, corresponding to the transverse component in the rotating coordinate system. The expectation value of an operator is given by the trace of the operator with the density matrix,

$$< I_x + iI_y > = \sum_L P^L \, \mathrm{Tr} \; \rho^L (I_x + iI_y)^L = \sum_{L,i,j} P^L \rho^L_{ij} (I_x + iI_y)^L_{ji} . \quad (43)$$

Since ρ^L is the density matrix for an individual species, it is necessary to weight the individual absorbances by the population, P^L, in Eq. (43). Finally, the absorption is the imaginary component,

$$S = \mathrm{Im} < I_x + iI_y > = \sum_{L,i,j} P^L (I_x + iI_y)^L_{ji} \; \mathrm{Im} \; \rho^L_{ij} . \quad (44)$$

In Eq. (44) $(I_x + iI_y)_{ji}$ is zero unless state j differs from state i by +1 in the z component of the magnetic moment. Therefore, it is only necessary to obtain the density matrix elements which satisfy this requirement on i and j. To determine which density matrix elements are coupled together by Eqs. (40) to (42), we must investigate the properties of the T, U, and V matrices.

Equation (21) can be rewritten for a matrix element of T as

$$T_{ij} = \sum_k a_{ik} b^T_{kj} , \quad (45)$$

where b^T_{kj} is the transpose of b_{kj}. T is thus the usual product matrix of two unitary matrices. These are both diagonal in blocks, corresponding to different values of $F_z = \sum_i M^i_z$,[19] so that T is also diagonal in the same blocks.

The density matrix elements needed to calculate the absorption

correspond to transitions between adjacent blocks ($F_z = \pm 1$). In Eq. (40) for ρ^A_{ik}, this means subscripts i and k on $T_{it}T_{kv}$ refer to adjacent blocks on the T matrices. The sum over the other two subscripts will have non-zero terms only when t and v also belong to these two blocks. Consequently density matrix elements can only couple with each other if they correspond to the same set of transitions. For example, the elements for the $F_z = 3/2$ to $F_z = \frac{1}{2}$ transition are not coupled to the elements for the $F_z = \frac{1}{2}$ to $F_z = -\frac{1}{2}$ transition.

The number of energy levels for each possible value of F_z are given by the usual binominal coefficients. For the three spin case these are 1:3:3:1. There are three sets of transitions between different F_z values, with 3, 9, and 3 transitions, respectively. Since there are three rotamers, this means that sets of 9, 27, and 9 density matrix elements must be determined. Each set requires the solution of 9, 27, and 9 simultaneous equations, respectively. To solve 27 equations in 27 unknowns for each frequency in a spectrum becomes very time consuming, even on an IBM 7090 computer. However, insertion of the ABX approximation greatly increases the number of blocks in the a, b, and c matrices, thereby increasing the number of sets and reducing the transitions per set. For the three rotamer case there are seven sets, with 3, 3, 6, 6, 6, 6, and 12 transitions, respectively (three transitions have zero intensity and are not included).

The transverse relaxation time is introduced by comparison of the results with the solution obtained above from the modified Bloch equations. The latter were derived for three nuclei, each resonating at a different frequency, undergoing exchange. If there is only one spin, each density matrix has only one independent off-diagonal element. There is only one

wave function, so that the a, b, c, T, U, and V matrices all have only one element, 1. Thus all the summations vanish in Eq. (40). Dividing through by τ_A gives

$$(\tau_A^{-1} + \alpha'^A)\rho^A = H_1 I_x^A M_o + \tau_{AB}^{-1} \rho^B + \tau_{AC}^{-1} \rho^C. \qquad (46)$$

ρ^A is the absorption per molecule whereas G_A in Eq. (7) is the total absorption of the A species. The two are related by $P_A\rho^A = G_A$. Making this substitution in Eq. (46), multiplying through by P_A, and using Eq. (6) gives an equation identical in appearance to Eq. (7). This similarity justifies the introduction of the transverse relaxation time by replacing α'^A with $\alpha^A = 1/T_2 + \alpha'^A$.

The set of Eqs. (40) to (42) are all complex equations in which it is only desired to obtain the imaginary component of the density matrix elements. The equations are reduced to a set of real equations in real unknowns by the following transformations.

The set of N equations, after division by τ_A, can be written as

$$(\tilde{\alpha} + \tilde{A})\vec{\rho} = -i\vec{M} \qquad (47)$$

where $\tilde{\alpha} = i\omega - i\tilde{X}$, ω is the frequency, $\tilde{X}$ is a diagonal matrix whose elements are the transition frequencies, $\tilde{A}$ is a real matrix including $1/T_2$ on the diagonal and the coefficients of the terms in the summation as off-diagonal elements, $\vec{\rho}$ is a complex vector of the density matrix elements, and $\vec{M}$ is a real vector propotional to I_x. (Note that $E_i - E_j$ in α_{ij} is the difference between a transition frequency and the spectrometer frequency.) Only the relative values of a particular linear combination of the density matrix elements are of interest, so that the

absolute value of H_1M_o is taken as unity. Substituting $\vec{\rho} = \vec{u} + i\vec{v}$, where u and v are real, and equating the real and imaginary parts gives

$$(\tilde{X} - \omega\tilde{I})\,\vec{v} + \tilde{A}\,\vec{u} = 0 \tag{48}$$

$$(\omega\tilde{I} - \tilde{X})\,\vec{u} + \tilde{A}\,\vec{v} = -\,\vec{M} \tag{49}$$

where $\tilde{I}$ is the unit matrix. Then the set of simultaneous equations for v are obtained directly as

$$\tilde{E}\,\vec{v} = [-\tilde{X}\,\tilde{A}^{-1}\,\tilde{X} + \omega(\tilde{X}\,\tilde{A}^{-1} + \tilde{A}^{-1}\tilde{X}) - \omega^2\,\tilde{A}^{-1} - \tilde{A}]\,\vec{v} = \vec{M}. \tag{50}$$

The values of v obtained from the solution of Eq. (50) are inserted into Eq. (44) to give the absorption.

Computer programs for the IBM 7094 have been written to calculate spectra for the case of three rotamers with AB, ABX, or ABC spectra. If one of the rotamers has identical nuclei, or if two of the rotamers are identical, it is still possible to calculate the spectra with the equations above. For example, two of the three rotamers of CF_2Br-CCl_2Br (see section V-B) have identical AB spectra. However rotation between the identical configurations (II and III) interchanges the environment of the fluorines and therefore affects the spectrum. In order to calculate the correct spectra it is necessary to make the chemical shift between nuclei A and B positive in one rotamer, and negative in the other, so that the interconversion of II and III actually changes the environment of the fluorines. This makes the ordering of the eigenvalues and the signs of the unitary matrices different for the two rotamers.

Alexander[7] has considered the identical problem of deriving a general theory of exchange starting from the derivative of the equation used by Kaplan (Eq. (39) above) for the self-consistent average density matrix.

Alexander's papers are considerably more detailed than Kaplan's, including several equations for the limiting cases of slow and fast exchange. For the special case of internal rotation between identical species, the qualitative appearance of the spectrum is given, in the slow exchange limit, by

$$\frac{1}{T_2'} = \frac{1}{\tau}\left[1 \mp \frac{J}{(\delta^2 + J^2)^{\frac{1}{2}}}\right], \tag{51}$$

where $1/T_2'$ is the additional broadening due to exchange, δ the chemical shift, and the minus sign applies to the center two lines of an AB spectrum, the plus sign to the outer two lines. If the coupling constant and chemical shift are the same, the equation reduces to

$$\frac{1}{T_2'} = \frac{1}{\tau}\left(1 \mp \frac{1}{\sqrt{2}}\right), \tag{52}$$

so that the outer lines will be substantially broader than the inner ones as the exchange rate increases. This description is generally applicable to the AB part of the AB and ABX spectra discussed below in the sections on $CF_2Br\text{-}CCl_2Br$ and $CF_2Br\text{-}CFBr_2$.

C. Application to Three Spin Problems

The equations developed in section B have been specialized to the case of three spins on three rotamers, and computer programs have been written to calculate the spectra.

The Hamiltonian matrix elements for a three spin system can be obtained in the usual manner,[19] and are given in Table I. There are eight energy levels, and the secular equation is diagonal in four blocks.

TABLE I. Basic Functions and Matrix Elements for Three Nuclei

Basic Function[a]	F_z	Diagonal Matrix Element H_{nn}
1. $\alpha\alpha\alpha$	3/2	$\frac{1}{2}(\nu_A + \nu_B + \nu_C) + \frac{1}{4}(J_{AB} + J_{AC} + J_{BC})$
2. $\beta\alpha\alpha$	1/2	$\frac{1}{2}(-\nu_A + \nu_B + \nu_C) + \frac{1}{4}(-J_{AB} - J_{AC} + J_{BC})$
3. $\alpha\beta\alpha$	1/2	$\frac{1}{2}(\nu_A - \nu_B + \nu_C) + \frac{1}{4}(-J_{AB} + J_{AC} - J_{BC})$
4. $\alpha\alpha B$	1/2	$\frac{1}{2}(\nu_A + \nu_B - \nu_C) + \frac{1}{4}(J_{AB} - J_{AC} - J_{BC})$
5. $\alpha\beta\beta$	-1/2	$\frac{1}{2}(\nu_A - \nu_B - \nu_C) + \frac{1}{4}(-J_{AB} - J_{AC} + J_{BC})$
6. $\beta\alpha\beta$	-1/2	$\frac{1}{2}(-\nu_A + \nu_B - \nu_C) + \frac{1}{4}(-J_{AB} + J_{AC} - J_{BC})$
7. $\beta\beta\alpha$	-1/2	$\frac{1}{2}(-\nu_A - \nu_B + \nu_C) + \frac{1}{4}(J_{AB} - J_{AC} - J_{BC})$
8. $\beta\beta\beta$	-3/2	$\frac{1}{2}(-\nu_A - \nu_B - \nu_C) + \frac{1}{4}(J_{AB} + J_{AC} + J_{BC})$

Off-diagonal Matrix Elements

$$H_{34} = H_{56} = \tfrac{1}{2}J_{AB}, \quad H_{24} = H_{57} = \tfrac{1}{2}J_{AC}, \quad H_{23} = H_{67} = \tfrac{1}{2}J_{BC}$$

[a] The spins are written in serial order, e.g. $\alpha\alpha\beta = \alpha_A\alpha_B\beta_C$.

H_{11} and H_{88} are uncoupled, whereas H_{22}, H_{33}, and H_{44} are the diagonal elements of one 3x3 secular equation, and H_{55}, H_{66}, and H_{77} the diagonal elements of the other 3x3 secular equation. The a, b, and c matrices required to diagonalize the Hamiltonian are similarly diagonal in four blocks. Note that $a_{11} = a_{88} = 1.0$. The discussion following Eq. (45) proves that the T, U, and V matrices are also diagonal in the same manner.

The I_x matrix elements, which are the square roots of the transition amplitudes in the representation in which the Hamiltonian is diagonal, are also obtained by the usual methods. The only non-zero elements are given in Table II.

The first three transitions ($I_{x,1i}$ for i = 2, 3, and 4) result in a change of the z component of the magnetic moment, F_z, from +3/2 to +1/2. The next nine transitions are the $F_z = +1/2$ to $F_z = -1/2$ transitions, and the last three the $F_z = -1/2$ to $F_z = -3/2$ transitions. From the discussion above it then follows that ρ_{12}, ρ_{13}, and ρ_{14} are coupled together for the three rotamers, corresponding to the $F_z = 3/2$ to 1/2 transition. The $F_z = -1/2$ to -3/2 transitions couple ρ_{58}, ρ_{68}, and ρ_{78}. Finally the $F_z = +1/2$ to -1/2 transitions couple the ρ_{ij} for i = 2, 3 and 4 and j = 5, 6, and 7. For each rotamer it is than necessary to consider the density matrix elements listed above, or 15 elements per rotamer.

All of the compounds studied herein could be approximated by ABX spectra, i.e. $\nu_X - \nu_A$, $\nu_X - \nu_B \gg J_{AX}$, J_{BX}, so that the 3x3 secular equations could be reduced to a 2x2 and a 1x1. Labelling the basic functions as in Table I, the H_{44} and H_{77} are now uncoupled, and $a_{11} = a_{44} = a_{77} = a_{88} = 1.0$. The only other nonzero a_{ij} elements are a_{22}, a_{23}, a_{32}, a_{33}, a_{55}, a_{56}, a_{65}, and a_{66}. The I_x matrix elements are still given in Table II, but many of the terms are zero. For example, $I_{x,12} = a_{22} + a_{23}$,

TABLE II. I_x matrix elements in the representation in which the Hamiltonian is diagonal

$I_{x,1i} = \sum_{u=2}^{4} a_{iu}$,	for i = 2, 3, and 4
$I_{x,ij} = \sum_{u=2}^{4} \left[\sum_{v=5}^{7} a_{iu}\, a_{jv} - a_{iu}\, a_{j,u+3} \right]$	for i = 2, 3, and 4 and j = 5, 6, and 7
$I_{x,i8} = \sum_{u=5}^{7} a_{iu}$,	for i = 5, 6, and 7

$I_{x,14} = 1.0$, and $I_{x,47} = 0.0$.

In the ABX approximation the number of density matrix elements which are coupled together is substantially reduced. To demonstrate how this occurs, consider Eq. (40) with i = 1 and j = 2:

$$(1 + \alpha^A_{12}\tau_A)\rho^A_{12} - \sum_{t,v}\left[\frac{\tau_A}{\tau_{AB}} T_{1t}T_{2v}\rho^B_{tv} + \frac{\tau_A}{\tau_{AC}} U_{1t}U_{2v}\rho^C_{tv}\right] = H_1 I^A_{x,12} M_o \tau_A \quad (53)$$

The discussion in section IIB proved that T, U, and V are diagonal in the same blocks as the a matrix. Therefore $T_{1t} = 0.0$ unless t = 1, in which case $T_{11} = 1.0$, and $T_{2v} = 0.0$ unless v = 2 or 3. Therefore

$$(1 + \alpha^A_{12}\tau_A)\rho^A_{12} - \frac{\tau_A}{\tau_{AB}}(T_{22}\rho^B_{12} + T_{23}\rho^B_{13}) - \frac{\tau_A}{\tau_{AC}}(U_{22}\rho^C_{12} + U_{23}\rho^C_{13})$$

$$= H_1 I^A_{x,12} M_o \tau_A \quad . \quad (54)$$

The equation for ρ^A_{13} (that is, with i = 1 and j = 3) is similar to Eq. (54), but with T_{22}, T_{23}, U_{22}, and U_{23} replaced by T_{32}, T_{33}, U_{32}, and U_{33}. Equations (41) and (42) yield similar results, from which it is concluded that ρ_{12} and ρ_{13} form one set of interacting density matrix elements for the three rotamers.

The equation with i = 1 and j = 4 is particularly simple since $T_{1t}\,T_{4v}$ is nonzero only if t = 1 and v = 4, so that ρ^A_{14}, ρ^B_{14}, and ρ^C_{14} form another set of three interacting density matrix elements. The remaining five sets are found in a similar manner.

A computer program has been written to calculate NMR spectra for AB and ABX systems of three exchanging species (or rotamers). The program can calculate about 10 points per second in a spectrum, which is sufficiently fast to merit its use in many other rate problems. The Fortran

listing and the use of the program is discussed in Appendix B. Appendix C describes in detail the method of calculation used in the program.

The results for several molecules will be discussed in section V.

III. KINETICS

The theory discussed above describes spectra as a function of the rates of exchange between three molecules. In the particular problem of internal rotation, we wish to associate a barrier height with the correlation time, or rate of exchange.

A. Populations of the Rotamers

Before discussing the approximations necessary to obtain the rates, we shall determine the populations of the rotamers, P_i, which are also necessary to calculate the spectra. The populations at low temperatures can be determined from the relative peak areas due to each rotamer. Assuming a Boltzmann population distribution, the energies, E_i, of the rotamers can be obtained. E_i is the difference in energy between the potential minimum of rotamer i and rotamer 1 (see Fig. 2). At other temperatures the relative populations, X_i, are given by (taking $E_1 = 0$)

$$X_1 : X_2 : X_3 = Q_1 : Q_2 e^{-E_2/RT} : Q_3 e^{-E_3/RT} . \tag{55}$$

The Q_i are the partition functions of the rotamers, excluding the internal rotation coordinate, whose contribution is given by the exponential. Assuming the partition functions are the same (this will be discussed in detail below), one can reduce Eq. (55) to

$$X_1 : X_2 : X_3 = 1 : e^{-E_2/RT} : e^{-E_3/RT} . \tag{56}$$

The populations, P_i, are obtained from Eq. (56) after division by $X_1 + X_2 + X_3$ for normalization.

B. Averaged Coupling Constants and Chemical Shifts

Gutowsky et al.[1,2] first pointed out that the coupling constants and chemical shifts which are observed in systems underoing fast chemical exchange should be time-weighted averages for each of the various species that is undergoing transformation. In the case of substituted ethane molecules in particular, the high-temperature coupling constants and chemical shifts have been assumed to be weighted averages of the coupling constants and chemical shifts for the three individual rotamers. Indeed, Gutowsky, Belford, and McMahon[20] have attempted to calculate the chemical shifts and coupling constants for the three rotamers by least-squares fitting of the observed high-temperature coupling constants and chemical shifts as a function of temperature.

In order to analyze the spectra at intermediate rates of exchange for several of the halogenated ethanes it has been necessary to make qualitative use of the equation for the average value of a coupling constant or chemical shift, which is given by the coupling constant of each rotamer weighted by its populations,

$$\langle F^i \rangle_{Av} = P_1 F_1^i + P_2 F_2^i + P_3 F_3^i , \tag{57}$$

where the subscripts refer to the three rotamers, P_k is the mole fraction of the kth rotamer, and F_k^i is the ith chemical shift or coupling constant of the kth rotamer. Substituting from Eq. (56),

$$\langle F^i \rangle_{Av} = \frac{F_1^i + e^{-E_2/RT} F_2^i + e^{-E_3/RT} F_3^i}{1 + e^{-E_2/RT} + e^{-E_3/RT}} . \tag{58}$$

The expression above should be exactly correct if the distribution of molecules as a function of dihedral angle in the energy levels in the potential wells for the torsional vibration (Fig. 2) is unchanged with temperature, and if intermolecular effects can be neglected. If the populations of the excited vibrational levels change appreciably and if the coupling constants or chemical shifts change nonlinearly with dihedral angle (assuming the barriers are reasonably large), then it would be necessary to average over the new population distribution weighted by the coupling constant at each angle.

The spectrum of CF_2Br-CFBrCl has been studied at low and high temperatures in order to test the validity of the above equation. The results have been published elsewhere,[21] and only the conclusions will be described briefly here. The equation holds reasonably well for the coupling constants — the calculated values were about 10% higher than the experimental values at high temperatures. The source of this discrepancy is not known; it may be attributable to either population of excited torsional states or temperature dependent intermolecular associations.

The chemical shifts of the three nuclei from the solvent, $CFCl_3$, were also determined. The calculated values differed appreciably from the experimental values, implying that the chemical shifts are temperature-dependent. This difference was linear within experimental error over the high temperature region. It should extrapolate to zero at exactly 150°K, the temperature at which the low temperature data was obtained. However the chemical shifts extrapolate to 136° and 171° (see Fig. 3 of Ref. 21), indicating some nonlinearity occurs in the temperature region between 150° and 242°K, the temperature of the last point on the straight line. The nonlinear effect, although beyond experimental error, is

nevertheless small.

The chemical shift results are explained by temperature-dependent intermolecular associations, which affect nuclei in different environments to different extents. An alternative explanation, the excitation of torsional modes, would not predict the observed fact that the average value for the chemical shift between two fluorines on the same carbon atom satisfies Eq. (58) extremely well. The results on CF_2Br-CCl_2Br and CF_2Br-CHBrCl substantiate this conclusion. In CF_2Br-CCl_2Br the chemical shift between the two fluorines on the same carbon is the same, within experimental error, from 191°K to 220°K. The chemical shift from the solvent changes over 7 cps in the same temperature range (see section V-B). In CF_2Br-CHBrCl the chemical shift between the two fluorines could be observed for all three rotamers. The calculated chemical shift from Eq. (58) was within experimental error of the observed one (see section V-F).

In order to quantitatively compare experimental chemical shifts with calculated ones using the equations in section II-B it has been necessary to correct the results below for the temperature dependent intermolecular associations. The chemical shifts measured at slow and fast rates of exchange could be accurately obtained. It was then possible to determine the correction due to the intermolecular interaction at intermediate rates of exchange, where the lines are broad, by assuming a linear dependence with temperature.

C. Rates of Exchange

From absolute reaction rate theory[22] there are two equivalent forms for the rate expression which we consider.

$$k_{ij} = \kappa \frac{kT}{h} e^{-\Delta F^{\ddagger}/RT} \tag{59}$$

and

$$k_{ij} = \kappa \frac{kT}{h} \frac{Q^{\ddagger}}{Q^{o}} e^{-E_o/RT}, \tag{60}$$

where k_{ij} is the rate of exchange from species i to j, k the Boltzmann constant, T the temperature, h Planck's constant, R the gas constant, $\Delta F^{\ddagger}$ the free energy of activation, Q^{o} the partition function for the reactant (or the rotamer in the staggered configuration), $Q^{\ddagger}$ the partition function for the activated complex (the rotamer in the eclipsed form), and E_o the activation energy. E_o is the energy of the eclipsed form minus that of the staggered form and is the barrier. κ is the transmission coefficient, defined as the fraction of crossings of the barrier that are successful in leading to the final products.

Neglecting vibration-rotation interaction, the ratio of the partition functions in Eq. (60) is

$$\frac{Q^{\ddagger}}{Q^{o}} = \frac{Q^{\ddagger}_{translation}\, Q^{\ddagger}_{rotation}\, Q^{\ddagger}_{vibration}}{Q^{o}_{translation}\, Q^{o}_{rotation}\, Q^{o}_{vibration}} . \tag{61}$$

This expression can be approximately evaluated if we neglect intermolecular effects. The translational partition functions depend only on the total mass and cancel exactly. The rotational partition function ratio is given by $(I^{\ddagger}_x\, I^{\ddagger}_y\, I^{\ddagger}_z)^{\frac{1}{2}}/(I^{o}_x\, I^{o}_y\, I^{o}_z)^{\frac{1}{2}}$, i.e., by the square root of the ratio of the product of the moments of inertia. For CF_2BrCCl_2Br the products of the moments of inertia have been calculated, assuming tetrahedral bond angles, for the two staggered and two eclipsed forms. The results are 2.5, 3.0, 2.7 and 3.0 x 10^{-111} gm^3cm^6, respectively. The

value depends primarily on the relative positions of the heavy bromine atoms. Thus the ratio of the products differs from unity by at most 20%, so that neglecting the difference introduces an error of less than 10% in the frequency factor.

The partition functions for vibration are all of the order of magnitude of unity at the temperatures of interest (150° to 300°K), and the frequencies are also unlikely to change drastically between the eclipsed and staggered forms. Mizushima[23] gives plots of calculated symmetric and anti-symmetric deformation frequencies of CH_2Br-CH_2Br as a function of azimuthal angle. The frequency differences between the gauche, trans, and eclipsed forms range up to 200 cm^{-1}, although the only observed frequencies are for the symmetric deformation in the gauche and trans forms, 231 and 190 cm^{-1}, respectively. If the vibrational frequency changes from 100 cm^{-1} in the ground state to 200 cm^{-1} in the activated complex then the ratio of the partition functions at 200 and 300°K is .67 and .62, respectively.

Bucker and Neilson[24] have assigned the fundamental vibrational frequencies in the Raman and infrared for CF_2Br-CH_2Br and CF_2Cl-CH_2Cl. In both cases the low frequency vibrations (below 500 cm^{-1}) are within 17 cm^{-1} of each other, and in many cases are identical. For the brominated compound the more stable form (probably trans) has vibrations at 170 and 299 cm^{-1}, the less stable rotamer at 187 and 282 cm^{-1}. These results, as well as Mizushima's calculation, show that frequency changes in one direction are usually compensated by other lines which show frequency shifts in the opposite direction. By the frequency sum rule, the sums of squares of the vibration frequencies of ethanes is independent of the azimuthal angle of internal rotation.[25] The CF_2Br-CH_2Br results also

indicate that the frequency differences may be less for the perhalogenated ethanes, but on the other hand there are more low frequency vibrations. Thus, it will be a reasonable, although not an excellent, approximation to cancel all the vibrational partition functions, except for the torsional vibration, which is present only in the reactant. Thus the rate expression, Eq. (60), simplifies to

$$k_{ij} = \kappa \frac{kT}{h} \frac{1}{Q_v} e^{-E_o/RT} \quad . \tag{62}$$

We can obtain a qualitative value for the torsional frequency, ν, by assuming a simple potential function for the barrier (which should be qualitatively correct despite the non-equivalence of the three rotamers, since the potential maxima are much higher than the minima), $V(\theta) = \frac{1}{2}V_o(1 - \cos 3\theta)$. (A more realistic potential function is seen in Fig. 2.) Inserting this potential into the Schroedinger Equation, one finds, in the harmonic oscillator approximation, that $\nu = \frac{3}{2\pi}\sqrt{E_o/2I_r}$, where E_o is the barrier and I_r the reduced moment of inertia.[26] If the two rotors are symmetric,

$$I_r = I_1 I_2/(I_1 + I_2), \tag{63}$$

where I_1 and I_2 are the moments of inertia of the rotors about the axis of rotation. For an asymmetric rotor the exact expression for I_r is quite complicated.[27] It has been used to calculate I_r for the trans form of meso-CFClBr-CFClBr, yielding $I_r = 2.611 \times 10^{-38}$ gm cm^2. The simplified formula, Eq. (63), gives $I_r = 3.29 \times 10^{-38}$ gm cm^2. For CF_2BrCCl_2Br, I_r calculated by Eq. (63) is 3.00×10^{-38} gm cm^2.

The barriers in CFClBr-CFClBr and CF_2BrCCl_2Br are about 10 kcal/mole, yielding torsional frequencies of 59 and 54 cm^{-1}, respectively. For

$CF_2BrCFBrCl$ a torsional frequency of the 68 cm^{-1} has been observed in the Raman by Glockler and Sage.[28] The other molecules studied should have torsional frequencies of the same order of magnitude.

The partition function for a vibration is

$$Q_v = \frac{1}{1 - e^{-u}}, \quad u = h\nu/kT, \tag{64}$$

measured from the zero-point vibrational level. (This differs from the bottom of the potential curve by only $\frac{1}{2}\nu \cong 30$ cm^{-1} = .08 kcal/mole). For a torsional frequency of 60 cm^{-1}, $Q_v = 2.9$ at 200°K and increases to 4.0 at 300°K.

Because of the approximations involved in neglecting the ratio of the vibrational partition functions, and since the torsional frequency is only approximate, Eq. (59) has been used in the experiments described below to determine the free energies of activation. It can be rewritten in terms of the enthalpy and entropy of activation as

$$k_{ij} = \kappa \frac{kT}{h} e^{-\Delta H^{\ddagger}/RT} e^{\Delta S^{\ddagger}/R} . \tag{65}$$

Comparing Eqs. (62) and (65), note that the temperature dependence of the torsional partition function is small so that $\Delta H^{\ddagger}$ and E_o should be almost the same. The entropy of activation should be given, approximately, by $e^{\Delta S^{\ddagger}/R} = \frac{1}{Q_v} = \frac{1}{3.5}$ or $\Delta S^{\ddagger} = -2.5$ eu. Because of the many approximations involved to reduce Eq. (61) to $1/Q_v$, further accuracy here is unjustified. Then $E_o \cong \Delta H^{\ddagger} = \Delta F^{\ddagger} - \Delta S^{\ddagger}T = \Delta F^{\ddagger} - 2.5T$, in cal/mole. Thus, at 300°K, the barrier is roughly .7 kcal/mole less than the free energy of activation.

The above results must now be applied to the problem of internal

rotation between three species, A, B, and C. There are three independent rates to be deduced, k_{AB}, k_{AC}, and k_{BC}. The principle of detailed balance, Eq. (6), determines the three reverse rates from the populations of the rotamers. There appear to be two reasonable choices for the rate of exchange, which differ primarily in the value of the transmission coefficient. The first (method 1) was used in the paper on CFClBr-CFClBr.[16]

Consider a potential curve as in Fig. 2. To evaluate k_{12}, note that a molecule in configuration 1 must attain at least energy E_5 before it can rotate to configuration two. Method 1 assumes that if rotamer 1 is excited with sufficient energy to exceed the barrier E_5, it remains in the excited state for a sufficiently long time that it will rotate several times in the large well bounded on both sides by barrier E_4, and will have a 1/3 chance of falling into potential wells 1, 2, or 3. Using Eq. (62), this gives

$$k_{12} = \frac{1}{3}\kappa' \frac{kT}{h} \frac{1}{Q} e^{-(E_5 - E_1)/RT} , \tag{66}$$

where κ' is the transmission coefficient excluding the factor of 1/3. Note that the exponential factor corresponds to the number of molecules with energy greater than E_5. For k_{13}, if the energy is greater than E_6 but less than E_5, then the rotamer has a 50:50 chance to go into wells 1 or 3. When the energy is greater than E_5, the probability of falling into well 3 reduces to 1/3. Therefore,

$$k_{13} = \frac{1}{2}\kappa' \frac{kT}{h} \frac{1}{Q_v} \left[e^{-(E_6-E_1)/RT} - e^{-(E_5-E_1)/RT} \right] +$$

$$\frac{1}{3}\kappa' \frac{kT}{h} \frac{1}{Q_v} e^{-(E_5-E_1)/RT}$$

$$= \frac{1}{2}\kappa' \frac{kT}{h} \frac{1}{Q_v} e^{-(E_6-E_1)/RT} - \frac{1}{6}\kappa' \frac{kT}{h} \frac{1}{Q_v} e^{-(E_5-E_1)/RT} . \tag{67}$$

The spectra are independent of barrier E_4 (the highest barrier) in method 1, because complete rotation is possible whenever a rotamer's energy exceeds E_5. By similar considerations, the other four rates were determined.[16] In the actual calculations for CFClBr-CFClBr, Q_v was incorporated into the barrier energies. κ' was also taken as 1, which is unrealistic in this case since it is the number of times that the molecules rotates around without actually falling into a potential well. Thus if 100 rotations occurred, κ' would be 1/100.[29]

The alternative choice (method 2) for the rate of exchange is that the rate between any two potential minima depends only on the barrier height between them, and any activated complex rotates only 120° to the next minimum. In this case the highest barrier affects the kinetics directly, although its effect is reduced by the fact that, for the example in Fig. 2, configuration 1 can rotate to 3 via configuration 2. The six rates are given by

$$k_{ij} = \kappa \frac{kT}{h} \frac{1}{Q_v} e^{-(E_{ij}-E_i)/RT} \tag{68}$$

i=1 to 3, j=1 to 3, and $i \neq j$. E_i is the energy of the potential minimum and E_{ij} is the energy of the barrier between minima i and j. Thus, in Fig. 2, $E_4 = E_{12}$, $E_5 = E_{23}$, and $E_6 = E_{31}$. Again, $1/Q_v$ is absorbed into the barrier height for the actual calculations, so that the free energy of activation is calculated. Note that even if the three barriers are equivalent, Eqs. (66-68) do not give the same rates, but differ by 1/3. This difference is due to the different definition of the transmission coefficient for methods 1 and 2.

The choice of unity for the transmission coefficient assumes that

deactivation occurs almost instantaneously after a rotation occurs. Classically, the angular velocity of rotation, ω, can be calculated from the kinetic energy, K_E, from

$$K_E = \frac{1}{2} I\omega^2. \qquad (69)$$

If the molecule is just above the barrier, its kinetic energy is about .3 kcal/mole. The moment of inertia, I, about the axis of rotation is about 1×10^{-37} gm cm^2 for a perhalogenated ethane. The angular velocity is much faster when the molecule is over the potential minimum and possesses mostly kinetic energy. Approximating the potential function in Fig. 2 by three rectangular wells, it is seen that the molecule spends half of its time with a small kinetic energy and the other half with a larger kinetic energy. Therefore the angular velocity calculated from Eq. (69) with $K_E = 0.3$ kcal/mole is the rate for a half revolution. Under these assumptions, the angular velocity is 1×10^{12} radians per second.

The primary source of deactivation in solution is probably collisions, and it is necessary to compare the collision rate with the angular velocity. Frost and Pearson[30] justify using elementary collision theory to calculate frequency factors for reactions in solution. The number of collisions per second, Z_A, is given by

$$Z_A = \left(\frac{8\pi kT}{\mu}\right)^{\frac{1}{2}} \sigma_{AB}^2 \, n_B \quad . \qquad (70)$$

The calculation was performed for one molecule of $CF_2Br\text{-}CCl_2Br$ (M.W.=293) in $CFCl_3$. The density of the solvent, n_B, is 1.49 gm/cc. σ_{AB} is the mean radius of A and B, taken as 4Å, and μ is the reduced mass. The number of collisions/second is 1×10^{12}. Although this provides an

order of magnitude result, Benson[31] points out that if one chooses a reasonable interaction potential between molecules in a solution, such as the hard sphere well model, then the potential energy of interaction between a molecule with its 4 to 12 nearest neighbors is always of the order of magnitude of kT (thermal energy). Thus it is reasonable that the transmission coefficient should be near unity.

Deviation of κ from the assumed value of unity will result in a larger value of the entropy of activation. Alternatively, the experimental free energy of activation will be too high. This is seen by supposing $\Delta G^{\ddagger}$ is the true free energy, with $\kappa = \frac{1}{m}$. Then $\Delta F^{\ddagger}$, calculated assuming $\kappa = 1$, is related to $\Delta G^{\ddagger}$ by $\frac{1}{m} e^{-\Delta G^{\ddagger}/RT} = e^{-\Delta F^{\ddagger}/RT}$, or $\Delta G^{\ddagger} = \Delta F^{\ddagger} - RT (\ln m)$. Method 1 inherently requires that κ be small, probably less than 1/10, which would decrease the calculated values of $\Delta F^{\ddagger}$ by 1.15 kcal/mole at 250°K.

The spectra of $CF_2Br\text{-}CCl_2Br$ provide experimental evidence in favor of method 2. In this molecule configurations 2 and 3 are identical minima, and E_4 and E_6 identical barriers by symmetry. Choosing barrier E_5 less than or equal to E_4 does not predict the observed spectra, as will be seen in Sec. IV-B. Since method 1 is independent of the value of the highest barrier, it is necessary to use method 2 (and in this case the additional parameter available, E_5) in order to calculate the observed spectrum.

Since method 1 fails to predict the observed spectra, κ is unlikely to be significantly less than 1, and in the absence of a better choice we take κ as 1 in Eq. (59). Cagle and Eyring[29] show that internal rotation of the type predicted by method 1 is nonexistent for the internal rotation of substituted biphenyls, and conclude that κ must be

near unity.

The choice of method 2 for the kinetics corresponds exactly with that used by Anet[32] to calculate barriers of internal rotation between identical species. He has studied the interconversion of substituted benzaldehydes by rotation about the $C_1 - C_\alpha$ bond (see Fig. 3). Here the kinetics involved a straightforward application of Eq. (59). The rate is given by

$$k_{12} = 2 \frac{kT}{h} e^{-\Delta F^{\ddagger}/RT}, \qquad (71)$$

where the 2 is inserted since I may rotate to II either by a clockwise or counter-clockwise rotation. Imagining a three molecule system where A=I, B=II, and C=II, and where B and C are exchanging very rapidly, then we have the same conditions as above, but in which the kinetics of Eq. (59) can be used. Choosing $E_2 = E_3 = 278.2$ cal/mole, the population of A is 50% at 202°K. Then the calculation using the kinetics of Eq. (68) in the formulas developed in section IIA gives exactly the same result as using the kinetics of Eq. (71) in the theory developed by Gutowsky and Holm[33] for exchange between two species, at all temperatures for any value of T_2. (In both calculations the coupling constant is neglected.)

The experimental accuracy is insufficient to justify the approximations made above from plots of log k against various parameters. Results for the different molecules considered are consistent because the same approsimations are used throughout.

To summarize, in all of the calculations below the rate of exchange from species i to species j is

$$k_{ij} = \frac{kT}{h} e^{-(E_{ij} - E_i)/RT} , \qquad (72)$$

where $F_{ij} = (E_{ij} - E_i)$ is the free energy of activation, and E_i is the energy of rotamer i. Note that E_{ij} differs by a small constant from the true barrier height. Since $F_{ij} \neq F_{Ji}$, the values of E_{ij} have been tabulated in section V below.

IV. EXPERIMENTAL

$CFCl_2$-$CFCl_2$ was obtained from K & K Laboratories and CF_2Br-CCl_2Br from Peninsular Chemresearch Inc. The CFClBr-CFClBr was provided by Dr. Paul Resnick of this department. CF_2Br-$CFBr_2$, CF_2Br-CHBrCl, and CF_2Br-CFBrCl were prepared by bromination of CF_2=CFBr, CF_2=CFCl (both from Peninsular Chemresearch) and CF_2=CHCl (from Allied Chemical Corp). The brominations were carried out in a sealed tube. The ethylene was used in excess and allowed to boil off from the product which was then used without further purification.

Spectra were studied of approximately 25% to 50% by volume solutions of the perhalogenated ethanes in CS_2, $CFCl_3$, CF_2Cl_2, or CF_3Br. Although the CF_3Br has a lower melting point than CF_2Cl_2, it was found that the ethane solutions of the latter usually froze at a lower temperature. Most spectra were taken with the freon solvents because sidebands of the solvent could be used to calibrate the spectrum. The freon peak was also a direct measure of the magnetic field inhomogeneity.

The spectra were recorded on a Varian HR-60 spectrometer operating at 56.4 Mc/sec equipped with a flux stabilizer and integrator. It was possible to record most spectra without the use of the integrator serving as a base line stabilizer which eliminated the undesirable 2000 and 4000 cps sidebands of the solvent. Chemical shifts and coupling constants were determined by the usual audio sideband technique, when the resonance lines were sharp. At intermediate rates of exchange the lines were broad and two sidebands of the freon solvent were used, one on each side of the peaks of interest.

Most of the spectra were obtained at fairly rapid sweep rates (about 200 cps/minute), using short response times, in order to avoid saturating the broad peaks at reasonable power levels.

All the frequency differences and line widths tabulated in the tables are the average of at least 8 spectra. The experimental errors are the root-mean-square deviations. The frequency differences and line widths were measured to one-half or 1 cps from the computer spectra, depending on the width of the peak. The computer results for $CF_2Br—CCl_2Br$ were obtained more accurately below 220°C by interpolation from the printed absorbances in order to observe small differences in the widths.

The variable temperature insert was constructed in this laboratory. It is substantially similar to the one described by Petrakis.[34] The Bakelite insulator ring has been replaced by a quartz disk with a small hole for the receiver coil wires. The quartz is used so that the positioning of the receiver coil was not drastically changed as the temperature was changed. The coolant was provided from a liquid nitrogen boiler in the earlier experiments, and by means of a stream of gaseous nitrogen through a coil immersed in liquid nitrogen in later experiments.

A copper-constantan thermocouple was placed in the insert at a point in the nitrogen path just ahead of the sample. The temperature of this thermocouple was compared with the temperature of another thermocouple placed in a dummy sample tube which was inserted in the probe. Depending on the nitrogen flow rate and the exact location of the thermocouple, these temperatures would differ by 1 to 10 degrees. The temperature of the thermocouple was compared with the dummy sample

thermocouple several times in each series of experiments, with consistent results. Consequently, although the absolute temperature is only known to ± 2 or 3°, the differences in temperature for spectra taken on a given run are known more accurately. The spectra are reproducible within the limits of the signal/noise.

V. RESULTS AND DISCUSSION

A. $CFCl_2$-$CFCl_2$

In the three rotamers of $CFCl_2$-$CFCl_2$ there are two identical rotamers with the fluorines gauche to each other, and the third rotamer has the fluorines trans. A 33% by volume solution in freon 11 ($CFCl_3$) was prepared. The compound was contaminated by about 25% CF_2Cl-CCl_3. The single resonant peak of the latter compound occurs 65.086 ± .004 ppm upfield from freon 11, and 2.722 ± .006 ppm downfield from $CFCl_2$-$CFCl_2$, and did not interfere with the latter peaks. Tiers[35] has obtained a shift of 2.755 ± .01 ppm at 21°C for a 90% solution of the difluoroethanes in $CFCl_3$; the difference is due to the chemical shift dependence on the temperature and solvent concentration.

At low temperatures exchange is sufficiently slow that the spectrum due to $CFCl_2$-$CFCl_2$ consists of two sharp lines, with relative areas of 1.00: 1.33 ± .03 at 151°K. Assuming the trans rotamer is the lowfield peak, then the degenerate gauche rotamers comprise the highfield peak. From the spectrum at 151°, the energy of the gauche forms is calculated to be 122 ± 7 cal/mole. At 300°K exchange between the rotamers is rapid and only one sharp line is seen. The relative populations at this temperature, from Eq. (56), are 1.00 : 1.63.

The chemical shifts, ν_1 and ν_2, of the rotamers from the solvent are tabulated in Table III. These have been plotted at low temperatures, where exchange does not affect the frequency separations. Extending the straight lines to 300°K gives chemical shifts of 3767. cps and 3866. cps, respectively. Inserting these results into Eq. (58), the chemical shift at 300° is calculated as 3828. cps, which compares well with the

TABLE III. Chemical shifts, peak widths, barrier to rotation, and form of the experimental spectra of $CFCl_2$-$CFCl_2$. All frequencies are in cycles per second.

Temp.	Doublet Separation	ν_1 [a]	ν_2 [a]
151°K	57.91 ± .25	3839.7 ± .5	3897.6 ± .5
154	58.9 ± .3	3837.4 ± .3	3896.3 ± .3
160	59.6 ± .3	3835.6 ± .5	3895.2 ± .5
167	61.9 ± .3	3831.6 ± .3	3893.5 ± .3

Temp.	$2/T_2$ [b]	Doublet Separation	Width [c] Peak 1	Width [c] Peak 2	Form [d]	Barrier [e]
177°K	2.6 ± .3	63.1 ± .5	6.8 ± .3	6.0 ± .3	d	9.5
186 ½	4.4 ± .3	62.6 ± .6	16.3 ± .6	13.0 ± .4	d	9.7
188	3.2 ± .3	62.4 ±1.1	17.7 ±1.0	13.1 ±1.0	d	9.7
191	7.0 ±1.0	52.8 ±3.	-	28. ±4.	d	9.6
194	4.6 ± .7	45. ±2.	-	30. ±4.	d	9.65
196 ½	6.4 ±1.0		(2.0)	61. ±3.	pws	9.6
198	2.8 ± .3		(1.5)	50. ±3.	ap	9.6
200	2.8 ± .4		(1.1)	38. ±2.	ap	9.6
204	2.6 ± .5			24. ±2.	sp	9.6
213	4.8 ±1.0			12.8 ± .6	sp	9.6

[a] Chemical shifts from the solvent, $CFCl_3$.

[b] Width at half height of freon sideband.

[c] Width at half height. Above 190°K there is only one peak; its width is given in the peak 2 column. The numbers in parentheses in the peak 1 column denote the asymmetry of this peak, calculated as the ratio of the distance, at half height, from the center of the peak to the low field side divided by the distance from the center to the high field side, where the center is that point under the maximum of the peak.

[d] d--doublet, broad lines; pws--peak with shoulder; ap--asymmetrical peak; sp--symmetrical peak.

[e] The barrier is obtained by comparison to the calculated spectra in Table IV.

experimental value of 3824. cps, considering the narrow temperature region over which the chemical shift of the individual rotamers has been obtained.

The alternative assignment of the low temperature spectrum, choosing the trans rotamer as the highfield peak, yields gauche rotamer energies of 294 cal/mole. Then the spectrum observed at 194°K should consist of two peaks of equal intensity, contrary to experiment. Further, the chemical shift at room temperature, calculated from Eq. (58), would be 3811. cps.

The experimental spectra at temperatures near the coalescence temperature are shown in Fig. 4, and the line widths and chemical shifts are tabulated in Table III. Since exchange between the two gauche rotamers does not change the environment of the fluorine atoms, this rate is unobservable. There is then only one barrier that we can obtain, which is for the rotation between the trans form and either one of the gauche forms. The spectra were calculated usings Eqs. (7-9), with Eq. (72) for the rates. Identical results can be obtained using the equations developed by Gutowsky and Holm,[33] but with an additional factor of two in the rate to account for the two possible paths of rotation (see section III-C).

As indicated above, the chemical shift between the gauche and trans rotamers has a considerable temperature dependence, linear within experimental error. Between 151°K and 167°K the frequency separation of the two rotamers increases by .20 cps/degree. It was assumed that the temperature dependence remained linear with temperature through the coalescence region, and the spectra were calculated at higher temperatures using a chemical shift between rotamers calculated for that particular temperature,

$$\nu_T = \nu_{150} + 0.20\ (T - 150), \tag{73}$$

where ν_T is the chemical shift at temperature T. Thus in Table IV ν increases with temperature by 7 cps over the coalescence region.

The calculated spectra appear, for the proper exchange rate, like the experimental spectra. The line widths, etc., of these spectra for various varriers and temperatures are tabulated in Table IV. The inhomogeneity of the magnetic field is obtained from the width of the freon sidebands used to calibrate the spectrum. Since these widths, at some temperatures, contribute significantly to the width of the peak, they have been included in the calculation. For a single peak, the width due to exchange and the width due to the inhomogenous field simply add. This is qualitatively true for the more complex spectra, as seen by the results tabulated in Table IV at 191° for two values of the natural line width.

The barrier is obtained at each temperature by comparison of the calculated spectra and the experimental spectra, and the best value at each temperature is also tabulated in Table III. The result is 9.6 ± .1 kcal/mole.

These results prove that a one parameter theory can reproduce exactly the experimental results in the absence of spin-spin coupling. In the next section we consider an experimental spectrum in which the spin-spin coupling must be added to reproduce the spectrum.

Table IV. Spectra of $CFCl_2$-$CFCl_2$ calculated with Eqs. (7-9) and Eq. (72).

Temp.	ν[a]	$2/T_2$[b]	Barrier	Doublet Separation	Width[c] Peak 1	Width[c] Peak 2	Form[d]
177.°K	63.4	2.6	9.4	62.5	9.0	6.5	d
			9.5	63.0	7.0	5.5	d
			9.6	63.0	6.0	5.0	d
186 ½	65.3	4.4	9.6	63.0	19.5	14.5	d
			9.7	63.5	16.0	12.0	d
			9.8	64.5	13.0	10.5	d
188.	65.6	3.2	9.6	62.0	23.0	15.5	d
			9.7	63.0	17.5	12.5	d
			9.8	64.0	13.5	10.5	d
191.	66.2	7.0	9.5	48.		47.	d
			9.6	56.		29.	d
			9.7	60.		23.	d
191.	66.2	2.0	9.4	-	(3.3)	60.	pws
			9.5	50.		31.	d
			9.6	57.		22.	d
194.	66.8	4.6	9.5		(2.5)	59.	pws
			9.6		(3.7)	66.	pws
			9.7	54.		30.	d
			9.8	60.		23.	d
196 ½	67.3	6.4	9.5		(1.5)	47.	ap
			9.6		(2.4)	58.	pws
			9.7		(3.1)	66.	pws
198.	67.6	2.8	9.5		(1.2)	37.	ap
			9.6		(1.5)	48.	ap
			9.7		(2.6)	57.	pws
200.	68.	2.8	9.5		(1.1)	30.	ap
			9.6		(1.2)	38.	ap
			9.7		(1.7)	48.	ap

Temp.	ν[a]	$2/T_2$[b]	Barrier	Doublet Separation	Width[c] Peak 1	Width[c] Peak 2	Form[d]
204.	68.8	2.6	9.5			18.	sp
			9.6			22.	sp
			9.7			30.	sp
213.	70.6	4.8	9.5			10.5	sp
			9.6			12.0	sp
			9.7			14.0	sp

[a] Chemical shift obtained from Eq. (73).

[b,c,d,] Same as in Table III.

B. $CF_2Br-CCl_2Br$

This compound was first studied qualitatively in an approximately 25% by volume solution of carbon disulfide. Because the results were of considerable interest in choosing between the two kinetic models, the spectra were rerun in a 25% mole fraction solution of $CFCl_3$. More quantitative results were obtained by first adjusting the field homogeneity using the sharp solvent peak, since the homogeneity changed considerably with temperature.

The low temperature spectrum at 191°K, shown in Fig. 5, consists of a large peak about 3313 cps upfield from the solvent (labelled peak 1 in Table V and the discussion below) and an AB quartet of peaks centered 205.9 cps upfield from peak 1. From the schematic diagram of the three rotamers of $CF_2Br-CCl_2Br$ in Fig. 6, it is seen that rotamer I has a plane of symmetry which makes the two fluorines equivalent. Rotamers II and III are mirror images, differing only by the interchange of the two fluorines. Consequently peak 1 is unambiguously assigned to rotamer I and the quartet to the pair of rotamers II and III. The chemical shift, $\nu_A - \nu_B$, and the coupling constant, J_{AB}, of the two fluorines on II are 184.8 ± .6 and 155.8 ± .6 cps, respectively. The results in CS_2 were 171.5 and 154.3 cps.

The ratio of the areas of peaks 3 and 4 relative to 1 and 2 is easily obtained with the Varian integrator. From the known coupling constants and chemical shifts of the AB quartet, it is possible to calculate the contribution of peak 2, and then obtain the relative populations of I:(II + III) = 1.16 ± .06 : 1.00. The relative energy of rotamer II is 320 ± 20 cal/mole. In the CS_2 solution the energy

is 420 cal/mole.

As the temperature is increased the peaks broaden. At 198°K peak 2 is unobservable due to the 5 cps half width of the much larger peak 1. Above 206° peak 5 is not distinguishable from the noise. However, the coalescence of the remaining three peaks, 1, 3, and 4, was carefully studied as the temperature was increased. Initially it was attempted to fit the spectra using the kinetics of method 1 (section III-C) in which the highest barrier does not affect the rates. Choosing all three barriers the same or the barrier between rotamers II and III less than the other two barriers gives calculated spectra which show peaks 3 and 4 coalescing prior to the coalescence of peaks 1 and 3. Since this is not observed, it was necessary to use the kinetics of method 2 for the rates, in which it is possible to make E_5, the barrier between rotamers II and III, higher than E_4, the barrier between I and II, and E_6, the barrier between I and III. E_4 and E_6 are identical by symmetry. If all three barriers are the same, then the spectra calculated by the two methods are identical, except that the barriers using method 2 are all higher by RT ln 3 due to the additional factor of 1/3 in Eq. (66). Therefore in the discussion of the spectra below all of the calculations have been performed using method 2, and it is shown that the calculated spectra with all the barriers equal do not reproduce the observed spectra.

Before describing the spectra, it is first necessary to consider the temperature dependence of the intermolecular interaction with the solvent on the chemical shifts. Unlike $CFCl_2$-$CFCl_2$, the two fluorines are on the same carbon atom and should be equally affected by the intermolecular interaction. This conclusion is confirmed by observing (see Table V) that the chemical shift between peaks 3 and 4 is constant, within

experimental error, from 191°K to the temperature of coalescence of the peaks, about 222°K. There remains a temperature dependence of the chemical shift from the solvent. The frequency of the observed, symmetrical, singlet peak at 257°K is 2300.1 ± .8 cps upfield from the solvent. The frequency of the peak at 257°K is calculated to be 2318.0 ± .5 cps from the chemical shifts measured at 198°, and is independent of small changes in the barriers. It is also clear from the downfield shift of peak 1 at 206° and 208° that there is a temperature-dependent shift of the solute peaks, since coalescence of the peaks would cause an upfield shift. In order to compare the observed shifts of peak 1 (and, at higher temperatures, the large single peak) with the calculated ones, it is easiest to correct the experimental shifts. From the results at 198° and 257°, and assuming a linear function, the correction is given by

$$\nu'_{obs} = \nu_{obs} - 0.305\ (T - 198), \qquad (74)$$

where T is the absolute temperature. For convenience in comparing the experimental and calculated spectra, the observed chemical shifts in Table V have been corrected. The scale in the figures is also adjusted so that the chemical shift of peak 1 is given by ν'_{obs}, and the zero frequency has been chosen 3112.6 cps upfield from the solvent at 198°K. The experimental chemical shifts from the solvent have been tabulated in footnote a of Table V.

The experimental chemical shifts and line widths are tabulated in Table V. The spectra are discussed for each temperature below:

At 198°K the spectrum calculated with E_4 = 10.85 kcal/mole reproduces the observed width of peak 1. It is necessary that E_5 be at least 12.0 kcal/mole in order to obtain the proper width for peaks 3 and 4.

TABLE V

Calculated and observed frequency separations and line widths for $CF_2Br\text{-}CCl_2Br$ in $CFCl_3$.[a] Peaks are numbered as in Fig. 5. The experimental spectra are shown in Figs. 7 to 16, and the calculated spectra with an asterisk have also been reproduced in the figures. All values are in cps, at 56.4 Mc/sec.

Temp.	E_4[b]	E_5[b]	ν'_{obs}[b]	$\nu_1-\nu_3$	$\nu_3-\nu_4$	$W_1^{\frac{1}{2}}$[d]	$W_3^{\frac{1}{2}}$[d]	$W_4^{\frac{1}{2}}$[d]
198°K	Exp.		0.0 ±.4	162.3 ±.4	86.3 ±.4	5.0 ±.2	4.9 ±.2	4.9 ±.2
	10.8	12.0	0	162½	86	5.4	5.7	5.6
	10.85	10.85	0	162½	86	4.9	6.2	6.2
	10.85	11.6	0	162½	86	4.9	5.3	5.3
	10.85	12.0	0	162½	86	4.9	5.2	5.2
	10.85	13.0	0	162½	86	4.9	5.2	5.2
	10.9	12.0	0	162½	86	4.6	4.9	4.8
206	Exp.		-0.2 ±.3	162.9 ±1.4	87.0 ± .8	12.2 ±.5	13.7 ± .6	13.6 ± .9
	10.75	12.0	1	161	86	13.1	15.3	15.0
	10.8	10.8	½	161½	86	12.5	17.5	17.3
	10.8	11.6	1	161	86	12.1	14.1	13.9
	10.8	12.0*	1	161	86	12.1	13.9	13.8
	10.8	13.0	1	161	86	12.1	13.7	13.5
	10.85	13.0	1	161	86	11.4	12.5	12.4
208	Exp.		0.9 ±.5	160.7 ± 0.6	86.7 ± .5	13.5 ± .3	17.2 ±1.5	16.9 ±1.5
	10.75	11.6	1½	160	86	14.5	18.8	18.2
	10.8	10.8	½	161	86	14.1	21.0	20.6
	10.8	11.2	1	160½	86	13.6	17.8	17.5
	10.8	11.6*	1	160½	86	13.4	16.7	16.3
	10.85	11.6	1	160½	86	12.3	14.9	14.7
216½	Exp.		2.1 ±.6	156.6 ± 1.5	87.2 ±1.5	30.2 ±1.2	33.7 ±2.0	33.8 ±2.0
	10.75	13.0	3	154	87	31½	40.	40½
	10.8	12.0	3	154½	87	29½	37.	37½
	10.8	13.0	3½	154½	87	28½	36½	37
	10.85	10.85	3	157	84	32	43½	46
	10.85	11.6	3	156	87	28½	37½	38
	10.85	12.0*	3	156	86	27½	34	34
	10.85	13.0	3	156	86	26½	33½	33½
	10.9	10.9	3	157	84	28	41½	45½
	10.9	11.3	2½	156½	87	27½	34	34½

Temp	E_4^b	E_5^b	$\nu'^{\,b}_{obs}$	$\nu_1-\nu_3$	$\nu_3-\nu_4$	$W_1^{\frac{1}{2}d}$	$W_3^{\frac{1}{2}d}$	$W_4^{\frac{1}{2}d}$
219½°	Exp.		6.1 ±.3	148.3 ± 1.1	86.5 ± .9	45.3 ±1.7	47.2 ±2.7	51.3 ±2.5
	10.75	12.0	6½	144½	89	44	51	c
	10.8	11.4	6	148	87	43½	50½	c
	10.8	12.0*	5½	148½	88	41	48	52
	10.8	13.0	5½	148½	88	39½	47	50
	10.85	10.85	6	151	81	43½	58	c
	10.85	11.2	5½	150½	86	41½	49	58½
	10.85	12.0	5	151	87	37½	44½	48½

Temp.	E_4^b	E_5^b	$\nu^{\,b}_{obs}$	$\nu_1-\nu_3$	$\nu_3-\nu_4$	$W^{3/4d}$	$W^{2/3d}$
222½°	Exp.		14.5 ±1.2	122. ± 7.	83. ±7.	49.3 ±2.5	61.6 ±2.5
	10.7	11.6	16	112	84	51	63½
	10.7	12.0*	15	115	90	48½	62½
	10.75	10.75*	17	121	c	52½	65½
	10.75	11.2*	15	123	82	48	59½
	10.75	11.6	13	126	88	43½	54½
	10.75	12.0*	12	126	92	41½	51
	10.8	10.8*	14	134	c	45½	56
224°	Exp.		17.0 ±2.7	114. ± 7.	84. ±5.	61. ±4.	-
	10.7	13.0	19	c	c	64	87½
	10.75	12.0	17	c	c	54½	69½
	10.75	13.0	15	103	92	52½	67
	10.8	11.6	15	120	88	47	59½
	10.8	12.0*	13	122	92	44	57½
	10.8	13.0	13	122	92	43½	54½
	10.85	10.85	15	129	c	49½	60½
	10.85	11.0	15	128	c	47½	59½
	10.85	11.3	13	129	83	43½	54½
	10.9	10.9	12	138	c	43½	52½

Temp.	E_4^b	E_5^b	$\nu'^{\,b}_{obs}$	$W^{3/4\,d}$	$W^{2/3\,d}$
225°	Exp.		30.6 ±4.	101. ± 7.	136. ± 7.
	10.65	12.0	37	110	130
	10.65	13.0*	34	113	132½
	10.7	10.7	40	99	129
	10.7	11.2	34	94½	125
	10.7	11.6*	30	93½	125
	10.7	12.0	27	93	125
	10.75	10.75*	31	80½	112
	10.75	11.6	23	69½	92½
230°	Exp.		76 ±8.	93. ±4.	111. ±4.
	10.75	10.75	78	88	106
	10.75	11.2	75	85	102½
	10.75	11.6	75	86	103
	10.75	12.0*	76	87	105
	10.8	10.8*	71	98½	117½
	10.8	11.2	68	94½	114
	10.8	11.6	69	97	116
	10.8	12.0*	69	101	118½
	10.85	11.2	58	103	123

Temp.	E_4^b	E_5^b	$\nu'^{\,b}_{obs}$	$W^{\frac{1}{2}\,d}$
234°	Exp		84.4 ±4.	112. ± 6.
	10.75	11.6	86	101
	10.8	10.8	91	112
	10.8	11.6	84	110
	10.8	12.0*	84	110
	10.8	13.0	84	110
	10.85	12.0	82	122
247°	Exp		100.3 ± 2.1	48.1 ±2.3
	10.8	12.0	101	44
	10.85	11.4	102	44
	10.85	12.0*	101	48
	10.85	13.0	100	49½
	10.9	10.9	103	41½
	10.9	11.4	101½	47½
	10.9	12.0	100	51½
	11.0	11.0	102½	51

Temp	E_4 [b]	E_5 [b]	ν'_{obs} [b]	$W^{\frac{1}{2}}$ [d]
257°	Exp		105.5 ± .8	23.1 ±1.0
	10.8	12.0	$105\frac{1}{2}$	20.9
	10.85	11.0	$105\frac{1}{2}$	18.3
	10.85	12.0	$105\frac{1}{2}$	22.3
	10.85	13.0	$105\frac{1}{2}$	23.5
	10.9	10.9	$105\frac{1}{2}$	19.2
	10.9	12.0	$105\frac{1}{2}$	24.0
	11.0	11.0	$105\frac{1}{2}$	22.5

[a]Spectra were calculated using Eqs. (40-42) and (72) using the computer program in Appendix B. The observed chemical shift from $CFCl_3$ and the width of a sideband of the solvent peaks were 3112.6 ± .4 and 2.0 cps at 198°, 3110.0 ± .3 and 3.0 (206°), 3110.4 ± .5 and 2.1 (208°), 3109.1 ± .6 and 2.7 ($216\frac{1}{2}$°), 3112.2 ± .3 and 3.7 ($219\frac{1}{2}$°), 3119.6 ± 1.2 and 2.9 ($222\frac{1}{2}$°), 3121.7 ± 2.7 and 3.3 (224°), 3135.0 ± 2.4 and 2.3 (225°), 3179.0 ± 8.5 and 3.0 (230°), 3186.0 ± 4.0 and 3.0 (234°), 3198.0 ± 2.1 and 5.0 (247°), and 3200.1 ± .8 and 3.8 cps at 257°.

[b]E_4 is the barrier between rotamer I and II, E_5 between II and III, in kcal/mole. ν'_{obs} is the chemical shift corrected according to Eq. (74), and less 3112.6 cps.

[c]coalesced.

[d]$W^{3/4}$ is the width of the main peak at 3/4 height, etc. At $216\frac{1}{2}$° and $219\frac{1}{2}$° the width is obtained from the dashed line shown in Figs. 9 and 10.

At 206° (Fig. 7) the best fit to the observed spectrum is obtained with E_4 = 10.8 and E_5 at least 12.0. As with 198° results, $E_5 = E_4$ makes the width of peak 3 much larger than the width of peak 1.

At 208° (Fig. 8) the experimental error of the line width is considerably larger, due primarily to fluctuations of the temperature during this experiment. The best value for E_5 is slightly lower at 11.4, with E_4 equal to 10.8 kcal./mole.

At 216½° (Fig. 9) there is a set of values of E_4 and E_5 which will reproduce the observed spectra: 10.8 and 13.0, 10.85 and 12.0, or 10.9 and 11.3. If $E_4 = E_5$ then the difference in width of peaks 1 and 3 is much larger than observed. In neither case is the fit perfect, but the experimental error is reasonably large. Note that the half-widths have been measured from the dashed line in the spectra, which introduces an added uncertainty of choosing the proper base line. It is impossible to measure the half width of peaks 3 and 4 from the true base line due to overlap with peak 1. The calculated half widths have been determined in an identical manner from the plots.

At 219½° (Fig. 10) the best fit is given by E_4 = 10.8 and E_5 = 12.0, although the width of peak 1 is not well reproduced. Although other sets of barriers come close to reproducing the observed line widths, this is the only one which also gives the proper frequency separations.

Several spectra at 222½° are reproduced in Fig. 11. The calculated spectra with $E_4 \doteq E_5$ clearly show peaks 3 and 4 coalescing before peaks 1 and 3 coalesce, whereas the experimental spectrum shows both 3 and 4 as discernible peaks on the side of peak 1. E_4 = 10.7, $E_5 \doteq$ 12.0 and E_4 = 10.75, E_5 = 11.2 both duplicated the experimental spectrum.

At 224° (Fig. 12), as usual, a range of values for E_4 and E_5 reproduce the appearance of the spectrum: 10.75 and 13.0, 10.8 and 12.0 and 10.85 and 11.3. It is impossible to reproduce the width of peak 1 while still observing peaks 3 and 4 in the calculated spectra, but this may be due to saturation of the peak. If E_4 = 10.75, decreasing E_5 below 13.0 reduces peaks 3 and 4 to shoulders. As at 222½°, if the barriers are the same, then it is impossible to observe peak 3 while obtaining the observed chemical shift between peaks 1 and 2. Since the calculated spectra resemble those at 222½°, only one has been reproduced.

At 225° the experimental accuracy is insufficient to decide which of the many calculated curves is best. The three curves reproduced in Fig. 13 duplicate the general appearance of the observed spectrum— E_4 = 10.7 and E_5 = 11.6 give the best widths and frequency of the main peak. Increasing E_4 to 10.75 or above mades the peak too sharp.

At 230° (Fig. 14) the set of barriers includes E_4 = 10.8, E_5 = 11.2 and E_4 = 10.85, E_5 = 12.0, which are both within experimental error of the observed spectra. Choosing both barriers the same can reproduce the observed line widths and frequency at this relatively high temperature, but that is because of the symmetrical appearance of the spectrum. Note that $E_4 = E_5$ = 10.8 has approximately the same width as E_4 = 10.8 and E_5 = 12.0, but that the former is a more symmetrical peak whereas the latter has a much larger upfield tail. At high values of E_5 an upfield peak (due to rotamers II and III) is being superimposed on the main peak of sufficient intensity to cause a slight increase in the widths.

At 234° (Fig. 15) the width of the peak is so broad that the half width is essentially independent of E_5, which affects, very slightly, the asymmetry of the peak. E_4 is 10.8.

At 247° (Fig. 16) and 257° there is a set of barriers which will fit the observed spectrum. At these relatively high temperatures the lines are narrower and the effects of E_5 on the spectra are readily noticed. If the barriers were the same it would be necessary to make $E_4 = E_5 = 11.0$, whereas $E_4 = 10.85$ and $E_5 = 12.0$ provides an equally good fit.

The arguments in section III indicate that the barriers should be approximately constant over a limited temperature range. The above data show that choosing the barriers in $CF_2Br\text{-}CCl_2Br$ as $E_4 = 10.8 \pm .1$ and $E_5 = 12.0 \pm .5$ can reproduce the experimental spectra over the 60 degree temperature range in which the coalescence of the peaks can be observed.

The qualitative results in CS_2 solution indicated that the lower barrier was the same, and possibly slightly lower, than in the $CFCl_3$ solution. Since it is impossible to estimate the field homogeneity, quantitative comparisons are impossible. At 206° the width of peaks 1 and 3 were 15 and 17 cps, respectively, from which E_4 is estimated to be 10.6 or 10.7 kcal/mole. The spectra at other temperatures had the same appearance as the spectra in $CFCl_3$.

C. $CF_2Br\text{-}CFBr_2$

The low temperature spectrum of the three rotamers of $CF_2Br\text{-}CFBr_2$ in carbon disulfide was first observed by Manatt and Elleman.[36] Spectra were first taken in CS_2, but the sample always froze before the low intensity peaks of the spectrum, broadened by exchange, could be observed. A solution 40% by volume in CF_2Cl_2 could be studied at much lower temperatures. The barriers were obtained in this solution.

The three rotamers are drawn in Fig. 17, and the spectrum at 152°K

is given in Fig. 18. Rotamers I and II have identical ABX spectra, and peaks 1-8 and 11-13 are clearly attributed to this rotamer. The remaining 5 peaks comprise an A_2X spectrum due to rotamer III, in which two of the fluorines are equivalent. The additional peaks between peaks 8 and 9 in Fig. 18 are due to impurities; these peaks remained sharp at all temperatures. Peaks 1, 2, 7, and 8 are as sharp as peaks 3-6 at 145°K, but it is then impossible to observe the triplet of rotamer III, as the population of this rotamer decreases rapidly with temperature. However, the coupling constants and chemical shifts (in cps from the solvent) of rotamer I could be accurately determined at this temperature.

The coupling constant and chemical shifts for the third rotamer were obtained at 150°K. The results are tabulated in Table VI, along with the constants obtained in CS_2 at about 160°K. At 146°K the relative areas of peaks 7-8 and 9-10 is 1:2.023 ± .14, from which the energy of rotamer III (relative to rotamer I) is calculated to be 759 ± 30 cal. for the CF_2Cl_2 solution. A similar experiment yields an energy of 701 ± 30 cal. in CS_2.

Manatt and Elleman showed that J_{AX} and J_{BX} in rotamer I are negative in sign, assuming J_{AB} is positive. Presuming that Eq. (58) is qualitatively correct, the coupling constant at room temperature can be calculated with both positive and negative sign for J_{AX} in rotamer III. The results are -15.3 and -17.6. The experimental value in CS_2 is $|17.1|$, from which it follows that J_{AX} is negative in rotamer III too.

As the temperature is increased above 150° the AB peaks (1-8) begin to coalesce to a broad line about 90 cps wide at 171°. As the temperature is increased further this begins to sharpen into a doublet, observed at 185°. At higher temperatures this doublet coalesces and the triplet

TABLE VI

Coupling constants and chemical shifts of the rotamers of CF_2Br-$CFBr_2$. The chemical shifts in CF_2Cl_2 are from the solvent, those in CS_2 from the center of the AB octet.

	CF_2Cl_2	CS_2[a]
Rotamer I		
J_{AB}	168.1 ± .2	165. ± 2.
J_{AX}	-16.1 ± .3	-15.7± .3
J_{BX}	-18.4 ± .3	-19.1± .3
ν_A	2843.5 ± .5	-94.9± .6
ν_B	3014.2 ± .5	94.9± .6
ν_X	3616.9 ± .3	705.9± .7
Rotamer III		
J_{AX}	-21.45± .2	-21.7± .3
ν_A	3330.5 ± .4	397.5± .4
ν_X	3885.2 ± .5	958.1± .5

[a] Manatt and Elleman[36] obtained 165, -16.2, -18.6, and -18.8 for the coupling constants, respectively.

(peaks 11-13), which remains sharp until 185°, begins to broaden, coalescing at about 197°K. Above 213° the triplet reappears, while the doublet forms at 217°. At room temperature an A_2X spectrum consisting of five sharp lines is observed.

The results are quantitatively explained using the theory developed in sections II and III above for the ABX case. E_4, the barrier between rotamers I and II, is much less than E_5, the barrier between rotamers II and III. By symmetry, E_6, the barrier between I and III, is equal to E_5. Rotation from I to II occurs at relatively low temperatures, which interchanges the position of the A and B fluorines, but does not change the environment of the X nucleus. Only rotation from I or II to III affects the X region of the spectrum and the doublet of rotamer III, and this only occurs at an appreciable rate at a higher temperature. Thus the triplets remain sharp until 185°. The doublet in the AB region is observed from 185° to about 197° since the exchange between I and II has become so fast that the fluorines are almost averaged. E_4 has only a minor effect on the AB part of the spectrum above 200°. The X portion of the spectrum is independent of E_4 at all temperatures.

The experimental spectra are reproduced in Figs. 18 to 29, along with some of the theoretical spectra. The frequency separations and widths for the observed and calculated spectra at all temperatures are tabulated in Table VII for the AB region and in Table VIII for the X peaks. The zero on the scale in the figures is arbitrarily located about 3000 cps upfield from the freon solvent, the exact value chosen such that peak 5 is located at the same point as its calculated location from the computer spectra. Qualitatively, the chemical shifts tabulated in Table VII are explained as follows. There is a downfield shift of the AB octet with temperature, due to intermolecular interactions with

TABLE VII.

Calculated and observed frequency separations and line widths for the AB region of CF_2Br-$CFBr_2$ in CF_2Cl_2.[a] Peaks are numbered as in Fig. 17 at low temperatures. The doublet observed at temperatures above 167°K is labelled as peaks 4 and 5. $w_{1,2}$ is the width, at half height, of peaks 1 and 2 together. The experimental spectra are shown in Figs. 18 to 29, and the calculated spectra with an asterisk have also been reproduced in the figures. All values are in cps.

Temp.	E_4^b	E_5^b	$\nu_1 - \nu_2$	$w_{1,2}$
152°K	Exp.		16.3 ± .4	26 ± 1
	7.8	9.9	15½	30.2
	7.9	9.9	16½	27.6
	8.0	9.9	16½	25.2

Temp.	E_4^b	E_5^b	$\nu_3-\nu_4$	$\nu_4-\nu_5$	$\nu_5-\nu_6$	$w_{3,4}$	$w_{5,6}$
162	Exp.		15.9 ± .3	50.1 ± .6	17.5 ± .2	28.4 ±1.4	30.5 ± .8
	7.7	9.9	14	53	16	33½	35
	7.8	9.9	16	53	17½	29½	31½
	7.9	9.9	16	53½	18	27½	29
163	Exp.		11.1 ±1.0	47.9 ± .6	14.7 ± .6	38.5 ±2.0	39.6 ±2.0
	7.6	9.9*	12	51½	14½	41½	43½
	7.65	9.9	13½	52½	15½	38	39½
	7.7	9.9*	14	53	16	35½	36

Temp.	E_4^b	E_5^b	$\nu_4-\nu_5$	$w_{4,5}$
167°K	Exp.		54 ± 2	95 ± 2
	7.6	9.9*	47	95½
	7.7	9.9*	57	102½
168	Exp.		38 ± 3	91 ± 4
	7.5	9.9	c	82½
	7.6	9.9	40	96½
	7.7	9.9	52	102
174	Exp.		c	68 ± 2½
	7.6	9.7	c	58
	7.6	9.9*	c	58
	7.7	9.9*	c	73
	7.6	10.1	c	58

Temp.	E_4^b	E_5^b	$\nu_4-\nu_5$	$w_{4,5}$	ν_{AB}^d
185°	Exp.		9 ± 2	42 ± 1	2907.7 ± 1
	7.7	9.9*	14	36½	2929
	7.8	9.8*	9	41	2929
	7.8	9.9	9	40	2929
	7.8	10.0*	10	39½	2929
	7.9	9.9*	c	44	2929
	7.9	10.0	c	43½	2929
199	Exp		c	44.4 ± .8	2908.9 ± .5
	7.7	9.7	c	43½	2935½
	7.7	9.8	c	41½	2933
	7.7	9.9	13	38½	2931½
	7.9	9.5	c	48	2942
	7.9	9.7*	c	44½	2935½
	7.9	9.8	c	43	2933
	7.9	9.9*	11	40½	2931½
	8.1	9.7	c	47	2935½
210	Exp		c	49.0 ± 1.5	2924.5 ± 1.2
	7.7	9.8*	c	45½	2951
	7.7	9.9	c	47	2947½
	7.7	10.0*	c	47	2943½
	7.7	10.1	c	45½	2940
	7.9	9.9	c	47	2947½
216	Exp		c	39.4 ± 1.2	2932.9 ± .6
	7.7	9.8	14	38.8	2957½
	7.7	9.9	10[e]	41½	2956
	7.7	10.0	c	44½	2953

Temp.	E_4^b	E_5^b	$\nu_4-\nu_5$	$w_{4,5}$	ν_{AB}^d
219°K	Exp.		11.6 ± .5	39.7 ± .7	2934.3 ± .6
	7.7	9.9*	$14\frac{1}{2}$	38	2960
	7.7	10.0*	$11\frac{1}{2}$	$41\frac{1}{2}$	2957
	7.7	10.1	c	44	2955
237	Exp.		16.7 ± .9	9.5 ± .7	2934.6 ± .3
	7.7	10.0	$17\frac{1}{2}$	7.7	2965
	7.7	10.1	$17\frac{1}{2}$	9.6	2965

[a]Spectra were calculated using Eqs. (40-42) in the ABX approximation and Eq. (72) with the computer program described in appendices B and C. The natural line width, in the absence of exchange, used in the calculations was 2.9 cps (152°K), 3.0 (162), 2.6 (163), 3.2 (167), 2.8 (168), 2.5 (174, 185), 2.8 (199), 2.3 (210), 2.0 (216), 2.2 (219), and 1.8 (237).

[b]E_4 is the barrier between rotamers I and II, E_5 between II and III, in kcal/mole.

[c]lines coalesced.

[d]ν_{AB} is the chemical shift of the AB line(s) from the solvent. Below 185° the calculated values are all 2929 cps, the experimental values are 2920.5 (162°K), 2918.6 (163°), 2918.2 (167°), 2916.0 (168°), and 2908.1 (174°), all ± 1.0 cps. The chemical shifts corrected for the temperature dependent intermolecular solvent interaction (see text) are 2929 (185°), $2932\frac{1}{2}$ (199°), 2950 (210°), $2962\frac{1}{2}$ (219°), and 2965 cps (237°).

[e]The spectrum is similar to the one with E_5 = 10.0 at 219° in which the peaks are almost coalesced (Fig. 29).

TABLE VIII

Calculated and observed frequency separations and line widths for the X region of CF_2Br-$CFBr_2$ in CF_2Cl_2.[a] Only the triplet, peaks 11-13 in Fig. A2, was studied. $w^{\frac{1}{4}}$ is the width at $\frac{1}{4}$ height of peak 12, and $w^{\frac{1}{2}}$ is the width at $\frac{1}{2}$ height. The latter, as seen from the spectra reproduced in Figs. 18, 23, 24, 27 and 28, usually includes part of peaks 11 and 13. The calculated spectra denoted with an asterisk have been reproduced in the figures.

Temp.	E_5	$\nu_{11}-\nu_{12}$	$\nu_{12}-\nu_{13}$	$w^{\frac{1}{4}}$	$w^{\frac{1}{2}}$
188°K	Exp.	17.0 ± .4	16.8 ± .5	-	8.7 ± .6
	9.7	17	17½		9½
	9.8	17½	17½		7½
	9.9	17½	17½		6½
193	Exp.	15.8 ± .9	15.7 ± 1.1	9.5 ± .9	-
	9.6	15½	15½	12	
	9.7	16½	16	9½	
	9.8	17	16½	7½	
196	Exp.	14.5 ± 1.0	15.7 ± 2.0	12.0 ± .8	39.3 ± 1.3
	9.7*	c	15	13½	41½
	9.75	15½	15½	12	41
	9.8*	15½	16½	10	40
199	Exp.	c	c	17.2 ± 1.0	42.4 ± .8
	9.7*	c	c	18½	43½
	9.8*	c	c	16	43
210	Exp.	c	c	22. ± 3.5	44.3 ± 1.5
	9.9*	c	c	16	43
	10.0*	c	c	19½	45
	10.1*	c	c	23	45
217	Exp.	16.8 ± .6	15.6 ± .8	9.4 ± .8	-
	9.8*	17	17	6½	
	9.9*	17	17	8	
	10.0*	17	15	10	

Temp.	E_5	$\nu_{11}-\nu_{12}$	$\nu_{12}-\nu_{13}$	$w^{\frac{1}{4}}$	$w^{\frac{1}{2}}$
238°K	Exp.	17.4 ± .3	17.2 ± .4	-	4.4 ± .2
	9.8	$17\frac{1}{2}$	$17\frac{1}{2}$		$3\frac{1}{2}$
	9.9	$17\frac{1}{2}$	$17\frac{1}{2}$		$4\frac{1}{2}$

[a] See footnote a, Table VII. Line widths used for spectra in this table are 1.8 cps (188°K), 2.0 (193), 1.9 (196), 2.1 (199), 3.2 (210), 2.2 (217), and 2.0 (238).

the solvent, until about 185°K. At this point the AB octet begins to coalesce with the much weaker doublet of rotamer III, and only an averaged AB spectrum is observed of all three rotamers at a weighted intermediate frequency. As the temperature rises, the population of rotamer III increases, which would shift the lines upfield. However, the downfield chemical shift of the individual rotamers with temperature causes an approximately equal and opposite effect, so that the frequency of the doublet is essentially unchanged from 219° to 237°.

The center of the AB region at 237° is observed 2937.6 cps upfield from the solvent, whereas the chemical shift is calculated to be 2965.0 cps. from the low temperature data, a discrepancy of 30.4 cps. At 185° the discrepancy between the observed and calculated value for the location of the AB octet is 21.5 cps, and at 152° the difference is about zero. Either a nonlinear temperature dependence or a substantially different temperature dependence for the chemical shifts of the two different rotamers appears necessary to explain these three points. Nevertheless, assuming the difference is linear between 185° and 237°, then the corrected values of the chemical shifts are within experimental error of the calculated values (see footnote d of Table VII.).

In Fig. 18 it is seen that peaks 1-2 and 7-8 of the AB octet are already significantly broader than peaks 3-6 at 152°K. As the temperature is increased further these peaks can no longer be distinguished from the noise, and only the central AB quartet was studied. At 163° this is about to coalesce into two peaks (Fig. 19). It is impossible to reproduce the peak 4 to peak 5 splitting at 163°, which may be due to a difference in the intermolecular solvent effect which changes the chemical shift of nucleus A as a function of temperature more than it affects nucleus B.

The results at low temperatures are insufficient to calculate the effect on A and B individually.

The entire spectrum at 167°K is reproduced in Fig. 20. All of the peaks are sharp except those due to the AB octet of rotamers I and II. In comparing the experimental spectrum with the theoretical one, note that the signal to noise renders impossible the observation of the low intensity peaks. These are easily seen on the computer output.

At 171°K the doublet was observed to coalesce, which is calculated to occur at E_4 = 7.7 kcal/mole. At 174° the spectrum (Fig. 21) is still independent of E_5, but at 185° (Fig. 22) changes in E_5 change the width slightly. This is clearly seen from Table VII.

As the temperature is increased further, the triplet (peaks 11-13) begins to coalesce. From Figs. 23 and 24 this is seen to occur between 196° and 199°. At 199° (Fig. 25) the spectrum of the AB region depends on both E_4 and E_5, and the choice of the barrier is not accurate. At 210° (Fig. 26 and 27) the spectrum is no longer dependent on E_4, as the I - II interchange is then occurring very rapidly. The spectrum of the AB region depends only on E_5. The width of the peak is at a maximum at 210°, and splits into a doublet again between 216° and 219° (Figs. 18 and 29). The spectra of the X region as it splits into a triplet again are in Figs. 18 and 28.

The best value of the barrier at each temperature is tabulated in Table IX. The mean values are E_4 = 7.7 kcal/mole and E_5 = 9.9 kcal/mole. Within experimental error in the temperature, the barriers are constant over the fifty degree temperature range in which they can be measured.

The above data show that the theory is able to quantitatively calculate ABX spectra as a function of the rate of exchange. The results are very sensitive to slight changes in the temperature or free energies.

TABLE IX. Best value of the barriers for $CF_2Br\text{-}CFBr_2$, in kcal/mole.

AB Region			X Region	
Temperature	E_4	E_5	Temperature	E_5
152°K	7.9		188°K	9.75
162	7.8		193	9.7
163	7.65		196	9.75
167	7.65		199	9.75
168	7.6		210	10.0
174	7.6		217	9.95
185	7.8		238	9.9
199	7.9	9.7		
210		10.0		
216		9.9		
219		10.0		
237		10.1		

The primary limitation is the determination of the temperature of the spinning sample, and these results clearly show it is worth undertaking such an improvement in the apparatus.

Preliminary results indicate the barrier E_4 with CS_2 as solvent is higher than in the CF_2Cl_2 solution. Since the change in barrier, about 0.4 kcal/mole, is just outside the experimental error, further investigation of this problem is not justified. A difficulty in obtaining accurate barriers in non-fluorinated solvents is that it is impossible to adjust for changes in the field homogeneity as the temperature is changed. However, in $CF_2Br\text{-}CFBr_2$ it is still possible to obtain E_4 accurately since the triplet peak remains sharp while the AB octet collapses, which would make this an excellent compound on which to study the effect of solvents

on barriers. In most compounds all the peaks become broad at the same temperature, and it would be necessary to employ an external standard to study the barrier quantitatively in other solvents.

D. CFClBr-CFClBr

Thompson, Newmark, and Sederholm[16] obtained the barriers in this compound using the modified Bloch equations, and method 1 (see section IIIC) for the kinetics. Since the density matrix theory can reproduce the observed doublets due to spin-spin splitting, the spectra have been recalculated. The results on CF_2Br-CCl_2Br indicated a better choice for the rates of exchange, so method 2 has been used in the recalculations. There are two isomers, each consisting of three rotamers, which are drawn in Fig. 30. The spectrum at 177° is in Fig. 31. The second and third rotamers of the first isomer are mirror images and have identical AX spectra. The fluorines in all the other rotamers are equivalent and only one line is observed for each rotamer.

The analysis of the low temperature spectra has been described in detail by Thompson et al.[16] Based on their assignment, IIa resonates at peak e in Fig. 31, IIb at peak a, and IIc at peak h. E_4' is the barrier between rotamers IIa and IIb, E_5' between IIa and IIc, and E_6' between IIb and IIc. Note that IIb has the bromines trans and is assumed to be the stable configuration. Primes have been used to distinguish the barriers in isomer II from those in isomer I. The assignment for rotamer I is unambiguous since Ib and Ic contribute equally to the doublet peaks b,c,f, and g. The remaining peak, d, is assigned to Ia. E_4 is the barrier between Ia and Ib, and is equal by symmetry to E_6, the barrier between Ia and Ic. E_5 is the barrier between the mirror image rotamers, Ib and Ic.

The exchange between the rotamers of the second isomer can be described exactly by the modified Bloch equations since no coupling is observable. The original impetus to this research was to calculate the spectrum of this molecule, including the coupling of the first isomer. The complexity of the spectrum is substantially increased by the presence of the two isomers, and the other molecules described above demonstrated the validity of the density matrix approach.

The spectra at intermediate rates of exchange have only been obtained in CS_2. Since the field homogeneity is not known, only qualitative results are reported here. There are two main differences between the barriers reported here and those determined previously. First, the kinetics of method 2 have been used, so that all the barriers are about .4 kcal/mole higher from the redefinition of the transmission coefficient (section IIIC). Second, it is possible to observe the two different barriers in the first isomer, since the doublets due to rotamers Ib and Ic were calculated.

The experimental spectrum and several calculated spectra at 194°K are shown in Fig. 32. A natural line width of 3.0 cps has been assumed for the calculations. This is reasonable since the spectra were taken after obtaining a good field at a temperature only 10° lower where the lines are sharp. The observed ratio of the heights of peaks 1 and 8 requires that E_5' and E_6' (denoted as EP5 and EP6 on the computer output) be about .8 kcal/mole greater than E_4'. Choosing either E_5' much larger, about 1 kcal/mole, than E_6', or E_6' much larger than E_5' makes peak 8 much sharper than peak 1. This effect occurs since either condition restricts the rotation of species IIc (peak h) significantly more than it affects IIa (peak a). IIa is already undergoing rapid exchange with IIb and its resonance becomes essentially independent of E_5' after E_5' becomes about

.5 kcal/mole greater than E_4'. A small difference between E_5' and E_6' is not detectable within the present experimental error, so the two barriers were set equal for the remainder of the calculations. The best width for peaks a and h is then obtained with $E_4' = 9.8$ kcal/mole and $E_5' = 10.5$ kcal/mole. Using these values, the observed width of peaks d and e is obtained with $E_4 = 10.1$ kcal/mole. Finally, the doublets are only observed if E_5 is increased substantially above E_4, to 11.0 or 12.0. Although the doublets could be observed by making E_4 and E_5 the same, about 10.4, the width of peaks d and e is much too sharp. This confirms the conclusions reached in the analysis of the CF_2Br-CCl_2Br data that the highest barrier is necessary to reproduce the observed spectra, and consequently the kinetics of method 2 must be used.

At 207°C it is possible to reproduce the experimental spectrum with $E_4' = 9.9$, $E_5' = 10.8$, $E_4 = 10.2$, and $E_5 = 12.0$ at a line width of 3.0 cps. That it is necessary to increase all the barriers approximately equally probably indicates a small error in the temperature. In Fig. 33 spectra have been calculated at 207° in which all the barriers have been changed by ±.2 kcal/mole (except for E_5) about the best values to indicate the changes which occur. The spectrum is insensitive to slight changes in E_5, so that it has been varied by 1.0 kcal/mole.

Spectra were first calculated at 233°K assuming a natural line width of 6 cps, and several calculated spectra are shown in Fig. 34, along with the experimental spectrum. It is necessary to increase E_4 to 10.6, with $E_5 = 12.0$, in order to reproduce the width of the main peak. If the three barriers in isomer one are the same, then it is necessary to increase them above 11.0. The smaller peak on the left of the spectra is from the second isomer, and if E_4' is greater than 10.0 the peak becomes much broader

and smaller than the main peak. Unfortunately, the spectra were taken in CS_2 and the field inhomogeneity may be considerable at this temperature. Spectra were calculated at the set of barriers which gave the best fit at 194°K for various values of the natural line width, and two of these are shown at the top of Fig. 34. It is seen that the observed spectrum can be reproduced if the width is about 20 cps. The magnet inhomogeneity may have been this large for these spectra.

In conclusion, the barriers for CFClBr-CFClBr are approximately those determined from the spectrum at 194°K. It would be interesting to reinvestigate the spectra of this compound in $CFCl_3$ in order to obtain reasonable results at higher temperatures. An accurate determination of the width of peaks a and h may permit the elucidation of all three barriers in the first isomer. The comparison of the barriers in this compound with those in CF_2Br-CCl_2Br will be discussed in the conclusions.

E. CF_2Br-CFBrCl

Brey and Ramey[37] first obtained the low temperature spectrum of the three rotamers of this compound. Newmark and Sederholm[21] made a detailed analysis of the low temperature spectrum as well as several time-averaged high temperature spectra in order to test the validity of Eq. (58) in section III-C. The assignment of the low temperature spectrum is discussed by Newmark and Sederholm.[21] The spectrum is shown in Fig. 30. Peaks 1-6, 10-11, and 16-18 are assigned to an ABX spectrum of rotamer I; peaks 9, 12-15, and 22-24 to rotamer III, and peaks 7-8 and 19-21 to rotamer II. The fluorines in II are nearly degenerate. The chemical shift between the fluorines in rotamer II was determined by fitting Eq. (58) to the high temperature spectra, in which this quantity was the only unknown.

The major experimental error in this calculation is the energy, E_3, of rotamer III, which introduces an uncertainty of about 11 cps in the value of $(\nu_A - \nu_B)_{II}$. Consistent results are obtained for the high temperature spectra for a range of chemical shifts and rotamer energies about the values used in the original calculation, E_3 = 746 cal/mole and $(\nu_A - \nu_B)_{II}$ = -11.0 cps.

As the temperature is increased to 154°K (Fig. 36), lines 7-8 and 19-21 of rotamer II coalesce. At 158°K (Fig. 37) all the pairs of doublets have coalesced except peaks 12-15 and 22-24, which are shown in the experimental spectrum at a higher gain. The temperature must be increased above 165°K (Fig. 39) before these peaks coalesce. To calculate this feature it is clearly necessary that rotamer III be isolated from the other two rotamers, which are interchanging fairly rapidly at 165°K. The calculated spectra will only reproduce the experimental ones if both E_5, the barrier between rotamers II and III, and E_6, the barrier between rotamers III and I, are at least 8.8 kcal/mole. Then the proper widths and appearance for the other peaks are obtained with E_4, the barrier between rotamers I and II, about 7.8 kcal/mole. The observed width of peak 11, 7 ± 2 cps at 154°K, 9 ± 2 at 158°K, and 13 ± 2 at 162°K, can be reproduced either by taking $E_5 = E_6$, or choosing one of the two barriers higher than the other. Because exchange is occurring so rapidly between rotamers I and II, the calculated spectrum depends primarily on the total rate of exchange of I and II with III. At higher temperatures peaks 11-14 have coalesced with peaks 1-10. A large number of spectra were calculated at 186° and 196° in which E_5 and E_6 were separately varied in the range 9.0 to 10.5 kcal/mole. However, the spectra calculated with E_5 not equal to E_6 could always be obtained with both barriers the same, at some intermediate value of E_5

and E_6. For example, the calculated spectrum with $E_5 = 10.0$ and $E_6 = 9.0$ differs negligibly from the one with $E_5 = E_6 = 9.1$ at 186°K. Consequently, in the discussion which follows all spectra were calculated with E_5 equal to E_6.

The observed width of peak 11 is obtained with $E_5 = 9.0$ at 154°K, 9.1 at 158°K, and 9.2 kcal/mole at 162°K. This large variation is partially due to varying degrees of saturation of the peaks, which was necessary in order to observe them. Saturation introduces additional broadening of the peaks, so that the true widths should be narrower, and the actual energy slightly higher. The form of the rest of the spectrum is accurately reproduced with $E_4 = 7.8$ kcal/mole at these three temperatures (Figs. 37-39). In particular, at 158°, the width of peaks 5-6 is calculated to be $38\frac{1}{2}$ cps for $E_4 = 7.7$, and 33 cps for $E_4 = 7.8$. The experimental value is 34 ± 2 cps. At 162° the results for the width are 45 cps (7.7), 55 cps (7.8), and 51 ± 4 cps (experimental). The frequency separations are unchanged, within experimental error, from those observed at 150°K. Note that decreasing E_5 to 9.0 in Fig. 38 makes peaks 11-15 much broader.

The spectrum at 165°K (Fig. 39) is reproduced best with $E_4 = 7.9$ and $E_5 = 9.2$. Peaks 12-15 are clearly not coalesced; their width was impossible to obtain because of the low signal/noise. Increasing the temperature to 171°K (Fig. 40) coalesces peaks 11 and 12, and 13 and 14. The frequency separation between peaks 3-4 and 5-6 (the latter is the large peak at 400 cps on the scale in the figure) has decreased at this temperature to 119 ± 4 cps, and this difference continues to decrease as the temperature is raised until it is only 21.7 cps at 321°K. At most intermediate temperatures it is a sensitive function of the barrier. For example, it is 102 cps for $E_4 = 7.8$ and 116 cps for $E_4 = 7.9$ at 171°. The observed

width, 61 cps for peaks 5-6, is somewhat larger than that calculated (47 cps for the 7.9 barrier). The splitting of peaks 16-18 into a triplet occurs at $E_4 = 7.8$, $E_5 = 9.2$ or $E_4 = 7.9$, $E_5 = 9.4$. This shows exchange between rotamers I and II is occurring so rapidly that the fluorines are averaged. The triplet is still observed at 175° (Fig. 41), but is coalesced again at 186° (Fig. 42) as the exchange with rotamer III becomes effective. The spectrum at 175° is approximately reproduced with $E_4 = 7.9$ and $E_5 = 9.4$. Increasing E_4 coalesces the triplet peaks, and decreasing it makes the other peaks too sharp.

At 186°K (Fig. 42) the experimental frequency difference between peaks 3-4 and 5-6 is 60 ± 4 cps, and the width of peak 5-6 is 43 ± 2 cps. The calculated spectrum with $E_4 = 8.1$ and $E_5 = 9.0$ gives 64 and 46 cps, respectively. If E_4 is between 7.6 and 8.0, then the frequency separation is 68 cps and the 400 cps peak is much sharper. The considerable discrepancy between the energies required to calculate the spectra at 186° compared to the other temperatures may be due to an abnormally large error in the temperature calibration.

An alternative explanation is the error in the energy of the third rotamer, which directly affects the chemical shifts of rotamer II used in the calculation. At 186° the exchange between I and II is rapid, so that the calculated chemical shifts are independent of E_4 if it is less than 8.1. Exchange with III is sufficiently slow that the effect of E_5 and E_6 is slight. If E_3 were 50 cal/mole higher, the calculated chemical shifts would be about 5 cps smaller at 186°K. At other temperatures a small adjustment in the barriers, about .1 kcal, changes the calculated chemical shifts sufficiently that an error in E_3 would be unnoticed.

At 196° and above, exchange between rotamers I and II is so rapid

that the spectrum depends only on the value of E_5. The choice of $E_5 = 9.2$ gives the best fit to the experimental spectrum (Fig. 43), in which the experimental and calculated chemical shift between peaks 3-4 and 5-6 are both 54 cps. However the width at half height of the large peak is calculated to be only 40 cps, whereas the experimental value is 48 ± 4 cps. The width for the peak at 950 cps is calculated to be 47, and the experimental result is 52 ± 4 cps. Changing the barriers does not make the peaks significantly broader, but does change the chemical shift by about 5 cps for each .1 kcal, so that the discrepancy between the observed and calculated width may again be due to a slight saturation of the peaks.

At 205° (Fig. 44) the barrier E_5 is about 9.3 kcal. The AB part of the spectrum (from 200 to 600 cps) is becoming the usual octet of peaks for an ABX spectrum, and the X part of the spectrum sharpens into a triplet. The peak at 430 cps (on the scale in the figure) is due to the A fluorine in the notation used by Newmark and Sederholm.[21] Referring to Table I of their paper, ν_A in the three rotamers at 150°K is 3438.8, 3474.5, and 3639.9 cps upfield from the solvent, respectively, whereas the chemical shifts for ν_B are 3194.2, 3485.4 and 3859.2 cps. Thus the A fluorine resonates in three environments whose chemical shifts differ by only 200 cps, and should produce a much sharper signal than the B fluorine, in which the chemical exchange must be sufficient to average over three environments whose frequencies differ by 650 cps. The exchange rate must be three times faster for the B fluorine in order to make its peaks as sharp as those for the A fluorine. The splitting of the A peaks due to coupling with the F_X nucleus can also be observed at a lower temperature. This qualitatively explains the appearance of the spectra above 180°.

At 220° (Fig. 45) the choice of E_5 = 9.5 kcal/mole gives the best fit to the spectrum, reproducing the width of peak 5 (11. ± 1. cps) and the peak 4-5 frequency difference of 26 cps. Increasing E_5 to 9.6 coalesces peaks 3 and 4. At 231° (Fig. 46) a barrier of 9.4 or 9.5 reproduces the observed spectrum within experimental error.

In conclusion, it has been possible to determine only the lowest barrier to internal rotation in CF_2Br-CFBrCl, as 7.9 ± .1 kcal/mole. The experimental spectra can be reproduced choosing the two higher barriers equal to 9.3 ± .2 kcal/mole. However, since the spectrum is only a function of the total rate of exchange with the third rotamer, it is impossible to determine the two other barriers separately. If the two higher barriers are different, a lower limit of 8.8 kcal/mole can be set on one of them.

The three rotamers are drawn in Fig. 47. From steric considerations, rotamer I is assigned to drawing A, II to B, and III to C. Although the calculations are independent of this assignment, it can be used to determine the form of the activated complex for the three possible rotations. When the substituted methyl group, CFClBr, on A rotates 120 degrees to form rotamer B, it is necessary that the chlorine move pass the fluorine, the bromine pass the second fluorine, and the fluorine pass the bromine. In the transition state these three pairs of atoms are presumably eclipsed. The results on CF_2Br-$CFBr_2$ and CF_2Br-CCl_2Br, in which the assignment of the rotamers is unambiguous, indicate that if two large halogens, such as a bromine and chlorine or two bromines, are eclipsed, then the barriers are much larger. This evidence is reviewed in detail in the next section. In CF_2Br-CFBrCl it is seen that the AC and BC exchange requires eclipsing two large halogens. The assignment made above is then completely consistent with the barrier determination, since E_4, the lowest barrier, is

between rotamers I and II, or A and B.

F. CF_2Br-CHBrCl

CF_2Br-CHBrCl was studied as an approximately 25% by volume solution in CF_2Cl_2. The low temperature fluorine spectrum of this molecule is shown in Fig. 48, and the frequencies and relative areas of the peaks are tabulated in Table X. The spectrum should consist of the superposition of three AB quartets, one for each rotamer. In analogy to CF_2Br-CFBrCl, the AB coupling constant should be about 165 cps. The spectrum is substantially different from that of CF_2Br-CFBrCl, and the assignment was finally made by a careful consideration of the relative areas of the peaks. Note in Table X that the area of peak 1, A_1, is the same as the total area of the doublet peaks 6 and 7, $A_{6,7}$. Similarly, $A_2 = A_{10,11}$, $A_3 = A_{8,9}$, and $A_4 = A_{12,13}$. These considerations lead to the following assignment for the three rotamers. Peaks 1, 2,6,7,10, and 11 for the two AB quartets of rotamer I, and peaks 3,4,8,9,12, and 13 for the AB quartets of rotamer III. The remaining peak, number 5, is from rotamer II. As in CF_2Br-CFBrCl, the two fluorines are nearly degenerate in one rotamer. Peaks 1 through 4 should be doublets, but no splitting was ever observed on these peaks, indicating that several of the HF coupling constants are almost zero. Peak 5 was obtained as a quartet on two occasions, and the four peaks are tabulated in Table X as 5a through 5d. The 146°K proton spectrum consists of two broad, overlapping peaks.

The spectra of the three rotamers were analyzed as ABX spectra to obtain the chemical shifts listed in Table XI. Although all the H-C-C-F coupling constants reported have the same sign, the results have only been obtained in substituted ethanes at room temperature, and on one substituted ethylene. The data presented here suggest the coupling constants

TABLE X. Frequency and relative intensity of the peaks in the fluorine spectrum of CF_2Br-CHBrCl at 123°K. Chemical shifts are from the solvent, CF_2Cl_2.

Peak	Frequency (cps)	Relative Intensity (%)
1	2181.8	10.6
2	2342.6	14.2
3	2381.0	4.2
4	2540.1	5.3
5a	2602.2	26.6
5b	2604.6	
5c	2607.5	
5d	2610.3	
6	3215.2	15.8
7	3234.1	
8	3293.0	6.7
9	3311.5	
10	3375.5	11.3
11	3394.4	
12	3452.3	5.2
13	3469.0	

observed for the substituted ethanes are the superposition of large values for some rotamers and small ones in the others. In particular, the small coupling constants may have the opposite sign of the large ones. In the analysis of the spectrum for rotamer II it has been assumed that both coupling constants are positive. The coupling constants in rotamers I and III were taken directly from the observed splittings. As a check on the assignment, the intensity of the peaks in each rotamer can be calculated from the chemical shifts and coupling constants. The intensity of peak 1 (or 10 and 11) should be 75% of that of peak 2 (or 8 and 9), and peak 3 (or 12 and 13) should be 70% of peak 4 (or 8 and 9). The data in Table X are within experimental error of these values.

The spectrum has been analyzed at 229°K and 303°K, where averaged chemical shifts and coupling constants are observed. These are also listed in Table XI. The proton spectrum at room temperature at 60 Mc. consists of four peaks of equal intensity. Using Pople's notation for an ABX system,[19] $2(D_+ - D_-) = 1.9$ cps and $J_{AX} + J_{BX} = 14.1$ cps. This agrees with the results obtained from the fluorine spectrum. The intensity of the two peaks comprising each doublet in the room temperature fluorine spectrum are the same. The fluorine spectrum is exactly analogous to peaks 1-8 in Fig. 18 for the AB peaks of rotamer I of $CF_2Br\text{-}CFBr_2$. Consequently the two HF coupling constants must have the same sign at 303°K. From the qualitative application of Eq. (58) for the averaged coupling constants it then follows that the two large coupling constants in rotamers I and III have the same sign. The energies of the rotamers were obtained from the average of several integral spectra. The results are $E_2 = 167 \pm 13$ cal/mole and $E_3 = 248 \pm 20$ cal/mole.

TABLE XI. Chemical shifts and coupling constants for the three rotamers of CF_2Br-CHBrCl at 146°K, and of the averaged spectrum at 229°K and 303°K. All values are in cycles per second.

	J_{AB}	J_{AX}	J_{BX}	ν_A[a]	ν_B[a]	$\nu_B-\nu_A$[a]
I	160.8 ± .5	< 2.	18.9 ± .3	2268.4	3298.8	1030.4
II	-	1.8 ± .4	3.4 ± .4	2584.3	2628.2	42.9
III	159.0 ± .7	18.5 ± 1.0	< 2.	3374.8	2467.4	-907.4
229°K	161.6 ± .4	5.2 ± .3	8.9 ± .3	2630.8	2862.5	231.7
303°K	162.2 ± .4	5.65 ± .2	8.6 ± .2	2631.3	2819.1	187.8

[a]The root-mean-square deviation in the chemical shifts is 2.0 for rotamers I and III, 5.0 for II, 0.7 at 229°K, and 0.5 at 303°.

TABLE XII. Calculated chemical shifts and coupling constants at high temperatures using weighted averages of the low temperature data for CF_2Br-CHBrCl.

	$\nu_B-\nu_A$	J_{AX}	J_{BX}	ν_A
229°K	233.7	5.3	9.3	2647.6
303°	187.6	5.7	8.8	2672.1

The averaged coupling constants and chemical shifts at high temperatures have been calculated with Eq. (58). The unobserved coupling constants were assumed to be zero. The results are in Table XII. The calculated coupling constants are larger than the observed ones (in Table XI) by approximately the same amount as the results obtained in CF_2Br-CFBrCl.[21] The discrepancy would be larger if some finite values were assumed for the near-zero coupling constants. In any case, the trend of the two coupling constants is quantitatively reproduced. The calculated value of the chemical shift between the two fluorines on the same carbon is within experimental error of the observed values. The observed discrepancies between the calculated and observed shift from the solvent peak are the usual order of magnitude. These results substantiate the conclusions drawn from the CF_2Br-CFBrCl data and reviewed in section III-B concerning the validity of Eq. (58) for the chemical shifts.

The spectra at intermediate rates of exchange are shown in Figs. 49 to 51. The situation is analogous to the experimental results of CF_2Br-CFBrCl — the peaks of one rotamer, in this case rotamer II, are not broadened by exchange whereas the other two rotamers are undergoing rapid exchange. Barriers E_4 and E_5 must be at least 7.8 kcal/mole to calculate the experimental spectrum with a sharp peak 5. The choice of E_6 = 6.9 kcal/mole (Fig. 49) gives the observed width, 70 ± 10 cps, for peak 2 in the figure (the peaks are numbered according to Fig. 48). The calculated width for E_6 = 6.8 is 95 cps, and 40 cps if E_6 = 7.0 kcal/mole.

Spectra were calculated with E_4 equal to E_5 since the previous results on CF_2Br-CFBrCl showed that the spectra will only depend on the total rate of exchange of II with III or I.

The choice of $E_4 = E_5 = 8.2$ kcal/mole at 147°K reproduces the observed width of the sharp peak, $13\frac{1}{2}$ cps. Changing E_4 by .1 kcal changes the width by less than a cycle at this low temperature.

When the temperature is increased to 156° the small peaks become extremely broad, and it was impossible to determine their width. $E_4 = 8.1$ reproduces the width of the main peak, 26±2 cps, E_6 between 6.7 and 6.9 reproduces the general appearance of the spectrum for this value of E_4. At 168° (Fig. 50) another peak 385±20 cps upfield from the main peak is observed. $E_4 = 8.0$ reproduces the width of the large peak, 165±20 cps, and the observed chemical shift. Changing E_6 has a small effect on the width.

At 190°K (Fig. 51) the AB part of an ABX spectrum is observed, in which the downfield pair of peaks are much sharper than the upfield pair. This appearance is explained in exactly the same manner as the CF_2Br-CFBrCl spectra above 205°. The observed spectrum is reproduced with $E_4 = 8.2$, $E_6 = 6.9$, or $E_4 = 8.1$, $E_6 = 7.0$. Both barriers have a noticeable effect on the spectrum. E_6 is still important at this relatively high temperature because of the large chemical shift between rotamers I and III.

At 210° (Fig. 50) the experimental spectrum can be reproduced for values of E_4 about 8.2 and E_6 about 6.9. The changes in the widths upon small variations of these parameters is insufficient to choose an exact value of the barrier at this temperature.

In conclusion, the lower barrier in CF_2Br-CHBrCl is 6.9±.2 kcal/mole, and the higher barriers are at least 7.8 kcal/mole. The experimental spectra can be reproduced by choosing the higher barriers the same, and equal to 8.2 kcal/mole.

If steric hindrance of the bromines determines the relative stability

of the rotamers, then drawing A of Fig. 1 is assigned as rotamer I, B as II, and C as III. In this case no simple explanation for the variation of the HF coupling constants is possible. However, only drawings A and B have the proton trans to a fluorine, and the probable explanation for the observed spectrum is that the gauche HF coupling constant is small and the trans one large. Then drawing A is assigned to rotamer I, C to II, and B to III. F_A is a doublet in rotamer I, and F_B a doublet in rotamer III, and the chemical shift relationships in Table XI are satisfied.

The barriers to internal rotation show unequivocably that the barrier between rotamers I and III is over 1 kcal/mole less than the other two barriers. From the steric consideration discussed in section V-E on CF_2Br-CFBrCl, the activated complex for the lowest barrier should have the fluorines and the proton each eclipsing a larger halogen. Therefore the lowest barrier occurs between the rotamers represented by drawings A and B in Fig. 1. Rotamer C must be assigned to peak 5, or rotamer II. This shows that the second assignment of rotamers to the drawings is correct, and presumably that the trans HF coupling constants are substantially larger than the gauche ones. Since the coupling is transmitted through the bonds, it is unlikely that it should have extreme fluctuations with small changes in dihedral angle.

This interpretation of the coupling constant is supported by other evidence. Abragam and Bernstein[38] have studied the temperature dependence of J_{HF} in $CFCl_2$-$CHCl_2$. Although they were unable to reach a low enough temperature to freeze out the rotamers, the results could be explained by fitting the observed averaged coupling constant using Eq. (58) above, with $E_2 = E_3 = 400$ cal/mole, $J_{trans} = 18.08$ cps, and $J_{gauche} = 1.03$ cps. Although it has been shown that this method of analysis is not quantitative,

it should be qualitatively correct.[21,39]

Fessenden and Waugh,[40] from a similar study of $CHCl_2$-CF_2Cl, find two sets of solutions to Eq. (58) for the two rotational isomers in this compound. The solution in which the more stable rotamer has all the chlorines gauche to one another (similar to drawing C in Fig. 1) gives $J_{trans} = 10$ and $J_{gauche} = 5$ cps. The results on CF_2Br-CHBrCl studied here indicate this assignment of the relative stability of the rotamers is likely to be correct.

The relative stability of the rotamers may be explained by a consideration of the dipole moment of the C-H bond and C-halogen bonds.

The C-H dipole is much less than the C-halogen dipole, so that the dipole moment perpendicular to the C-C axis in rotamer C may be less than in rotamer B. This effect could be studied by determining the relative energies of the three rotamers of CF_2Br-CHBrCl in solvents of different dielectric strength.

VI. CONCLUSIONS

The experimental results on $CF_2Br-CCl_2Br$ and $CF_2Br-CFBr_2$ have been presented in considerable detail to show that the modification of the theory of exchange developed in section II can accurately reproduce experimental spectra. For the more complex molecules studied it was impossible to obtain the free energies of activation between all three rotamers. However, the theory is still capable of reproducing the observed spectra within experimental error in the parameters used in the calculation. The results for the chemical shifts and free energies of activation for the molecules studied follows.

A. Chemical Shifts

The chemical shifts between two fluorine atoms on the same carbon varies by more than 15 ppm in the molecules discussed. Although this seems rather large, similar differences are obtained for methylene fluorines in cyclic compounds.[41] The results on $CF_2Br-CFBrCl$ and $CF_2Br-CHBrCl$ indicate that the smaller values usually observed in molecules undergoing free rotation result from an averaging of larger values of different signs in the various configurations.

That the spectrum of the three rotamers of $CF_2Br-CHBrCl$ is very different from the one of $CF_2Br-CFBrCl$ shows that substitution of a proton for a fluorine has a large effect on the electron distribution of the molecule. This is certainly reasonable in view of the change in magnitude of the dipole moment for the C-F compared to the C-H bond.

No correlation between the substituents gauche to the AB fluorines and their relative chemical shift has been noticed. Thus, in isomer I of $CF_2Br-CFBr_2$ (Fig. 17), one of the fluorines is gauche to a fluorine

and bromine, and the other gauche to two bromines. The two equivalent fluorines in isomer III are gauche to a fluorine and a bromine, yet their resonance is several hundred cycles upfield from the resonance of I. Similar results are true for the other compounds. The distortion of the molecule from tetrahedral symmetry, due to the large bromine substituents, may be the main source of changes in the chemical shift between rotamers. In all the molecules studied the resonance of the fluorines in the high energy form are at higher magnetic field. The high energy form probably has the bromines gauche, and consequently the greatest distortion. This is definitely the case in CF_2Br-CCl_2Br and CF_2Br-$CFBr_2$ where the two isomers have different spectra. In the other molecules it is impossible to assign the rotamers to the spectrum from such considerations because each rotamer has an ABX spectrum. However, in analogy to the first two molecules, and other halogenated ethanes which have been studied by different techniques,[42] the highest energy form probably has the largest substituents gauche to each other. This is reasonable from steric and dipole moment considerations for the perhalogenated ethanes. This assignment was made in CFClBr-CFClBr and CF_2Br-CFBrCl in order to correlate the barriers in the next section. The assignment of CF_2Br-CHBrCl was discussed in section V-F. Apparently this molecule is an exception to the usual rule that the high energy form has the large halogens gauche to each other.

In CF_2Br-$CFBr_2$ and CF_2Br-CFBrCl there is some consistency in the resonance of the single upfield fluorine (F_X). In the two rotamers (III of CF_2Br-$CFBr_2$ in Fig. 17 and C of CF_2Br-CFBrCl in Fig. 47) where this fluorine is gauche to the two other fluorines it is several hundred cycles upfield from the resonance when the fluorine is gauche to a fluorine and a bromine or chlorine.

B. Barriers

The free energies of activation, termed for simplicity the barriers, of the halogenated ethanes which have been determined in this work are listed in Table 13. The free energies are measured from the potential minimum of the most stable rotamer. The barriers of four additional perhalogenated ethanes determined from infrared and electron diffraction measurements have also been listed for comparison. Presumably the large barriers for the ethanes with bulky substituents like chlorine or bromine are steric in origin, and one would anticipate a correlation between the size of the substituent and the barrier. To show this correlation, the pairs of atoms which are eclipsed in the activated complex when the rotation occurs are also indicated in the Table.

Comparing the results in the compounds with two fluorines to those with three fluorines, it is clear that adding a bulky chlorine or bromine significantly increases the barrier.

The geometry of the molecule substantially affects the magnitude of the barriers. Thus, E_4 in CF_2Br-CCl_2Br has exactly the same pairs of atoms eclipsed in the activated complex as E_4 in CFClBr-CFClBr, yet the two barriers differ by .7 kcal./mole. There is a similar lack of agreement between E_5 of the former molecule and E_5' of the latter, although the experimental error is greater in this case. Although the CFClBr-CFClBr measurements were performed in CS_2 solution while the CF_2Br-CCl_2Br measurements were made in $CFCl_3$, sufficient measurements of the latter compound in CS_2 showed that the lower barrier did not change with solvent. The higher barriers in CF_2Br-CCl_2Br may be explained by observing that one of the carbons has three bulky substituents in this isomer. Distorting the bond angles from tetrahedral symmetry to move

TABLE XIII

The pairs of atoms which are eclipsed in a rotation, and the associated free energy of activation, in kcal/mole.

Molecule	Barrier	Eclipsed Pairs
CF_2Br-CCl_2Br	$E_4 = 10.8 \pm .1$	Br-Cl, Br-F, Cl-F.
	$E_5 = 12.0 \pm .5$	Br-Br, 2 Cl-F.
$CFCl_2$-$CFCl_2$	$E = 9.65 \pm .1$	Cl-Cl, 2 Cl-F.
CFClBr-CFClBr	$E_4 = 10.1 \pm .2$	Br-Cl, Br-F, Cl-F.
	$E_5 = 12.0 \pm 1.5$	Br-Br, Cl-Cl, F-F.
	$E_4' = 9.9 \pm .2$	2 Br-F, Cl-Cl.
	$E_5' = 10.6 \pm .3$	Br-Br, 2 Cl-F.
	$E_6' = 10.6 \pm .3$	2 Br-Cl, F-F.
CF_2Br-$CFBr_2$	$E_4 = 7.7 \pm .2$	3 Br-F.
	$E_5 = 9.9 \pm .2$	Br-Br, Br-F, F-F.
CF_2Br-CFBrCl	$E_4 = 7.9 \pm .1$	2 Br-F, Cl-F.
	$E_5 = 9.3$[a]	Br-Br, Cl-F, F-F.
	$E_6 = 9.3$[a]	Br-Cl, Br-F, F-F.
CF_2Br-CHBrCl	$E_4 = 8.1$[b]	Br-Cl, Br-F, F-H.
	$E_5 = 8.1$[b]	Br-Br, Cl-F, F-H.
	$E_6 = 6.9 \pm .2$	Br-F, Br-H, Cl-F.
CF_3-CF_3[c]	$E = 4.35$	3 F-F.
CF_3-CF_2Cl[d]	$E = 5.67$	Cl-F, 2 F-F.
CF_3-CF_2Br[d]	$E = 6.4$	Br-F, 2 F-F.
CCl_3-CCl_3[e]	$E = 10.8 \pm .3$	3 Cl-Cl.

[a] The lower limit to this barrier is 8.8.

[b] The lower limit to this barrier is 7.8.

[c] Reference 12.

[d] Reference 15.

[e] Reference 13.

the bromines further apart in the eclipsed state is then rendered more difficult.

It is reasonable that the barrier will be the sum of three terms, corresponding to the three pairs of eclipsed atoms in the activated complex. Let E(Br-F) denote the contribution to the total barrier of a bromine atom and a fluorine atom which are eclipsed. It is possible to obtain barrier contributions from each pairwise interaction, although the conclusions already drawn show these may have little significance. It is nevertheless interesting to obtain an independent result from the other molecules studied. From the CF_3-CF_3 and CF_3-CF_2Br results, E(F-F)= 1.45 kcal./mole, and E(F-Br) = 3.50 kcal./mole. However, E(F-Br) = 2.75 kcal./mole is calculated from E_4 of CF_2Br-$CFBr_2$, 25% lower than 3.50. Further consideration of pairwise contributions to the barrier in different molecules is clearly unwarranted.

It is interesting that the two barriers in an asymmetric compound are significantly different (2.2 kcal./mole in CF_2Br-$CFBr_2$). A theory to quantitatively predict the results cannot depend linearly on the size of the substituents. Thus, E(Br-Br) + E(F-F) $\neq$ 2 E(Br-F). In Table XIV the distance from a substituent on an ethane to the plane bisecting the carbon-carbon bond is given. These values can be compared to the Van der Waals radii, also given in the Table. The bromine and chlorine Van der Waals radii extend much further than the bisecting plane. The overlap of the eclipsed atoms, corresponding to E(Br-Br), E(F-F), and E(Br-F), are 1.06, .24, and .65 Å, respectively. A linear theory would postulate that the barrier contribution is directly proportional to this overlap, and conclude that $E_4 = E_5$ in CF_2Br-$CFBr_2$. However the results prove that the barrier is proportional to some power

of the overlap distance. In fact the overlap is so great that some distortion of the carbon bonding orbitals undoubtedly occurs to reduce it in the transition state, which eliminates simple correlations of the data. In this respect, it is interesting to note that the distance between two bromines on a tetrahedral carbon atom is 3.17 Å, or .34 Å further apart than the two eclipsed bromines.

Table XIV. The distance from a halogen or proton substituted on an ethane to the plane bisecting the carbon-carbon bond, D, and its Van der Waals radius, R. All distances are in Angstroms.

Substituent	C-X distance[a]	D[b]	R[c]	D - R
H	1.095	1.13	1.2	-0.07
F	1.375	1.23	1.35	-0.12
Cl	1.78	1.36	1.80	-0.44
Br	1.94	1.42	1.95	-0.53

[a] From L. E. Sutton, "Table of Interatomic Distances and Configurations in Molecules and Ions," The Chemical Society, London, 1958.

[b] The calculation assumes tetrahedral bond angles.

[c] L. Pauling, "The Nature of the Chemical Bond," Cornell University Press, Ithaca, New York, 1960, p. 260.

The series of compounds, CF_2Br-CClBrX, X=H, F, and Cl has been studied. A significant increase, 1.0 kcal./mole, in the magnitude of the barrier occurs with substitution of a fluorine for a proton. This

substantial increase in the barrier may be a steric effect. In one case the bromine is eclipsed with a proton, in the other case with a fluorine. In addition a contributing factor to the difference may be the change in the magnitude and possibly direction of the bond dipole upon substitution of the fluorine for the proton. Changing the fluorine to a chlorine increases the barrier even more, by 3.0 kcal./mole. The significant increase in the barrier with substitution of a chlorine occurs because in CF_2Br-CCl_2Br any rotation requires that two large halogens be eclipsed.

Finally, the free energies of activation are independent of temperature, within experimental error. The results presented show the theory is sufficiently sensitive to small changes in the barriers that it should be possible to measure the temperature dependence of the barriers with experimental apparatus which provide more accurate temperature control. The error in the barrier is directly proportional to the absolute error in the temperature because of the exponential dependence of the rate laws used in this work.

ACKNOWLEDGEMENTS

I wish to express my sincere thanks to Professor Charles Sederholm for introducing me to this research. His advice on many problems and invaluable help in the construction of experimental equipment is greatly appreciated.

I have benefited immeasureably from discussions with my fellow graduate students and acknowledge their many helpful suggestions. I wish to thank Mr. Frank Papen for much advice and help with the electronics of the spectrometer.

Finally, Mrs. Linda Cantor and Mrs. Pat Cookson have helped prepare the final manuscript.

I gratefully acknowledge fellowship aid from the National Science Foundation. Financial support was also received from the United States Atomic Energy Commission through the Lawrence Radiation Laboratory.

APPENDICES

A. The Solution to the Modified Bloch Equations

Setting the time derivatives equal to zero, Eqs. (T7 to T9) reduce to three equations in three unknowns, G_A, G_B, and G_C. Only the total magnetization $G = G_A + G_B + G_C$ is desired. Since the main contribution to the transverse relaxation times in the three configurations in the absence of exchange is the magnetic field inhomogeneity, it is possible to set $T_{2A} = T_{2B} = T_{2C} = T_2$. The solution is most easily obtained as the ratio of two complex numbers using Cramer's rule (the method of determinants),

$$G = \frac{U + iV}{X + iY},$$

where U, V, X, and Y are real, and i is the square root of -1. Since most chemical shifts and half widths are given in cycles per second instead of radians per second, the units have been changed to give τ_{ij}^{-1} and T_2^{-1} in cps. Thus τ_{ij} and T_2 are in seconds/cycle, which is a factor of 2π larger than the definition for the lifetime and transverse relaxation time. Since only the inverse of τ_{ij} and T_2 are used, this should not prove confusing.

For convenience the following definitions are used in the equations for U, V, X, and Y shown below:

$$k_{ij} = \tau_{ij}^{-1} \; ; \; k_i = k_{ij} + k_{il} \quad (i, j, l \text{ all different})$$

$$T^{-1} = T_2^{-1} \; ; \quad R = k_A + k_B + k_C \; ;$$

$$Q = k_A k_B + k_A k_C + k_B k_C - k_{AB} k_{BA} - k_{AC} k_{CA} - k_{BC} k_{CB}$$

$$U = [(k_{BC} + k_C)p_B + (k_{CB} + k_B)p_C]\nu_A + [(k_{AC} + k_C)p_A + (k_{CA} + k_A)p_C]\nu_B$$

$$+ [(k_{AB} + k_B)p_A + (k_{BA} + k_A)p_B]\nu_C +$$

$$+ T^{-1} [p_A(\nu_B + \nu_C) + p_B(\nu_A + \nu_C) + p_C(\nu_A + \nu_B)]$$

$$V = -p_A\nu_B\nu_C - p_B\nu_A\nu_C - p_C\nu_A\nu_B + Q + T^{-1} R + T^{-2}$$

$$X = k_A\nu_B\nu_C + k_B\nu_A\nu_C + k_C\nu_A\nu_B + T^{-1}(\nu_A\nu_B + \nu_A\nu_C + \nu_B\nu_C - Q) - T^{-2} R - T^{-3}$$

$$Y = (k_{BA}k_C + k_{BC}k_{CA})\nu_A + (k_{CB}k_A + k_{CA}k_{AB})\nu_B + (k_{AC}k_B + k_{AB}k_{BC})\nu_C +$$

$$-\nu_A\nu_B\nu_C + T^{-1} [k_C(\nu_A + \nu_B) + k_B(\nu_A + \nu_C) + k_A(\nu_B + \nu_C)] +$$

$$+ T^{-2} (\nu_A + \nu_B + \nu_C)$$

Finally, the absorption is proportional to the imaginary component of G and is given by

$$\mathrm{Im}\ G = \frac{V\ X - U\ Y}{X^2 + Y^2} .$$

B. ABXIR Computer Program

The program calculates NMR spectra as a function of the rate of exchange between three species, each with two or three nuclei of spin $\frac{1}{2}$. If there are three nuclei, one nucleus must, to second order, be uncoupled from the other two (ABX approximation). The rate of exchange is obtained from the three barrier heights and the temperature using absolute reaction rate theory (Eq. (72)). The method used in the calculation is described in Appendix C. Input to the program consists of the chemical shifts, coupling constants, and the relative energies of the three species.

The program is written in Fortran IV and requires about 13,069 cells of memory. It is written for a fortran monitor which uses one input tape (number 2) and one output tape (number 3). It is possible to use an optional subroutine to produce California Computer Products plots; although this subroutine is included in the listing it is written for the University of California, Lawrence Radiation Laboratory, Berkeley, Computer Center and will have to be modified for most other installations.

The MAP listing for the subroutine which solves the simultaneous equations is not included. The subroutine, F4 BC SMQ4, is a modification of of F4GM SIMQ written for fortran IV by the University of California Computer Center, Berkeley.

The computer time required is about .05 seconds for each point in a spectrum.

Note that all the input to the program, and all of the rates calculated by the program, are in cycles per second. This consistency of units avoids multiplying and dividing by 2π. However the inverse of the rates is no longer the correlation time, but it is a factor of 2π larger. In subroutine TAU the rates are divided by 2π to convert from radians/sec to cycles/sec.

Input Data Cards:

The first card contains a flag to indicate the start of a new problem, -7, in columns 1 and 2. The remaining 78 columns are used for identification and are printed at the top of each spectrum.

The second card contains parameters required for the problem.

Col. Nos.	
1 - 2	KSET – Since at different temperatures it is usually desired to calculate spectra at different barrier energies, frequencies, and line widths, the cards with these parameters are separated in sets. The number of sets is KSET.
3	ICON – controls plotting in subroutine NMPLOT. If plotting occurs on the monitor tape using the PL11 version, then ICON = 2 normalizes the plot so that the largest value of the absorbance has a value of 100. If ICON = 1 or 3, then the program must read a nonzero value of YH (columns 17 -22). Points are then plotted so that an absorbance of YH has an ordinate of 100 if ICON = 1, or an ordinate of 1 if ICON = 3. If the alternative plotting routine is used to produce Cal Comp plots (PLOT7 version), then ICON = 1 writes plots and ICON = 2 skips the plotting sequence.
4	NSPIN – the number of spins, 2 or 3. If any other number the program calls EXIT and terminates.
5 - 10	E2 – energy, in cal./mole, of the second species (II) relative to an energy of zero for the first species. The format is F6.3, so that the decimal point is between columns 7 and 8. Punching the decimal point always overrides the format specification.

11 - 16 E3 – the energy of the third species. (III). Format F6. 3.

17 - 22 YH – see explanation for ICON above. Format F6. 3.

The next three cards provide the chemical shifts and coupling constants for species (or rotamers) I, II, and III, respectively. Each card has the same format, 6F10.3 (six fields, each 10 columns wide, with the decimal point 3 columns to the left of the end of each field), for the six constants ν_A, ν_B, ν_X, J_{AB}, J_{AX}, and J_{BX} (all in cycles per second) for each rotamer. It is important that the chemical shifts are ordered such that, under exchange or rotation, nucleus A of species I converts to nucleus A of species II, etc. If there are only two spins, then ν_X, J_{AX}, and J_{BX} must be zero.

A "set" of cards (described above under card 2) contains a minimum of 4 cards. The first one contains necessary control parameters for the remaining cards in the "set", describing the number of barriers and temperatures at which spectra will be calculated. The first card also contains a number of options which can reduce significantly the time required for the calculations in subroutine MASGEN, as well as print out intermediate results. The program does not utilize any option unless a nonzero number is entered for that option.

<u>Col. Nos.</u>

1 - 2 IMAX – the number of groups of 3 energy barriers. Maximum value is 15.

3 - 4 JMAX – the number of temperatures. Maximum value is 20.

5 - 6 IDELMX – the number of groups of frequencies (see below). Maximum value is 75.

7 - 10 WIDTH – the natural line width in the absence of exchange (in cps). This must be nonzero to prevent a singularity in

the calculation. Format F4.0. All of the remaining fields on this card have format F5.0, so that the decimal point, unless punched, is assumed all the way to the right of the field.

11 - 20 VV(996) and AB(996), currently unused.

21 - 25 VV(997) = ISKIPG (in subroutine MASGEN). If this is equal to integer between 1 and 7, NE, the A and A^{-1} matrices are printed for inversion number NE.

26 - 30 AB(997) -- see VV(998) comment.

31 - 35 VV(998) = ISKIPF. If one, then the program only calculates the absorption in the AB region of the spectrum when the frequency is between AB(997) and AB(998), and in the X region when the frequency is between AB(999) and AB(1000). Usually these two regions do not overlap appreciably, even including the tails of the broad peaks at intermediate rates of exchange. If VV(998) is two, then only those matrices are solved when one of the transition frequencies associated with the matrix is within AB(1000) of the frequency being calculated. The latter approximation is useful only when the rate of exchange is slow. For a two spin system VV(998) must NOT be one.

36 - 40 AB(998) -- see VV(998) comment.

41 - 45 VV(999). If this is 7 (for three spins) or 4 (for two spins), the absorption calculated from the inversion of each of the matrices is printed at each frequency. In the output with with this option, for three spins, the first column is the frequency, the second the total absorption (the sum of the remaining columns), the 3rd, 4th, and 9th are the absorption

in the X region, and the 5th through 8th are the absorption in the AB region. This option enables one to determine, for later computer runs on the same compound, the best choices for the VV(998) option. The dimension statement allows at most 100 points to be calculated with this option. In the output for two spins, the first and second columns are still the frequency and total absorption. The 3rd and 4th columns are irrelevant, and the 5th and 6th are the absorption due to inversion of the individual matrices.

46 - 50 AB(999) -- see VV(998) comment

51 - 55 VV(1000) = ISKIP. If this is equal to an integer between 1 and 7, NE, the E matrix before inversion and the column vector result are printed for inversion number NE.

56 - 60 AB(1000) -- see VV(998) comment.

Following the first card in each set are IMAX cards with three energy barriers on each card:

1 - 10 E_4, the barrier between species I and II. The format for each barrier is F10.1, but punching the decimal point always overrides the format specification.

11 - 20 E_5, the barrier between species II and III.

21 - 30 E_6, the barrier between species I and III.

Following the barrier cards are (JMAX/13) cards containing the temperatures at which spectra are to be calculated at the above values of the barriers. Each card contains 13 consecutive fields six spaces wide, format 13F6.1, for the temperatures.

Finally there must be (IDELMX + 1)/8 cards with the frequencies at which the spectra will be calculated. These cards contain a series

of frequencies – VMIN(I) – and frequency differences – DELV(I). A spectrum is calculated at frequency intervals of DELV(I) from VMIN(I) to VMIN(I+1), where I ranges from 1 to IDELMX (specified on the first card in the set). This permits varying the frequency grid and calculating more points near the maxima of peaks without having to calculate an excessive number of points in the entire spectrum. Each card contains eight pairs of VMIN and DELV – in fields five spaces wide, format 16F5.0. For example, the first card contains VMIN(1), DELV(1), VMIN(2), DELV(2), ... , VMIN(8), DELV(8). It is necessary that the VMIN(I) monatonically increase from VMIN(1) to VMIN(IDELMX + 1). The program is dimensioned so that at most 995 points can be calculated in a spectrum. Although this number could easily be increased, it is desirable to keep it reasonably small so that the program will not calculate indefinitely if an error is made in the input. A frequent mistake is to have DELV equal to zero, in which case the computer will increment VMIN(I) by zero to attain VMIN(I + 1), and only stop when it exceeds 995 points.

Additional "sets" of cards may follow the last frequency card of a set. Following the last set another card with -7 in columns 1 and 2, and a comment in the remaining columns, signifies the start of another problem. Execution may be terminated by the computer reading an End-Of-File after the last data card, or by a -7 card followed by a blank card.

A sample problem follows the listing of the fortran decks. The first page of output contains the parameters necessary for the calculation which are derived from the coupling constants and chemical shifts. The energy levels are the elements of the diagonalized Hamiltonian,

and the unitary matrices are the transformation matrices from the basic product representation of the Hamiltonian to the diagonal representation. The transition frequencies and I_x matrix elements are also listed for each rotamer. The transition amplitude is given by $(I_x)^2$. The second, and succeeding pages, contain the spectra. At the top of each spectrum the temperature, barrier, rotamer energies, and the line width in the absence of exchange are listed, as well as the calculated rotamer mole fractions and inverse correlation times for the six possible interconversions.

In the sample problem the results of inverting the 7 matrices have been printed for the first set of data using the VV(999) option.

```
$IBFTC ABXIR
C       ABXIR -- MAIN PROGRAM TO CALCULATE NMR SPECTRA FOR EXCHANGE
C       BETWEEN THREE ABX (OR AB) SPECIES.
C       SUBROUTINES REQUIRED--BCSIMQ, INPUT, MASGEN, NMPLOT, PREP, TAU
        DIMENSION RECORD (13), VMIN(76), DELV(75), TT(20), E4(15), E5(15),
       1E6(15), FA(9), AB(1000), VV(1000)
        NDIM = 1000
        COMMONFA/CALC/N,NA,NE,M,MM/ PLOT / YH,ICON /ABX/ NSPIN,NMIN,NMAX
        L=1
C       FIRST CARD OF EACH PROBLEM CONTAINS -7 IN COLUMNS 1 AND 2.
C       RECORD IS A COMMENT PRINTED AT THE TOP OF EACH SPECTRUM.
1       READ (2,905) ICODE, (RECORD(I), I=1,13)
        IF (ICODE .NE. (-7)) GO TO 1
C       E2 AND E3 ARE THE ENERGIES, IN CAL./MOLE, OF ROTAMERS 2 AND 3
C       RELATIVE TO E1=0.0 FOR ROTAMER 1.
C       ICON AND YH ARE PARAMETERS FOR SUBROUTINE NMPLOT.
C       NSPIN IS NUMBER OF SPINS, KSET NUMBER OF SETS.
        READ (2,906) KSET,ICON,NSPIN,E2,E3,YH
        IF (NSPIN .LT. 2 .OR. NSPIN .GT. 3) CALL EXIT
        WRITE (3,909) (RECORD(I),I=1,13),L
        NMIN = 7 - 2*NSPIN
        NMAX = NSPIN/3 + 2*NSPIN
C       NMIN AND NMAX CONTROL THE NUMBER OF MATRICES SOLVED BY MASGEN.
        NSPIN=NSPIN-1
        L=L+1
C       INPUT CALCULATES TRANSITION FREQUENCIES AND UNITARY MATRICES
C       FROM THE COUPLING CONSTANTS AND CHEMICAL SHIFTS WHICH IT READS.
        CALL INPUT
        DO 76 KH=1,KSET
C       WIDTH IS THE NATURAL LINE WIDTH IN THE ABSENCE OF EXCHANGE -
C       WIDTH MUST NOT BE ZERO TO AVOID SINGULARITY IN MATRIX INVERSION
C       IN SUBROUTINE MASGEN.
C       (VV(I),AB(I),I=996,1000) ARE OPTIONS USED IN SUBROUTINE MASGEN.
        READ (2,913) IMAX,JMAX,IDELMX,WIDTH, (VV(I),AB(I),I=996,1000)
        IF (IMAX .GT. 15 .OR. IMAX .LT. 1 .OR. JMAX .GT. 20 . OR.
       1JMAX .LT. 1 .OR. IDELMX .GT. 75 .OR. IDELMX .LT. 1) GO TO 1
        TTINV = 0.5*WIDTH
C       ENERGY BARRIERS ARE STORED IN E4, E5, AND E6, TEMPERATURES IN TT.
        READ (2,916) (E4(I), E5(I), E6(I), I=1,IMAX)
        READ (2,918) (TT(I), I=1,JMAX)
C       SPECTRA ARE CALCULATED AT FREQUENCY INTERVALS OF DELV(I) FROM
C       VMIN(I) TO VMIN(I+1), FOR I = 1 TO IDELMX.
        READ (2,923) (VMIN(I), DELV(I), I=1,IDELMX), VMAX
        VMIN(IDELMX+1) = VMAX
        W= VMIN(1) - DELV(1)
        I=1
        IP = 0
45      W=W+ DELV(I)
        IP = IP + 1
        IF (IP .GT. 995) GO TO 60
        VV(IP) = W
        IF(W.LT.VMIN(I+1)) GO TO 45
        IF (W.GE.VMAX) GO TO 60
        I = I+1
        W = VMIN(I)
        GO TO 45
60      DO 76 JH = 1,JMAX
        DO 76 IH = 1, IMAX
        DO 61 I=1,IP
61      AB(I) = 0.0
```

```
$IBFTC TAU
      SUBROUTINE TAU (T,E2,E3, EFOUR, EFIVE, ESIX)
C     RATES ARE IN CYCLES PER SECOND, NOT RADIANS PER SECOND.
C     FOR THREE SPECIES, A, B, AND C, SUBROUTINE TAU CALCULATES THE
C     POPULATIONS (POPA,ETC.) AND THE RATES OF EXCHANGE (FAB IS THE RATE
C     FROM A TO B, ETC.) FROM THE ENERGY MINIMA (E1=0.0, E2, E3) AND THE
C     BARRIERS (EFOUR IS THE BARRIER BETWEEN 1 AND 2, EFIVE -- 2 AND 3,
C     ESIX -- 1 AND 3).
      COMMON FAB, FAC, FBC, FBA, FCA, FCB, POPA, POPB, POPC
C     ZT = K/(H*2*PI) = BOLTZMANN CONSTANT/ PLANCK CONSTANT/ TWO PI
      ZT = 3.3164E9* T
      F2 = EXP  (E2/(1.987*T))
      F3 = EXP  ( E3/(1.987 *T))
      TM = .001987*T
      F4 = EXP(-EFOUR/TM)
      F5 = EXP(-EFIVE/TM)
      F6 = EXP(-ESIX/TM)
      FAB = F4*ZT
      FAC   = F6*ZT
      FBC   = F2*F5*ZT
      FBA   = F2*F4*ZT
      FCA   = F3*F6*ZT
      FCB   = F3*F5*ZT
      POPA   = 1.0/(1.0 + 1.0/F2 + 1.0/F3)
      POPB = POPA/F2
      POPC = POPA/F3
      RETURN
      END
```

```
C     TAU CALCULATES POPULATIONS AND CORRELATION TIMES FOR EXCHANGE.
      CALL TAU (TT(JH), E2, E3, E4(IH), E5(IH), E6(IH))
      WRITE (3,931) (RECORD(I), I=1,13), L, E2, E3, TT(JH),
     1E4(IH), E5(IH), E6(IH), (FA(I),I=7,9),WIDTH, (FA(I),I=1,6)
C     PREP SETS UP THE MATRICES NEEDED TO CALCULATE SPECTRA.
      CALL PREP (TTINV)
      L=L+1
      DO 75 I= NMIN,NMAX
      NE = I
      NA =(NE+1)/2
      N = ((((NE+5) / 4)**2 ) / 3) * 3 + 3
C     MASGEN CALCULATES THE ABSORPTION FOR ONE OF THE MATRICES, AND IS
C     CALLED 2 TIMES IF NSPIN=2, 7 TIMES IF NSPIN = 3.
C     ABSORPTION AT FREQUENCY VV(I) IS STORED IN AB(I).
      CALL MASGEN (NDIM, AB, VV, IP)
      IF (M .GT. 1 .OR. MM .GT. 1) GO TO 1
75    CONTINUE
C     NMPLOT PRINTS THE SPECTRUM.  TWO VERSIONS EXIST, ONE PLOTS ON
C     THE MONITOR OUTPUT TAPE 3, ONE WRITES CAL COMP PLOTS.
76    CALL NMPLOT (NDIM, AB, VV, IP)
      GO TO 1
905   FORMAT (I2,13A6)
906   FORMAT (I2,2I1, 3F6.3)
909   FORMAT (1H1 13A6,47X I3)
913   FORMAT (3I2,F4.0, 10F5.0)
916   FORMAT (3F10.1)
918   FORMAT (13F6.1)
923   FORMAT (16F5.0)
931   FORMAT (36H1NMR SPECTRA OF EXCHANGING NUCLEI     13A6,9X 4HPAGEI3/
     128H ROTAMER ENERGIES (CAL)  0. 2F8.1,19H    TEMPERATURE (K)F7.2,
     230H   BARRIERS TO ROTATION (KCAL)3F10.3/23H ROTAMER MOLE FRACTIONS
     33F8.4,49H   2/T2 = LINE WIDTH IN ABSENCE OF EXCHANGE (CPS) F5.2/
     464H INVERSE CORRELATION TIMES (CPS)-TAB,TAC,TBC,TBA,TCA,TCB INVERS
     5E  1P6E11.3)
      END
```

```
$IBFTC PREP
      SUBROUTINE PREP (TTINV)
C     SUBROUTINE PREP CALCULATES THE ELEMENTS OF THE 7   A   MATRICES
C     FROM THE RESULTS OF SUBROUTINE INPUT.
C     THE THIRD SUBSCRIPT OF THE  A  MATRIX REFERS TO A SET OF DENSITY
C     MATRIX ELEMENTS WHICH  INTERACT DUE TO THE EXCHANGE.
      COMMON FA, A, ENX, XM, F
      DIMENSION A(12,12,4), FA(9),          F(4,4,3), XM(12,4), ENX(12,7)
      DO 105 K=1,2
      K1 = K+1
      DO 104 I=1,5,2
      A(I,I+1,K1) = 0.
104   A(I+1,I,K1) = 0.0
      DO 105 L = K1,3
      IT = K+L-2
      MIT = IT + 3
      A(K,L,1) =-FA(IT)
      A(L,K,1) =-FA(MIT)
      DO 105 I=1,2
      I2 = I + 2*(K-1)
      DO 105 J=1,2
      J2 = J+2*(L-1)
      A(I2,J2,2) = -F(I,J,IT)*FA(IT)
      A(J2,I2,2) = -F(I,J,IT) * FA(MIT)
      A(I2,J2,3) = -F(I+2,J+2,IT)*FA(IT)
      A(J2,I2,3) = -F(I+2, J+2, IT)*FA(MIT)
      DO 105 M=1,2
      M2 = 2*(I + 2*K -3) + M
      DO 105 N=1,2
      N2 = 2*(J + 2*L-3) + N
      A(M2,N2,4) = -F(I,J,IT)*F(M+2, N+2, IT)*FA(IT)
 105  A(N2,M2,4) = A(M2,N2,4) * FA(MIT)/FA(IT)
      DO 107 I=1,3
      FABO = FA(2*I) + FA(2*I - 1) + TTINV
      A(I,I,1) = FABO
      DO 106 J=1,2
      J2 = J + 2*(I-1)
      A(J2,J2,2) = FABO
106   A(J2,J2,3) = FABO
      DO 107 J=1,4
      J2 = J+4*(I-1)
      DO 107 K=1,4
      K2 = K+4*(I-1)
      A(J2,K2,4) = 0.0
107   A(J2,J2,4) = FABO
      RETURN
      END
```

```
$IBFTC MASGEN
      SUBROUTINE MASGEN (NDIM, AB, VV, IP)
C     SUBROUTINE MASGEN OBTAINS THE ABSORPTION BY THE SOLUTION OF A SET
C     OF SIMULTANEOUS EQUATIONS AT EACH FREQUENCY.  IN ORDER TO REDUCE
C     THE SET OF COMPLEX EQUATIONS TO A SET OF REAL EQUATIONS, IT IS
C     NECESSARY TO INVERT THE   A   MATRIX.  THIS INVERSION IS NECESSARY
C     ONLY WHEN NE IS ODD.
      COMMON DUMMY, POP, A, ENX, XM
C     NE=1,2,7 ARE MATRICES FOR THE X ABSORPTION, NE=3,4,5,6 ARE MA-
C     TRICES FOR THE AB ABSORPTION OF THE ABX MOLECULES.
      COMMON /CALC/ N,NA,NE , M, MM
      DIMENSION X(12), XMS(12), Q(12,12), R(12,12), DUMMY(6), ERASE(12),
     1ANEW(12,12), YM(12), E(12,12), ENX(12,7), XM(12,4), A(12,12,4), VV
     2(NDIM), POP(3), AB (NDIM) , ABN(100,6)
C     ISKIP, VV(NDIM-1), AND ISKIPG PERMIT PRINTING INTERMEDIATE RESULTS
      ISKIP = VV(NDIM) + .01
      ISKIPF = VV(NDIM-2) + 1.01
      ISKIPG = VV(NDIM-3)
      DO 28 I=1,N
      XMS(I) = XM(I,NA)
28    X(I) = ENX(I,NE)
      ISAVE = NE - 2*NA + 2
      GO TO (30,34), ISAVE
30    DO 31 I=1,N
      DO 31 J=1,N
      Q(I,J) = 0.0
31    R(I,J) = A(I,J,NA)
      DO 32 I=1,N
 32   Q(I,I) = 1.0
C     OPTION TO PRINT A MATRIX.
      IF (ISKIPG .EQ. NA) WRITE (3,820) ((R(I,J),J=1,N), I=1,N)
C     M=ISIMEQ(12,N,M,A,B,DET,ERASE) SOLVES THE EQUATION AX=B, WHERE
C     A IS AN N BY N MATRIX, B AN N BY M MATRIX FOR THE N BY M MATRIX X.
C     THE RESULT IS STORED COLUMNWISE IN A.  AVAILABLE FROM SHARE
C     LIBRARY -- F4 BC SMQ4, WRITTEN BY UNIVERSITY OF CALIFORNIA
C     COMPUTER CENTER, BERKELEY, CALIFORNIA.
C     THE VALUE OF THE DETERMINANT OF A IS STORED IN DET.
C     ERASE IS USED BY ISIMEQ TO STORE NUMBER OF PERMUTATIONS.
C     M=1 FOR NORMAL EXIT.
C     M=2 IS AN ERROR CODE THAT OVERFLOW HAS OCCURRED.
C     M=3 IS ERROR CODE IF SINGULARITY IN MATRIX INVERSION.
C     INVERT A MATRIX.
      M=ISIMEQ (12,N,N, R, Q, 0.0,ERASE)
      IF(M.GT.1) GO TO 98
C     OPTION TO PRINT A INVERSE MATRIX.
      IF (ISKIPG .EQ. NA) WRITE (3,820) ((R(I,J),J=1,N), I=1,N)
34    DO 41 I=1,N
      DO 41 J=1,N
      ANEW(I,J) = -A(I,J,NA) - R(I,J)*X(I)*X(J)
41    Q(I,J) = R(I,J)*(X(J)+X(I))
      DO 90 IR = 1,IP
      ABSH = 0.0
      W = VV(IR)
      GO TO (70,47,45), ISKIPF
C     IF ISKIPF = 2 A MATRIX IS SOLVED ONLY IF W IS SUFFICIENTLY CLOSE
C     TO X(I) -- SLOW EXCHANGE APPROXIMATION.
45    DO 46  I=1,N
      IF (AB(NDIM) - ABS(W - X(I))) 46,70,70
46    CONTINUE
      GO TO 85
```

```
      DO 73 I=1,IP
      IF(AB(I) .LE. YH) GO TO 73
      YH = AB(I)
73    CONTINUE
75    YSCALE = YHIGH/YH
      IF (XICON .LT. 3.3) GO TO 77
      CALL CCNEXT
      CCXMIN = 0.
      CCXMAX = XLONG/1024.
      CCYMIN = 100./1024.
      CCYMAX = 1000./1024.
      XMIN = VV(1)
      XMAX = VV(IP)
      YMIN = CCYMIN
      YMAX = CCYMAX
      IF(XICON .EQ. 5.0) CALL CCGRID (1,NDIVP, NDIVS, 6HNOLBLS,1,1,20)
      XICON = 1.0
77    YSET = (YHIGH + YSPACE) * (XICON - 1.0) + 110.0
      DO 79 I=1,IP
      IF(AB(I) .LT. YH) GO TO 79
      AB(I) = YH
79    AB(I) =(AB(I)*YSCALE + YSET)/1024.
      CALL CCPLOT(VV,AB,IP, 4HJOIN, ISYM, 1)
      IF (YH2 .EQ. 0.0) GO TO 81
      DO 80 K=1,L
      IF (ABSORB(K) .LT. YH2) GO TO 80
      ABSORB(K) = YH2
80    ABSORB(K) = (ABSORB(K) *YHIGH/YH2 + YSET)/1024.
      CALL CCPLOT (FREQ,ABSORB,L, 4HJOIN, 0,0)
81    I = 0
82    I = I + 1
      IF (I .GT. ILET) GO TO 95
      XLET(I) = XLET(I)/1024.
      YLET(I) = YLET(I)/1024.
      L = 2*I - 1
      WORD(2) = WORDS(L+1)
      WORD(1)=WORDS(L)
      CALL CCLTR (XLET(I),YLET(I), KRTUP, KSIZE, WORD, NOFCH(I))
      GO TO 82
95    IF (IEND .EQ. 2) CALL CCEND
601   FORMAT (F1.0, 7I1, I2,3F4.0, 4(F4.0,F3.0),E10.1, 2F5.2,E10.1/
     14I1,6X 8A6)
604   FORMAT (1H F7.1,E11.4,F7.1,E11.4, F7.1,E11.4,F7.1,E11.4,F7.1,
     1E11.4,F7.1,E11.4,F7.1,E11.4)
96    RETURN
      END
```

```
$IBFTC PL11
C       PL11
C     THIS SUBROUTINE NMPLOT PRINTS THE FREQUENCY, ABSORBANCE, AND PLOTS
C     THE SPECTRUM ON THE MONITOR OUTPUT TAPE 3.
      SUBROUTINE NMPLOT (NDIM, AB, VV, IP)
C     ICON=1 YIELDS PLOT WHERE ABSORBANCE=YH HAS AN ORDINATE OF 100
C     ICON=2 NORMALIZES PLOT SO THAT LARGEST ABSORBANCE HAS VALUE OF 100
C     ICON=3 YIELDS PLOT WHERE ABSORBANCE=YH HAS AN ORDINATE OF 1
      COMMON /PLOT/ YH,ICON
      DATABLNK,DOT/1H ,1H./
      DIMENSION VV(NDIM),AB (NDIM),X(34)
      GOTO(21,11,23),ICON
11    YH=0.0
      DO13I=1,IP
      IF(AB (I)-YH) 13,13,12
12    YH=AB (I)
13    CONTINUE
21    YH = YH * 0.01
23    DO 910 I=1,34
910   X(I) = BLNK
      DO 932 IH = 1,IP
      ABSORB = AB(IH)/YH
      IABSN = ABSORB + 1.0
      IF (IABSN- 100) 923,923,922
922   IABSN= 100
923   IGO = IABSN/34
      IABSN= IABSN- IGO*33 - IGO/2
      IGO = IGO+1
      X(IABSN)= DOT
      GO TO(926,927,928),IGO
C     THE USE OF THREE PRINT STATEMENTS REDUCES THE NUMBER OF SPACES
C     WHICH MUST BE PRINTED, SUBSTANTIALLY REDUCING PRINTER TIME -
C     DEPENDING ON THE TYPE OF PRINTER.
926   WRITE (3,946) VV(IH), AB(IH), (X(I),I =1,IABSN)
      GOTO932
927   WRITE (3,947) VV(IH), AB(IH), (X(I),I =1,IABSN)
      GOTO932
928   WRITE (3,948) VV(IH), AB(IH), (X(I),I =1,IABSN)
932   X(IABSN)= BLNK
946   FORMAT(1H F7.1, 1PE14.4, 33A1)
947   FORMAT(1H F7.1, 1PE14.4, 33X 34A1)
948   FORMAT(1H F7.1, 1PE14.4, 67X 33A1)
      RETURN.
      END
```

```
$IBFTC PLOT7
      SUBROUTINE NMPLOT (NDIM,AB,VV,IP)
C     PLOT7
C     THIS VERSION OF SUBROUTINE NMPLOT PRODUCES CALIFORNIA
C     COMPUTER PRODUCT PLOTS USING VARIOUS SUBROUTINES DESCRIBED
C     IN J6 EO CC94 -- WRITTEN AT E. O. LAWRENCE RADIATION
C     LABORATORY, BERKELEY, CALIFORNIA, COMPUTER CENTER.
C     THIS PROGRAM WILL HAVE TO BE MODIFIED FOR MOST OTHER INSTALLATIONS
      COMMON /CCPOOL/XMIN,XMAX,YMIN,YMAX, CCXMIN,CCXMAX,CCYMIN,CCYMAX
      COMMON /PLOT/ YH,ICON  / SAVE/ FREQ,ABSORB
      DIMENSIONVV(NDIM),AB(NDIM),WORDS(8), WORD(2),XLET(4),YLET(4),NOFCH
     1(4) , FREQ(144), ABSORB(144)
      WRITE (3,604)(VV(I),AB(I),I=1,IP)
C     ICON = 1 PRODUCES PLOT, ICON = 2 SKIPS PLOTTING.
      GO TO (1,96), ICON
C     XICON = 4 OR LARGER PREPARES FOR A NEW SET OF PLOTS.
C     XICON = 1 OR 4 OR LARGER PRODUCES PLOT AT BOTTOM OF PAGE.
C     XICON = 2 OR 3 PRODUCES PLOT YSET HUNDREDTHS OF AN INCH ABOVE
C     BASE LINE.  (SEE STATEMENT NUMBER 77)
C     XICON = 5 CAUSES FRAME TO BE DRAWN ABOUT PLOTS.
C     ISTART = 1 IF FIRST GRAPH, 2 OTHERWISE
C     IEND = 2 FOR LAST GRAPH, 1 OTHERWISE
C     ILET = NUMBER OF WORDS TO BE PRINTED.
C     ISYM = SYMBOL FOR POINTS PLOTTED.  IF ZERO NO SYMBOL USED.
C     KSIZE = APPROXIMATE SIZE OF LETTERS, IN TENTHS OF AN INCH.
C     KRTUP EVEN PRINTS HORIZONTAL LETTERS, ODD -- VERTICAL LETTERS.
C     NDIVS = NUMBER SECONDARY SUBDIVISIONS ALONG HORIZONTAL FRAME LINES
C     NDIVP = NUMBER PRIMARY SUBDIVISIONS ALONG HORIZONTAL FRAME LINES.
C     ALL DISTANCES READ BY PROGRAM ARE IN HUNDREDTHS OF AN INCH.
C     XLONG = HORIZONTAL WIDTH OF PLOT.
C     YHIGH = HEIGHT OF INDIVIDUAL PLOTS.
C     YSPACE = VERTICAL SPACING BETWEEN PLOTS.
C     XLET AND YLET  = BEGINNING OF PRINTED WORD RELATIVE TO ORIGIN
C     AT LOWER LEFT HAND EDGE OF PAPER.
C     YH = 0.0 NORMALIZES PLOT TO MAXIMUM ABSORBANCE.
C     OTHERWISE PLOT NORMALIZED TO VALUE OF YH.
C     IF WEAK PEAKS ARE PRESENT, A NONZERO YH2 CAUSES PLOT BETWEEN
C     VMIN AND VMAX (FREQUENCIES) TO BE PLOTTED ABOVE MAIN PLOT
C     NORMALIZED TO YH2.
C     NOFCH = NUMBER OF CHARACTERS IN A WORD TO BE PRINTED ON PLOT.
C     WORDS = COMMENTS ON GRAPH.
C     WORDS ARE PRINTED IN PAIRS, SO  FOR EXAMPLE, XLET(2),YLET(2),
C     NOFCH(2) REFER TO WORDS(3) AND WORDS(4).  THIS ALLOWS 9 LETTERS
C     TO BE WRITTEN CONVENIENTLY (NOT 12 DUE TO FORMAT OF NOFCH).
1     READ(2,601) XICON, ISTART, IEND, ILET, ISYM, KSIZE, KRTUP,
     1NDIVS,  NDIVP,  XLONG, YHIGH, YSPACE, (XLET(I),YLET(I), I=1,4),
     2YH,VMIN,VMAX, YH2, (NOFCH(I),I=1,4),(WORDS(I), I=1,8)
      GO TO (2,3),ISTART
2     CALL CCBGN
3     IF (YH2 .EQ. 0.0) GO TO 19
      I=0
      L=0
5     I=I+1
      IF(VMIN .GT. VV(I)) GO TO 5
6     L=L+1
      FREQ(L) = VV(I)
      ABSORB(L) = AB(I)
      I=I+1
      IF(VMAX .GT. VV(I) .AND. L .LE. 100) GO TO 6
19    IF (YH .NE. 0.0) GO TO 75
```

```
C       IF ISKIPF IS 1 THE SIMULTANEOUS EQUATIONS ARE ONLY SOLVED FOR
C       FREQUENCIES WITHIN THE BOUNDARIES SPECIFIED BY AB(NDIM-3) TO
C       AB(NDIM-2) FOR THE AB MATRICES, AB(NDIM-1) TO AB(NDIM) FOR X
C       MATRICES.
47      IF((NE.LE. 2 .OR. NE .EQ. 7).AND. W .GT. AB(NDIM-1) .AND. W
       1 .LT. AB(NDIM)) GO TO 70
        IF ( .NOT. (NE .GE. 3 .AND. NE .LE. 6 .AND. W.LT. AB(NDIM-2)
       1 .AND. W .GT. AB(NDIM-3))) GO TO 85
70      SQW = W**2
        DO 71 I=1,N
        YM(I) = XMS(I)
        DO 71 J=1,N
 71      E(I,J) = ANEW(I,J) + W*Q(I,J) - SQW*R(I,J)
C       OPTION TO PRINT E MATRIX.
        IF (ISKIP .EQ. NE) WRITE (3,820) ((E(I,J),J=1,N), I=1,N)
C       SOLVE SET OF SIMULTANEOUS EQUATIONS FOR DENSITY MATRIX ELEMENTS.
C       RESULT STORED IN FIRST COLUMN OF E.
        MM= ISIMEQ  (12, N, 1, E, YM, 0.0, ERASE)
        IF(MM.GT.1) GO TO 98
C       OPTION TO PRINT DENSITY MATRIX ELEMENTS.
        IF (ISKIP .EQ. NE) WRITE (3,820)  (E(I,1), I=1,N)
        DO 83 I=1,3
        N3 = N/3
        DO 83 J=1,N3
        J2 = J + N3*(I-1)
83      ABSH = ABSH + E(J2,1) * XMS(J2) * POP(I)
        AB(IR) = -ABSH + AB(IR)
C       OPTION TO PRINT RESULT OF INVERSION FOR EACH SET.
85      IF(NE-IFIX(VV(NDIM-1) + .01)) 86,89,90
86      ABN(IR,NE) = ABSH
        GOTO90
89      J2=NE-1
        WRITE (3,810) W,AB(IR),(ABN(IR,N3),N3=1,J2),ABSH
90      CONTINUE
        GO TO 99
98      WRITE (3,830) M,MM,NE
810     FORMAT (F10.1, 8E15.6)
820     FORMAT (1H 1PE10.3, 11E11.3)
830     FORMAT (50H OVERFLOW(2) OR SINGULARITY(3) IN MATRIX INVERSION 2I4
       1, 18H, INVERSION NUMBER I2)
99      RETURN
        END
```

```
$IBFTC INPUT
      SUBROUTINE INPUT
C     INPUT CALCULATES TRANSITION FREQUENCIES (ENX), ENERGY LEVELS (E),
C     UNITARY MATRICES (C), AND THE SQUARE ROOT OF THE TRANSITION AMPLI-
C     TUDES (XM) FOR EACH ROTAMER.  IT THEN OBTAINS THE F MATRICES FOR
C     EACH POSSIBLE EXCHANGE.
C     THERE ARE 6 2X2 UNITARY MATRICES FOR THE THREE ROTAMERS IN  C  .
      DIMENSION C(2,2,6), E(8), ENX(12,7),XM(12,4), DUMMY(585), F(4,4,3)
      COMMON DUMMY,ENX,XM,F / ABX / NSPIN, NMINP, NMAXP
      DO 58 I=1,3
      IT = I+3
      I21=2*I-1
C     VA,VB, AND VX ARE FREQUENCIES -- XJAB,XJAX,XJBX COUPLING CONSTANTS
C     FOR 2 SPIN PROBLEM, PROGRAM MUST READ VX = JAX = JBX = 0
      READ (2,901) VA,VB,VX, XJAB,XJAX,XJBX
      VT=0.5*(VA+VB+VX)
      XJT = 0.25*(XJAB+XJAX+XJBX)
      VP = VT-VX
      XJP = -XJT + 0.5* XJAB
      E(1)=VT+XJT
      E(4) = VP + XJP
      E(7) =-VP + XJP
      E(8)=-VT+XJT
      VP = VT-VA
      VT = VT-VB
      XJP = -XJT + 0.5* XJBX
      XJT = -XJT + 0.5*XJAX
      HAA = VP + XJP
      HBB = VT + XJT
      K=I
      J=2
      TANG = 1.0
14    HD = HAA-HBB
      IF (HD.EQ.0.) GO TO 17
C     DIAGONALIZE 2X2 MATRIX.  OFF-DIAGONAL TERM = HAB = 0.5*XJAB.
      TANG = SIGN(1.0,HD)*XJAB/ (ABS(HD) + SQRT(HD*HD + XJAB*XJAB))
17    COSINE = 1./SQRT(1.0 + TANG*TANG)
      SINE = TANG*COSINE
      HT = HAA
      HAA = COSINE*COSINE *(HAA + TANG*(XJAB+ TANG*HBB))
      HBB = COSINE*COSINE *(HBB - TANG*(XJAB- TANG*HT))
      E(J) = HAA
      E(J+1) = HBB
      C(1,1,K) = COSINE
      C(1,2,K) = SINE
      C(2,1,K) = -SINE
      C(2,2,K) = COSINE
      IF (J .EQ. 5) GO TO  25
      J=5
      K=I+3
      TANG = -1.0
      HAA =-VP + XJP
      HBB =-VT + XJT
      GO TO 14
25    XM(I,1) = 1.0
      ENX(I,1)=E(1)-E(4)
      ENX(I,2)=E(7)-E(8)
      L1=4*I-3
      DO 45 K=1,2
      K1= K+1
```

```
      XM(I21,2) = C(K,1,I) + C(K,2,I)
      ENX(I21,3) = E(1)-E(K1)
      ENX(I21,4) = E(K1) - E(7)
      IF (NSPIN .EQ. 1) GO TO 45
      DO 43 L=1,2
      XM(L1,4) = C(K,1,I)*C(L,2,IT) + C(K,2,I)*C(L,1,IT)
43    L1 = L1+1
      K5=K+4
      XM(I21,3)= C(K,1,IT) + C(K,2,IT)
      ENX(I21,5) = E(K5) - E(8)
      ENX(I21,6) = E(4) - E(K5)
      ENX(2*I21-1,7) = E(K1) - E(5)
      ENX(2*I21,7) = E(K1) - E(6)
45    I21=I21+1
      WRITE (3,903) I
      GO TO (46,47), NSPIN
46    WRITE (3,904) VA, VB, XJAB, (E(K), K=1,3), E(7), C(1,1,I),
     1C(1,2,I), C(2,1,I), C(2,2,I)
      GO TO 49
47    WRITE (3,906) VA,VB,VX, XJAB,XJAX,XJBX, (E(K),K=1,8),
     1(((C(L1,J,L), J=1,2), L=I,IT,3), L1=1,2)
49    WRITE (3,905)
      DO 58 K=NMINP,NMAXP
      L = (K+1)/2
      NOVER3 = ((((K+5) /4 )**2) /3) +1
      NMAX = NOVER3*I
      NMIN = NMAX-NOVER3 +1
58    WRITE (3,908) (ENX(N,K),XM(N,L), N=NMIN,NMAX)
      DO 117 M=1,2
      M1=M+1
      MT = M+3
      DO 117 N=M1,3
      IT = M+N-2
      NT = N+3
      DO 117 I=1,2
      DO 117 L=1,2
      F(I,L,IT)= 0.0
      F(I+2,L+2, IT) = 0.0
      DO 117 K=1,2
      F(I,L,IT) = C(I,K,M) * C(L,K,N) + F(I,L,IT)
 117  F(I+2,L+2,IT) = C(I,K,MT) * C(L,K,NT) + F(I+2,L+2,IT)
901   FORMAT (6F10.3)
903   FORMAT (8HOROTAMER I2)
904   FORMAT (1H  12X 16HVA, VB, AND JAB  3F11.2/1H012X16HENERGY LEVELS
     1  4F11.2/1H012X 17HUNITARY MATRIX   2F11.7/30X 2F11.7)
905   FORMAT (1H012X103HTRANSITION FREQUENCIES AND  I  SUB  X  MATRIX EL
     1EMENTS, WHICH ARE SQUARE ROOTS OF TRANSITION AMPLITUDES  )
906   FORMAT (1H 12X31HVA, VB, VX, JAB, JAX, AND JBX  6F11.2/1H012X
     116HENERGY LEVELS     8F11.2/1H012X17HUNITARY MATRICES 4F11.7/
     230X 4F11.7)
908   FORMAT (13X 4F11.3)
      RETURN
      END
```

CF2BR-CFBRCL. SAMPLE SPECTRUM. RICHARD NEWMARK. SEPTEMBER 25,1964. 1

ROTAMER 1

VA, VB, VX, JAB, JAX, AND JBX 438.80 194.20 921.80 170.00 -11.80 -14.80

ENERGY LEVELS 813.25 268.85 567.95 -95.25 -355.08 -651.72 193.55 -741.55

UNITARY MATRICES 0.9546679 -0.2976731 0.9538084 0.3004155
0.2976731 0.9546679 -0.3004155 0.9538084

TRANSITION FREQUENCIES AND I SUB X MATRIX ELEMENTS, WHICH ARE SQUARE ROOTS OF TRANSITION AMPLITUDES

508.500	1.000		
535.100	1.000		
544.404	0.657	245.296	1.252
75.296	0.657	374.404	1.252
386.472	1.254	89.828	0.653
259.828	1.254	556.472	0.653
623.924	0.003	920.568	1.000
523.032	1.000	1219.676	-0.003

ROTAMER 2

VA, VB, VX, JAB, JAX, AND JBX 474.50 485.40 980.20 167.30 -15.45 -12.53

ENERGY LEVELS 1004.88 532.15 364.40 38.67 -615.71 -448.14 58.97 -935.22

UNITARY MATRICES 0.7326931 0.6805592 0.7267517 -0.6869003
-0.6805592 0.7326931 0.6869003 0.7267517

TRANSITION FREQUENCIES AND I SUB X MATRIX ELEMENTS, WHICH ARE SQUARE ROOTS OF TRANSITION AMPLITUDES

966.210	1.000		
994.190	1.000		
472.727	1.413	640.483	0.052
473.183	1.413	305.427	0.052
319.512	0.040	487.078	1.414
654.378	0.040	486.812	1.414
1147.861	-0.009	980.295	1.000
980.105	1.000	812.539	0.009

ROTAMER 3

VA, VB, VX, JAB, JAX, AND JBX 639.90 859.20 1297.60 160.00 -20.30 -21.30

ENERGY LEVELS 1427.95 744.33 473.27 151.15 -824.73 -552.87 -50.35 -1368.75

UNITARY MATRICES 0.9505792 0.3104820 0.9509158 -0.3094499
-0.3104820 0.9505792 0.3094499 0.9509158

TRANSITION FREQUENCIES AND I SUB X MATRIX ELEMENTS, WHICH ARE SQUARE ROOTS OF TRANSITION AMPLITUDES

1276.800	1.000		
1318.400	1.000		
683.620	1.261	954.680	0.640
794.680	1.261	523.620	0.640
544.016	0.641	815.884	1.260
975.894	0.641	704.016	1.260
1569.064	0.001	1297.196	1.000
1298.004	1.000	1026.136	-0.001

NMR SPECTRA OF EXCHANGING NUCLEI CF2BR-CFBRCL. SAMPLE SPECTRUM. RICHARD NEWMARK. SEPTEMBER 25,1964. PAGE 2

ROTAMER ENERGIES (CAL) 0. 313.0 746.0 TEMPERATURE (K) 158.00 BARRIERS TO ROTATION (KCAL) 7.700 9.100 9.100

ROTAMER MOLE FRACTIONS 0.6840 0.2524 0.0635 2/T2 = LINE WIDTH IN ABSENCE OF EXCHANGE (CPS) 2.40

INVERSE CORRELATION TIMES (CPS)-TAB,TAC,TBC,TBA,TCA,TCB INVERSE 1.168E 01 1.352E-01 3.664E-01 3.167E 01 1.455E 00 1.455E 00

227.0	0.311482E-01	-0.253466E-05	-0.234654E-05	-0.219112E-01	-0.468780E-03	-0.510184E-03	-0.824828E-02	-0.487646E-05
233.0	0.486919E-01	-0.258085E-05	-0.238765E-05	-0.358063E-01	-0.459978E-03	-0.497286E-03	-0.119184E-01	-0.496359E-05
239.0	0.778065E-01	-0.262833E-05	-0.242986E-05	-0.587539E-01	-0.452700E-03	-0.487228E-03	-0.181026E-01	-0.505310E-05
245.0	0.112154E-00	-0.267715E-05	-0.247321E-05	-0.822004E-01	-0.446402E-03	-0.479580E-03	-0.290171E-01	-0.514508E-05
248.0	0.123159E-00	-0.270208E-05	-0.249533E-05	-0.848997E-01	-0.443422E-03	-0.476524E-03	-0.373288E-01	-0.519203E-05
251.0	0.128180E-00	-0.272736E-05	-0.251775E-05	-0.791729E-01	-0.440435E-03	-0.473903E-03	-0.480819E-01	-0.523963E-05
254.0	0.130242E-00	-0.275301E-05	-0.254047E-05	-0.683294E-01	-0.437341E-03	-0.471656E-03	-0.609930E-01	-0.528790E-05
257.0	0.131546E-00	-0.277902E-05	-0.256352E-05	-0.564892E-01	-0.434032E-03	-0.469715E-03	-0.741420E-01	-0.533685E-05
260.0	0.130339E-00	-0.280541E-05	-0.258688E-05	-0.459797E-01	-0.430403E-03	-0.468004E-03	-0.834505E-01	-0.538649E-05
263.0	0.123182E-00	-0.283218E-05	-0.261056E-05	-0.374672E-01	-0.426350E-03	-0.466438E-03	-0.848113E-01	-0.543684E-05
269.0	0.933168E-01	-0.288689E-05	-0.265893E-05	-0.256908E-01	-0.416678E-03	-0.463373E-03	-0.667349E-01	-0.553970E-05
275.0	0.641834E-01	-0.294323E-05	-0.270867E-05	-0.185996E-01	-0.405057E-03	-0.459682E-03	-0.447078E-01	-0.564555E-05
900.0	0.360001E-01	-0.212921E-01	-0.239292E-02	-0.636238E-04	-0.432685E-04	-0.625674E-04	-0.480857E-04	-0.120976E-01
910.0	0.101211E-00	-0.659796E-01	-0.467728E-02	-0.804836E-04	-0.373322E-04	-0.515774E-04	-0.526775E-04	-0.303320E-01
912.0	0.120833E-00	-0.776476E-01	-0.544880E-02	-0.854636E-04	-0.363147E-04	-0.497720E-04	-0.539891E-04	-0.375111E-01
914.0	0.139351E-00	-0.859340E-01	-0.639413E-02	-0.912251E-04	-0.353452E-04	-0.480728E-04	-0.554682E-04	-0.467923E-01
916.0	0.155126E-00	-0.885396E-01	-0.756294E-02	-0.979294E-04	-0.344204E-04	-0.464715E-04	-0.571361E-04	-0.587872E-01
918.0	0.168615E-00	-0.852758E-01	-0.902389E-02	-0.105778E-03	-0.335375E-04	-0.449604E-04	-0.590171E-04	-0.740716E-01
920.0	0.182061E-00	-0.779513E-01	-0.108651E-01	-0.115034E-03	-0.326939E-04	-0.435325E-04	-0.611409E-04	-0.929925E-01
922.0	0.197528E-00	-0.689893E-01	-0.132068E-01	-0.126040E-03	-0.318871E-04	-0.421817E-04	-0.635418E-04	-0.115068E-00
924.0	0.215100E-00	-0.601610E-01	-0.162188E-01	-0.139248E-03	-0.311149E-04	-0.409024E-04	-0.662614E-04	-0.138443E-00
926.0	0.231664E-00	-0.522690E-01	-0.201100E-01	-0.155270E-03	-0.303753E-04	-0.396893E-04	-0.693493E-04	-0.158990E-00
928.0	0.242628E-00	-0.455604E-01	-0.251669E-01	-0.174939E-03	-0.296663E-04	-0.385377E-04	-0.728660E-04	-0.171584E-00
930.0	0.244926E-00	-0.399882E-01	-0.317110E-01	-0.199427E-03	-0.289861E-04	-0.374435E-04	-0.768845E-04	-0.172884E-00

227.0	3.1148E-02
233.0	4.8692E-02
239.0	7.7807E-02
245.0	1.1215E-01
248.0	1.2316E-01
251.0	1.2818E-01
254.0	1.3024E-01
257.0	1.3155E-01
260.0	1.3034E-01
263.0	1.2318E-01
269.0	9.3317E-02
275.0	6.4183E-02
900.0	3.6000E-02
910.0	1.0121E-01
912.0	1.2083E-01
914.0	1.3935E-01
916.0	1.5513E-01
918.0	1.6861E-01
920.0	1.8206E-01
922.0	1.9753E-01
924.0	2.1510E-01
926.0	2.3166E-01
928.0	2.4263E-01
930.0	2.4493E-01

SAMPLE PROBLEMS

THE DATA CARDS READ BY THE COMPUTER ARE BELOW. AND THE FIRST TWO PAGES OF THE PRINTED OUTPUT FROM THE COMPUTER FOR THE FIRST PROBLEM FOLLOW THIS PAGE. THE OPTION TO PRINT OUT THE ABSORPTION FROM THE INVERSION OF EACH MATRIX HAS BEEN USED.

```
-7CF2BR-CFBRCL.  SAMPLE SPECTRUM. RICHARD NEWMARK.  SEPTEMBER 25,1964.
 123 313. 746.
438.80     194.20     921.80     170.0      -11.80      -14.80
474.50     485.40     980.20     167.3      -15.45     -12.53
639.90     859.20     1297.60    160.       -20.30     -21.30
 1 1 6 2.4                                   7.0
7.7        9.1        9.1
158.0
  227    6  245    3  263    6  275  625  900   10  910    2  930
```

THE FOLLOWING CARDS WERE USED TO PRODUCE SOME OF THE CF2BR-CFBR2 PLOTS IN SECTION VC. ONLY THE FIRST TWO SETS ARE INCLUDED. NOTE THAT TWO ADDITIONAL CARDS ARE REQUIRED FOR EACH PLOT. THE SIZE OF THE PLOT AND THE LETTERS PRINTED ON IT ARE INCLUDED ON THESE CARDS.

```
-7CF2BR-CFBR2.  CARDS USED TO CALCULATE CAL COMP PLOTS.  RICHARD A. NEWMARK.
 913 0.   759.
-156.51     14.17      616.91     168.05     -16.12      -18.44
14.17       -156.51    616.91     168.05     -18.44      -16.12
332.60      332.60     887.33                -21.45      -21.45
 2 1212.6                   -300.1.0  450.       450.       9999.
7.6        9.9        9.9
7.7        9.9        9.9
163.0
 -175   25 -150    5 -120    4 -112    1 -109    2 -107  2.5 -102    2 -1 0   1
  -96    2  -94    4  -90    5  -50    2  -48    1  -44    2  -42  2.5   37   2
  -33    1  -29    2  -25    5    5   10   25   25   75
4113020     250 163  41 166253 166233 166213
665        E4=7.6      E5=9.9      T=163
2213020     250 163  41 166457 166437 166417
665        E4=7.7      E5=9.9      T=163
 1 1312.1
10.8       11.6       10.8
208.0
 -100   50  -50   20  -30    5  -10    2    0    1    2    2    4    1    7  1.5
   10    5   30   20  130   10  140   5.  150  2.5  160    1  164    2  170    5
  240  2.5  245    2  247    1  250  2.5  255    5  270   10  300   20  360   10
  380    5  400    2  404    1  405  2.5  410    5  420   10  450   25    5
2213030         360      440800 440770 440740
775        E4=10.8     E5=11.6     T=208
```

C. Interpretation of ABXIR Computer Program

The calculation of the spectra ultize a straightforward application of the equations in section II. This section will explain the method of calculation used in the computer program in somewhat greater detail.

The parameters necessary are read by the computer in the main program and subroutine INPUT. The latter calculates the four diagonal energy levels, in the ABX approximation, $E_1 = H_{11}$, E_4, E_7, and E_8, which are listed in Table I. It then sets up the 2x2 secular equations and diagonalizes them. Note that the eigenvectors are the column vectors of the unitary matrix, whereas the equations in section II-B used the eigenvectors as the rows of the a,b, and c matrices (Eqs. (16-17)). Since the computation of the transition amplitudes requires knowing the expansion of the eigenvectors in the basic product functions, it is necessary to preserve the order of the eigenvalues in the program. If the chemical shifts are identical, a minus sign is introduced to compute the correct transition amplitudes. This is accomplished by the statement TANG = -1.0 in subroutine INPUT. Note that changing the sign of $\nu_A - \nu_B$ reverses the order of the second and third, and fifth and sixth eigenvalues, as well as changing the signs in the unitary matrix. The spectrum is unchanged but the environment of the two fluorines is different.

The a, b, and c matrices are stored in the C matrix in INPUT. The third subscript is used to distinguish among the six possible 2x2 unitary matrices in the three species. If the 3rd subscript is 1, 2, or 3 it refers to a unitary matrix for the energy levels with $F_z = \frac{1}{2}$. The subscript of 1 or 4, 2 or 5 and 3 or 6 refers to the 2x2 sections of the a, b, and c matrices, respectively.

The 14 allowed transition frequencies are stored in ENX, and the I_x matrix elements in XM. It was shown in section II-C that the density matrix elements are coupled together in 7 different sets, and it is important to keep these sets separate so that the computer solves the minimum number of simultaneous equations necessary to obtain the absorption.

Each off-diagonal density matrix element can be associated with an I_x matrix element and a transition frequency. The I_x matrix elements are obtained from Table II, section II-C, and are listed in Table XV.

Table XV I_x Matrix Elements in the Representation in Which the Hamiltonian is Diagonal for an ABX System

$I_{x,12} = a_{22} + a_{23}$	$I_{x,13} = a_{32} + a_{33}$
$I_{x,14} = 1.0$	$I_{x,25} = a_{22}a_{56} + a_{23}\,a_{55}$
$I_{x,26} = a_{22}a_{66} + a_{23}a_{65}$	$I_{x,27} = a_{22} + a_{23}$
$I_{x,35} = a_{32}\,a_{56} + a_{33}a_{55}$	$I_{x,36} = a_{32}a_{66} + a_{33}a_{65}$
$I_{x,37} = a_{32} + a_{33}$	$I_{x,45} = a_{55} + a_{56}$
$I_{x,46} = a_{65} + a_{66}$	$I_{x,58} = a_{55} + a_{56}$
$I_{x,68} = a_{65} + a_{66}$	$I_{x,78} = 1.0$

The transition frequencies are the difference in energy between the two energy levels associated with a given I_x matrix element. The density matrix elements for each species associated with each set number are given in Table XVI in the order used in the program. Thus set number 3 is a vector six elements long containing the following elements:

Table XVI Density Matrix Elements in Each Set

Set Number	Second Subscript of XM	Density Matrix Elements
1	1	ρ_{14}
2	1	ρ_{78}
3	2	ρ_{12}, ρ_{13}
4	2	ρ_{27}, ρ_{37}
5	3	ρ_{58}, ρ_{68}
6	3	ρ_{45}, ρ_{46}
7	4	ρ_{25}, ρ_{26}, ρ_{35}, ρ_{36}

ρ_{12}^{A}, ρ_{13}^{A}, ρ_{12}^{B}, ρ_{13}^{B}, ρ_{12}^{C}, and ρ_{13}^{C}. The second subscript of ENX gives the set number, and the transition frequencies are stored in order using the first subscript. Since the values of I_x are the same for sets 1 and 2, 3 and 4, and 5 and 6, the second subscript in XM corresponding to the 7 sets is also listed in Table XVI.

The only nonzero values of the T, U, and V matrices are stored in F, where the third subscript of F refers to the T, U, and V matrix, respectively. The upper left and lower right 2x2 blocks in the 4x4 F matrix are the only spaces used, corresponding to the upper and lower 2x2 blocks in the three matrices. It is important to remember that these have the same diagonal blocks as the a and b matrices.

In subroutine TAU the populations of the three species and the rates are calculated according to Eqs. (56) and (72) in section III. The results are stored in COMMON and referred to as the vector FA in the other routines.

Subroutine PREP sets up the A matrix defined in Eq. (47). The third subscript on the A matrix refers to the seven sets in the same way as the second subscript of XM, since A has the same degeneracy in sets as XM. The A matrices all have the same form, consisting of blocks for each rotamer and each possible exchange. In order to clarify the construction of the A matrix, the elements for the second A matrix, which is six rows by six columns, are explicitly listed below. This matrix is obtained directly from Eq. (54) and the five analogous equations:

$$
\begin{matrix}
\frac{1}{\tau_A} + \frac{1}{T_2} & 0.0 & T_{22}/\tau_{AB} & T_{23}/\tau_{AB} & U_{22}/\tau_{AC} & U_{23}/\tau_{AC} \\
0.0 & \frac{1}{\tau_A} + \frac{1}{T_2} & T_{32}/\tau_{AB} & T_{33}/\tau_{AB} & U_{32}/\tau_{AC} & U_{33}/\tau_{AC} \\
T_{22}/\tau_{BA} & T_{23}/\tau_{BA} & \frac{1}{\tau_B} + \frac{1}{T_2} & 0.0 & V_{22}/\tau_{BC} & V_{23}/\tau_{BC} \\
T_{32}/\tau_{BA} & T_{33}/\tau_{BA} & 0.0 & \frac{1}{\tau_B} + \frac{1}{T_2} & V_{32}/\tau_{BC} & V_{33}/\tau_{BC} \\
U_{22}/\tau_{CA} & U_{23}/\tau_{CA} & V_{22}/\tau_{CB} & V_{23}/\tau_{CB} & \frac{1}{\tau_C} + \frac{1}{T_2} & 0.0 \\
U_{23}/\tau_{CA} & U_{33}/\tau_{CA} & V_{32}/\tau_{CB} & V_{33}/\tau_{CB} & 0.0 & \frac{1}{\tau_C} + \frac{1}{T_2}
\end{matrix}
$$

The matrix above clearly consists of nine 2x2 blocks. The three blocks which include the diagonal elements are calculated in the DO loop to statement number 107. The other blocks are calculated in the DO loop to number 105. Each 2x2 block corresponds to one of the three possible pairwise exchanges – AB, AC, or BC. Note that the A matrix is not symmetric because $\tau_{AB} \neq \tau_{BA}$.

The absorption is obtained from the solution of the simultaneous equations in each set by subroutine MASGEN. For an AB system of two spins on the three species, it is only necessary to use the sets of matrices corresponding to one of the quartets in the AB part of the ABX spectrum. The main program sets up NMIN and NMAX so that subroutine MASGEN is called only for sets 3 and 4. There is also provision in INPUT to make the output for the two spin system include only the relevant data.

For each of the seven sets it is necessary to determine the E matrix at each frequency, which is defined in Eq. (50) of section II-B. The M vector in Eq. (50) consists of the I_x matrix elements stored in

XM. The solution of the simultaneous set of equations yields the v vector, which comprises the imaginary part of the density matrix elements. Before calculating E, A^{-1} is found. A^{-1} is calculated only when NE, the set number is, odd, since A is the same for NE = 1 and NE = 2, etc., as mentioned above. Referring to the listing for subroutine MASGEN, the matrix inversion is performed by the function ISIMEQ by setting Q equal to the unit matrix. A^{-1} is stored in R. Following statement number 34, the part of E independent of ω is stored in ANEW and the part which is proportional to ω is stored in Q. The DO loop to statement 71 sets up the E matrix and the following call to ISIMEQ solves Eq. (50). The imaginary components of the density matrix elements are stored in the first column of E. The absorption is then calculated according to Eq. (44), and the result is stored in ABSH. This is then added to AB(IR), where the subscript keeps track of the frequency. AB(IR) is set to zero before the matrices are solved, and the solution for each set is simply added to the result from the previous sets.

Various options in subroutine MASGEN provide for the output of intermediate results in the calculation. They also provide means of solving only for the AB part of the spectrum at specified frequencies, thereby avoiding the unnecessary solution of the simultaneous equations at frequencies where the absorption for that set is practically zero. These options, explained in Appendix B, are transferred to the subroutine from the main program through otherwise unused locations in the vectors VV and AB.

Finally, subroutine NMPLOT plots the spectrum, either as points on the monitor output tape or as a California Computer Products, Inc.,

plot. These routines simply plot the absorbance as a function of frequency. To understand the logic of the plots, the reader is referred to the write-up of the Share subroutine J6 EO CC94.

APPENDIX D. ABCIR COMPUTER PROGRAM.

```
$IBFTC ABCIR
C       SUBROUTINES REQUIRED--BCSIMQ,READY,DATABC,TAU,SIME,NMPLOT.
        DIMENSION RECORD (13), VMIN(76), DELV(75), TT(20), E4(15), E5(15),
       1E6(15), FA(9), AB(1000), VV(1000)
        NDIM = 1000
        COMMON FA / PLOT/YH,ICON
        L=1
C       THIS PROGRAM CALCULATES NMR SPECTRA OF THREE ABC SYSTEMS UNDER-
C       GOING EXCHANGE.  BECAUSE IT REQUIRES THE SOLUTION OF A 27X27
C       MATRIX TO CALCULATE THE ABSORPTION AT EACH POINT, IT HAS NOT BEEN
C       USED EXCEPT AS A TEST PROGRAM. NO KNOWN BUGS REMAIN.
C       THE PROGRAM IS WRITTEN IN ANALOGY TO THE ABXIR PROGRAM.
C       ONLY THE DIFFERENCES FROM THE ABXIR PROGRAM WILL BE NOTED IN THE
C       COMMENT CARDS.
C       INPUT TO THIS PROGRAM IS SUBSTANTIALLY LIKE ABXIR PROGRAM.
C       MAIN EXCEPTION IS INPUT TO SUBROUTINE DATABC.
C       OPTIONS USED IN SUBROUTINE SIME -- CORRESPONDING TO MASGEN -- ARE
C       INDICATED IN THE SUBROUTINE.
1       READ (2,905) ICODE, (RECORD(I), I=1,13)
        IF (ICODE .NE. (-7)) GO TO 1
C       NSPIN IS NOT READ AS IT MUST BE THREE.
        READ (2,906) KSET,ICON,E2,E3,YH
        WRITE (3,909) (RECORD(I),I=1,13),L
        L=L+1
        CALL DATABC
        DO 76 KH=1,KSET
        READ (2,913) IMAX,JMAX,IDELMX,WIDTH, (VV(I),AB(I),I=996,1000)
        TTINV = 0.5*WIDTH
        IF (IMAX .GT. 15 .OR. IMAX .LT. 1 .OR. JMAX .GT. 20 . OR.
       1JMAX .LT. 1 .OR. IDELMX .GT. 75 .OR. IDELMX .LT. 1) GO TO 1
        READ (2,916) (E4(I), E5(I), E6(I), I=1,IMAX)
        READ (2,918) (TT(I), I=1,JMAX)
        READ (2,923) (VMIN(I), DELV(I), I=1,IDELMX), VMAX
        VMIN(IDELMX+1) = VMAX
        W= VMIN(1) - DELV(1)
        I=1
        IP = 0
45      W=W+ DELV(I)
        IP = IP + 1
        IF (IP .GT. 995) GO TO 60
        VV(IP) = W
        IF(W.LT.VMIN(I+1)) GO TO 45
        IF (W.GE.VMAX) GO TO 60
        I = I+1
        W = VMIN(I)
        GO TO 45
60      DO 76 JH = 1,JMAX
        DO 76 IH = 1, IMAX
        DO 61 I=1,IP
61      AB(I) = 0.0
        CALL TAU (TT(JH), E2, E3, E4(IH), E5(IH), E6(IH))
        WRITE (3,931) (RECORD(I), I=1,13), L, E2, E3, TT(JH),
       1E4(IH), E5(IH), E6(IH), (FA(I),I=7,9),WIDTH, (FA(I),I=1,6)
        CALL READY (TTINV)
        L=L+1
        DO 75 I=1,3
```

```
810   FORMAT (F10.1, 8E15.6)
820   FORMAT (1H 1PE10.3, 11E11.3)
830   FORMAT (50H OVERFLOW(2) OR SINGULARITY(3) IN MATRIX INVERSION 2I4
     1, 18H, INVERSION NUMBER I2)
99    RETURN
      END
```

```
CEIGEN
C     FORTRAN 2 PROGRAM TO CALCULATE UNITARY MATRICES FOR ABCIR.
C     SUBROUTINE HDIAG IS USED TO DIAGONALIZE THE MATRICES, AVAILABLE
C     FROM SHARE LIBRARY.   VA,VB, AND VC ARE CHEMICAL SHIFTS.  XJAB,
C     XJAC, AND XJBC ARE COUPLING CONSTANTS.
      DIMENSION H(70,70), U(70,70), RECORD(12), HA(70,70),VT(4),XJT(4)
1     READINPUT TAPE 2, 11, (RECORD(I), I=1,12)
      READ INPUT TAPE 2,12,  VA, VB, VC, XJAB, XJAC, XJBC
      VT(1) = -VA + VB + VC
      VT(2) = VA - VB + VC
      VT(3) = VA + VB - VC
      VT(4) = VA + VB + VC
      XJT(1) = -XJAB - XJAC + XJBC
      XJT(2) = -XJAB + XJAC - XJBC
      XJT(3) = XJAB - XJAC - XJBC
      XJT(4) = XJAB + XJAC + XJBC
      H(1,2) = 0.5*XJAB
      HA(1,2) = H(1,2)
      H(1,3) = 0.5*XJAC
      HA(1,3) = H(1,3)
      H(2,3) = 0.5*XJBC
      HA(2,3) = H(2,3)
      DO 14 I=1,4
      H(I,I) = 0.5*VT(I) + 0.25*XJT(I)
14    HA(I,I) = -VT(I)*0.5 + 0.25*XJT(I)
      WRITE OUTPUT TAPE 3, 13, (RECORD(I), I=1,12), VA, VB, VC,
     1XJAB, XJAC, XJBC, H(4,4), HA(4,4)
      WRITE OUTPUT TAPE3,141,((H(I,J), J=1,3), (HA(I,K), K=1,3),I=1,3)
      N = 3
      IEGEN = 0
      CALL HDIAG (H,N,IEGEN,U,NR)
      WRITE OUTPUT TAPE 3,15,NR, (H(I,I), (U(I,J), J=1,3), I=1,3)
      CALL HDIAG (HA, N, IEGEN, U, NR)
      WRITE OUTPUT TAPE 3,15,NR,(HA(I,I), (U(I,J), J=1,3), I=1,3)
      GO TO 1
 11   FORMAT (12A6)
12    FORMAT (6F10.3)
13    FORMAT (1H1 12A6, 57H VA, VB, VC, JAB, JAC, JBC, EN(1), EN(8) RESP
     1ECTIVELY.      /8F14.4)
141   FORMAT (17H0INITIAL MATRICES  / (6F14.4))
15    FORMAT (57H0EIGENVALUES (FIRST COLUMN), UNITARY MATRIX.  NO. OF RO
     1T.   I5/(1H0 4E20.7))
      END
```

```
      NA = I
      N = (I/3)*18 + 9
      CALL SIME (NA,N,NDIM,AB,VV,IP)
       IF (NA .EQ. 5) GO TO 1
75    CONTINUE
76    CALL NMPLOT (NDIM, AB, VV, IP)
      GO TO 1
905   FORMAT (I2,13A6)
906   FORMAT (I2,I1,F7.3,2F6.3)
909   FORMAT (1H1 13A6,47X I3)
913   FORMAT (3I2,F4.0, 10F5.0)
916   FORMAT (3F10.1)
918   FORMAT (13F6.1)
923   FORMAT (16F5.0)
931   FORMAT (36H1NMR SPECTRA OF EXCHANGING NUCLEI     13A6,9X 4HPAGEI3/
     128H ROTAMER ENERGIES (CAL)  0. 2F8.1,19H     TEMPERATURE (K)F7.2,
     230H   BARRIERS TO ROTATION (KCAL)3F10.3/23H ROTAMER MOLE FRACTIONS
     33F8.4,49H   2/T2 = LINE WIDTH IN ABSENCE OF EXCHANGE (CPS) F5.2/
     464H INVERSE CORRELATION TIMES (CPS)-TAB,TAC,TBC,TBA,TCA,TCB INVERS
     5E  1P6E11.3)
      END

$IBFTC DATABC
C     DATABC READS IN THE UNITARY MATRICES, CPLUS AND CMINUS, WHICH COR-
C     RESPOND TO THE  C  MATRIX IN SUBROUTINE INPUT.  THESE MATRICES AND
C     THE EIGENVALUES MUST BE OBTAINED ELSEWHERE.
      SUBROUTINE DATABC
      DIMENSION  ENX(27,3), EIGEN(8), CPLUS(3,3,3), CMINUS(3,3,3),
     1FA(3,3,3), FB(3,3,3),  XM(27,3) , DUMMY(9), A(2187)
      COMMON DUMMY, FA, FB, A, ENX, XM
      DO 103 K=1,3
      READ (2,901) (EIGEN(I), I=1,8), ((CPLUS(I,J,K), J=1,3),
     1I=1,3), ((CMINUS(I,J,K), J=1,3), I=1,3)
      DO 102 I=1,3
      I2 = I + 3*K - 3
      ENX (I2,1) = EIGEN (1) - EIGEN(I+1)
      ENX(I2,2) = EIGEN (I+4) - EIGEN(8)
      XM(I2,1) = 0.0
      XM(I2,2) = 0.0
      DO 102 J=1,3
      J2 = J + 3*I + 9*K - 12
      XM(I2,1) = XM(I2,1) + CPLUS(I,J,K)
      XM(I2,2) = XM(I2,2) + CMINUS(I,J,K)
      XM(J2,3) = 00.0
      ENX(J2,3) = EIGEN (I+1) - EIGEN(J+4)
      DO 102 L1=1,3
      XM(J2,3) = XM(J2,3) - CPLUS(I,L1,K) * CMINUS(J,L1,K)
      DO 102 L2 =1,3
102   XM(J2,3) = XM(J2,3) + CPLUS(I,L1,K)*CMINUS(J,L2,K)
      WRITE (3,902)       K,          (EIGEN(I), I=1,8), ((CPLUS(I,J,K),
     1J=1,3), (CMINUS(I,L1, K), L1 = 1,3), I=1,3)
      J2SUB9 = J2 - 8
      I2SUB3 = I2 - 2
103   WRITE (3,904)                ((ENX(N,M),XM(N,M), N=I2SUB3,I2),
     1M=1,2), (ENX(N,3), XM(N,3), N=J2SUB9,J2)
      DO 117 M=1,2
      M1 = M+1
      DO 117 N=M1,3
      IT = M+N-2
```

```
      NA = I
      N = (I/3)*18 + 9
      CALL SIME (NA,N,NDIM,AB,VV,IP)
       IF (NA .EQ. 5) GO TO 1
75    CONTINUE
76    CALL NMPLOT (NDIM, AB, VV, IP)
      GO TO 1
905   FORMAT (I2,13A6)
906   FORMAT (I2,I1,F7.3,2F6.3)
909   FORMAT (1H1 13A6,47X I3)
913   FORMAT (3I2,F4.0, 10F5.0)
916   FORMAT (3F10.1)
918   FORMAT (13F6.1)
923   FORMAT (16F5.0)
931   FORMAT (36H1NMR SPECTRA OF EXCHANGING NUCLEI     13A6,9X 4HPAGEI3/
     128H ROTAMER ENERGIES (CAL)  0. 2F8.1,19H     TEMPERATURE (K)F7.2,
     230H   BARRIERS TO ROTATION (KCAL)3F10.3/23H ROTAMER MOLE FRACTIONS
     33F8.4,49H   2/T2 = LINE WIDTH IN ABSENCE OF EXCHANGE (CPS) F5.2/
     464H INVERSE CORRELATION TIMES (CPS)-TAB,TAC,TBC,TBA,TCA,TCB INVERS
     5E  1P6E11.3)
      END

$IBFTC DATABC
C     DATABC READS IN THE UNITARY MATRICES, CPLUS AND CMINUS, WHICH COR-
C     RESPOND TO THE  C  MATRIX IN SUBROUTINE INPUT.  THESE MATRICES AND
C     THE EIGENVALUES MUST BE OBTAINED ELSEWHERE.
      SUBROUTINE DATABC
      DIMENSION  ENX(27,3), EIGEN(8), CPLUS(3,3,3), CMINUS(3,3,3),
     1FA(3,3,3), FB(3,3,3),  XM(27,3) , DUMMY(9), A(2187)
      COMMON DUMMY, FA, FB, A, ENX, XM
      DO 103 K=1,3
      READ (2,901) (EIGEN(I), I=1,8), ((CPLUS(I,J,K), J=1,3),
     1I=1,3), ((CMINUS(I,J,K), J=1,3), I=1,3)
      DO 102 I=1,3
      I2 = I + 3*K - 3
      ENX (I2,1) = EIGEN (1) - EIGEN(I+1)
      ENX(I2,2) = EIGEN (I+4) - EIGEN(8)
      XM(I2,1) = 0.0
      XM(I2,2) = 0.0
      DO 102 J=1,3
      J2 = J + 3*I + 9*K - 12
      XM(I2,1) = XM(I2,1) + CPLUS(I,J,K)
      XM(I2,2) = XM(I2,2) + CMINUS(I,J,K)
      XM(J2,3) = 00.0
      ENX(J2,3) = EIGEN (I+1) - EIGEN(J+4)
      DO 102 L1=1,3
      XM(J2,3) = XM(J2,3) - CPLUS(I,L1,K) * CMINUS(J,L1,K)
      DO 102 L2 =1,3
102   XM(J2,3) = XM(J2,3) + CPLUS(I,L1,K)*CMINUS(J,L2,K)
      WRITE (3,902)       K,          (EIGEN(I), I=1,8), ((CPLUS(I,J,K),
     1J=1,3), (CMINUS(I,LI, K), LI = 1,3), I=1,3)
      J2SUB9 = J2 - 8
      I2SUB3 = I2 - 2
103   WRITE (3,904)                ((ENX(N,M),XM(N,M), N=I2SUB3,I2),
     1M=1,2), (ENX(N,3), XM(N,3), N=J2SUB9,J2)
      DO 117 M=1,2
      M1 = M+1
      DO 117 N=M1,3
      IT = M+N-2
```

```
      DO 117 I=1,3
      DO 117 J=1,3
      FA(I,J,IT) = 0.0
      FB(I,J,IT) = 0.0
      DO 117 K=1,3
      FA(I,J,IT) = CPLUS(I,K,M)*CPLUS(J,K,N) + FA(I,J,IT)
117   FB(I,J,IT) = CMINUS(I,K,M)*CMINUS(J,K,N) + FB(I,J,IT)
901   FORMAT (8F10.3/(3F10.8))
902   FORMAT (22H0CONSTANTS FOR ROTAMER I2, 15H, ENERGY LEVELS 8F11.2/
     139H0UNITARY  MATRICES  --MATRIX CPLUS        3F11.7, 11H  CMINUS
     2 3F11.7/(39X 3F11.7, 11X 3F11.7))
904   FORMAT (65H0TRANSITION FREQUENCIES AND SQUARE ROOTS OF TRANSITION
     1AMPLITUDES/(6F12.3))
      RETURN
      END

$IBFTC READY
      SUBROUTINE READY (TTINV)
C     THIS CORRESPONDS TO SUBROUTINE PREP.
      COMMON TAUINV, FA, FB, A
      DIMENSION A(27,27,3), FA(3,3,3), FB(3,3,3), TAUINV(9)
      DO  104  I=1,9
      DO 104 J=1,9
      A(I,J,3) = 0.0
      DO 104 K=1,2
      J2 = 9*K + J
      I2 = 9*K + I
      A(I,J,K) = 0.0
104   A(I2, J2, 3) =0.0
      DO 105 K=1,2
      K1 = K+1
      DO 105 L=K1,3
      IT = K + L - 2
      MIT = IT + 3
      DO 105 I=1,3
      I2 = I + 3*K - 3
      DO 105 J = 1,3
      J2 = J + 3*L - 3
      A(I2, J2, 1) = -FA(I,J,IT) *TAUINV(IT)
      A(J2,I2,1)  = -FA(I,J,IT)*TAUINV(MIT)
      A(I2,J2,2) = -FB(I,J,IT)*TAUINV(IT)
      A(J2,I2,2) = -FB(I,J,IT)*TAUINV(MIT)
      DO 105 M=1,3
      M2 = 3*I + 9*K - 12 + M
      DO 105 N=1,3
      N2 = 3*J + 9*L - 12 + N
      A(M2,N2,3) = -FA(I,J,IT) * FB(M,N,IT) * TAUINV(IT)
 105  A(N2,M2,3) = A(M2,N2,3) * TAUINV(MIT)/TAUINV(IT)
      DO 107 I=1,3
      FABO = TAUINV(2*I) + TAUINV(2*I-1) + TTINV
      DO 106 J=1,3
      J2 = J + 3*(I-1)
      DO 106 K=1,2
106   A(J2,J2, K) = FABO
      DO 107 J=1,9
      J2 = J + 9*I - 9
107   A(J2,J2,3) = FABO
      RETURN
      END
```

```
$IBFTC SIME
      SUBROUTINE SIME (NA,N,NDIM,AB,VV,IP)
      COMMON DUMMY, POP, DUMMYP, A, ENX, XM
      DIMENSION DUMMY(6), POP(3), DUMMYP(54), A(27,27,3), ENX(27,3),
     1XM(27,3),  X(27), XMS(27), Q(27,27), R(27,27), ERASE(27),  ANEW(27
     2,27), YM(27), E(27,27), VV(NDIM), AB(NDIM), ABN(2,250)
      ICON = VV(NDIM - 2) + .01
      ISKIPG = VV(NDIM - 3) + .01
      ISKIP = VV(NDIM) + .01
C     IF ICON = 2, SIME READS A INVERSE MATRIX, AND SKIPS THE TIME CON-
C     SUMING 27X27 MATRIX INVERSION.  IF ICON = 3, SIME WRITES THE R__
C     = A INVERSE MATRIX ON CARDS FOR FUTURE USE.
      IF (.NOT. (NA .EQ. 3 .AND. ICON .EQ. 2))GO TO 30
      READ (2,804) (ERASE(I), I=1,6), ((R(I,J), J=1,27), I=1,27)
      GO TO 36
30    DO 31 I=1,N
      X(I) = ENX(I,NA)
      XMS(I) = XM(I,NA)
      DO 31 J=1,N
      Q(I,J) = 0.0
31    R(I,J) = A(I,J,NA)
      DO 32 I=1,N
 32   Q(I,I) = 1.0
      IF (ISKIPG .EQ. NA) WRITE (3,820) ((R(I,J),J=1,N), I=1,N)
      M=ISIMEQ (27,N,N, R, Q, 0.0,ERASE)
      IF (M .GT. 1) GO TO 98
      IF (ICON .EQ. 3 .AND. NA .EQ. 3) WRITE (14,804) (DUMMY(I), I=1,6
     1), ((R(I,J), J=1,27), I=1,27)
      IF (ISKIPG .EQ. NA) WRITE (3,820) ((R(I,J),J=1,N), I=1,N)
36    DO 41 I=1,N
      DO 41 J=1,N
      ANEW(I,J) = -A(I,J,NA) - R(I,J)*X(I)*X(J)
41    Q(I,J) = R(I,J)*(X(J)+X(I))
44    DO 90 IR = 1,IP
      W = VV(IR)
      SQW = W**2
      DO 71 I=1,N
      YM(I) = XMS(I)
      DO 71 J=1,N
 71    E(I,J) = ANEW(I,J) + W*Q(I,J) - SQW*R(I,J)
      IF (ISKIP .EQ. NA) WRITE (3,820) ((E(I,J),J=1,N), I=1,N)
73    MM= ISIMEQ  (27, N, 1, E, YM, 0.0, ERASE)
      IF (MM.GT. 1) GO TO 98
      IF (ISKIP .EQ. NA) WRITE (3,820)  (E(I,1), I=1,N)
81    ABSH = 0.0
      DO 83 I=1,3
      N3 = N/3
      DO 83 J=1,N3
      J2 = J + N3*(I-1)
83    ABSH = ABSH + E(J2,1) * XMS(J2) * POP(I)
      AB(IR) = -ABSH + AB(IR)
85    IF(NA-IFIX(VV(NDIM-1) + .01)) 86,89,90
86    ABN(IR,NA) = ABSH
      GOTO90
89    WRITE (3,810) W,AB(IR),(ABN(IR,N3),N3=1, 2),ABSH
90    CONTINUE
      GO TO 99
98    WRITE (3,830) M,MM,NA
      NA = 5
804   FORMAT (1P7E11.4)
```

Bibliography

1. H. S. Gutowsky, D. W. McCall, and C. P. Slichter, J. Chem. Phys., 21, 279 (1953).

2. H. S. Gutowsky and A. Saika, J. Chem. Phys., 21, 1688 (1953).

3. J. J. Drysdale and W. D. Philips, J. Am. Chem. Soc. 79, 319 (1957).

4. P. M. Nair and J. D. Roberts, J. Am. Chem. Soc., 79, 4565 (1957).

5. H. M. McConnell, J. Chem. Phys., 28, 430 (1958).

6. J. Kaplan, J. Chem. Phys., 28, 278 (1958).

7. S. Alexander, J. Chem. Phys., 37, 967, 974 (1962).

8. R. J. Kurland and Wise, private communication.

9. J. Heidberg, J. A. Weil, G. A. Janusonis, and J. K. Anderson, J. Chem. Phys., 41, 1033 (1964).

10. C. S. Johnson, Jr., and J. C. Tully, J. Chem. Phys., 40, 1744 (1964).

11. E. B. Wilson, "Advances in Chemical Physics II," Interscience Publishers, Inc., New York, 1959.

12. E. L. Pace, J. Chem. Phys. 16, 74 (1948).

13. Y. Morino and E. Hirota, J. Chem. Phys., 28, 185 (1958).

14. C. R. Ward and C. H. Ward, J. Mol. Spec., 12, 289 (1964).

15. O. Risgin and R. C. Taylor, Spectrochim. Acta., 15, 1036 (1959).

16. D. S. Thompson, R. A. Newmark, C. H. Sederholm, J. Chem. Phys., 37, 411 (1962).

17. I. Solomen and N. Bloembergen, J. Chem. Phys., 25, 261 (1956).

18. U. Fano, Revs. Modern Phys., 29, 74 (1957).

19. J. A. Pople, W. G. Schneider, and J. H. Bernstein, "High-Resolution Nuclear Magnetic Resonance," McGraw-Hill Book Co., Inc., New York, 1959, chap. VI.

20. H. S. Gutowsky, G. C. Belford, and P. E. McMahon, J. Chem. Phys., 36, 3353 (1962).

21. R. A. Newmark and C. H. Sederholm, J. Chem. Phys., 39, 3131 (1963), and Lawrence Radiation Laboratory Report UCRL 10905, 1963, University of California, Berkeley, California.

22. A. A. Frost and R. G. Pearson, "Kinetics and Mechanism," John Wiley and Sons, New York, 1961, p. 61ff.

23. S. Mizushima, "Structure of Molecules and Internal Rotation," Academic Press, Inc., New York, 1954, p. 214.

24. H. P. Bucker and J. R. Nielsen, J. Mol. Spec., 11, 47 (1963).

25. Reference 23, p. 208.

26. K. S. Pitzer, "Quantum Chemistry," Prentice-Hall, Inc., New Jersey, 1953, p. 239.

27. K. S. Pitzer, J. Chem. Phys. 14, 239 (1946).

28. G. Glockler and C. G. Sage, J. Chem. Phys., 9, 387 (1941).

29. F. W. Cagle, Jr. and H. Eyring, J. Am. Chem. Soc., 73, 5628 (1951).

30. Reference 22, p. 130.

31. S. W. Benson, "The Foundations of Chemical Kinetics," McGraw-Hill Book Co., Inc., New York, 1960, chap. XV.

32. F. A. A. Anet and M. Ahmad, J. Am. Chem. Soc. 86, 119 (1964).

33. H. S. Gutowsky and C. H. Holm, J. Chem. Phys. 25, 1228 (1956).

34. L. Petrakis, Nuclear Magnetic Resonance Studies (Ph.D. Thesis), Lawrence Radiation Laboratory Report UCRL-9733, June 6, 1961 (unpublished).

35. G. V. D. Tiers, J. Phys. Chem. 67, 928 (1963).

36. S. L. Manatt and D. D. Elleman, J. Am. Chem. Soc., 84, 1305 (1962).

37. W. S. Brey, Jr., and K. C. Ramey, J. Chem. Phys. 39, 3546 (1963).

38. R. J. Abragam and H. J. Bernstein, Can. J. Chem. 39, 39 (1961).

39. R. J. Abragam and L. Cavalli, Mol. Phys., to be published.

40. R. W. Fessendem and J. S. Waugh, J. Chem. Phys. 37, 1466 (1962).

41. Reference 19, chap. XII

42. Reference 23, chap. II and III.

Figure Captions

1. The three rotamers of CF_2Br-CHBrCl.
2. A possible potential energy curve as a function of dihedral angle.
3. The two configurations of a substituted benzaldehyde.
4. Spectra of $CFCl_2$-$CFCl_2$ in $CFCl_3$ at several temperatures (°K). The sharp peaks on the left and right of each spectrum are sidebands of the solvent, $CFCl_3$. The sideband frequencies are 3780 and 3928 cps at 186-1/2°K, 3752 and 3956 cps at 196-1/2°, 3805 and 3916 cps at 200°, and 3794 and 3943 cps at all other temperatures.
5. Experimental spectrum of CF_2Br-CCl_2Br at 191°K.
6. The three rotamers of CF_2Br-CCl_2Br.
7. Experimental and calculated spectra of CF_2Br-CCl_2Br in $CFCl_3$ at 206°K.
8. Experimental and calculated spectra of CF_2Br-CCl_2Br at 208°K.
9. Experimental and calculated spectra of CF_2Br-CCl_2Br at 216-1/2°K. The sharp peaks are sidebands of the solvent, $CFCl_3$, at 3196 and 3444 cps upfield from the solvent peak.
10. Experimental and calculated spectra of CF_2Br-CCl_2Br at 219-1/2°K. Solvent sidebands are at 3038 and 3436 cps.
11. Experimental and calculated spectra of CF_2Br-CCl_2Br at 222-1/2°K. Solvent sidebands are at 2996 and 3419 cps.
12. Experimental and calculated spectra of CF_2Br-CCl_2Br at 224°K. Solvent sidebands are at 2986 and 3436 cps.
13. Experimental and calculated spectra of CF_2Br-CCl_2Br at 225°K. Solvent sidebands are at 2996 and 3419 cps.
14. Experimental and calculated spectra of CF_2Br-CCl_2Br at 230°K. Solvent sidebands are at 2986 and 3436 cps.
15. Experimental and calculated spectra of CF_2Br-CCl_2Br at 234°K. Solvent sidebands are at 2986 and 3436 cps.

16. Experimental and calculated spectra of $CF_2Br-CCl_2Br$ at 247°K. Solvent sidebands are at 2986 and 3436 cps.

17. The three rotamers of $CF_2Br-CFBr_2$.

18. Experimental spectra of $CF_2Br-CFBr_2$. The peaks are numbered in the spectrum at 152°K. The spectra at 162°K, 168°, 216°, and 237° show peaks 3 to 6 at higher temperatures. The spectra at 188°K and 238° show peaks 11 - 13 at higher temperatures. The sharp peaks on the high temperature spectra are sidebands of the solvent, CF_2Cl_2.

19. Experimental and calculated spectra of peaks 3 - 6 of $CF_2Br-CFBr_2$ at 163°K. The sharp peaks are sidebands of the solvent, CF_2Cl_2, at 2835 and 2998 cps upfield from the solvent peak.

20. Experimental and calculated spectra of $CF_2Br-CFBr_2$ at 167°K.

21. Experimental and calculated spectra of peaks 3 - 6 of $CF_2Br-CFBr_2$ at 174°K. Solvent sidebands are at 2835 and 2998 cps.

22. Experimental and calculated spectra of the peak 3 - 6 region of $CF_2Br-CFBr_2$ at 185°K. Solvent sidebands are at 2835 and 2998 cps.

23. Experimental and calculated spectra of peaks 11 - 13 of $CF_2Br-CFBr_2$ at 196°K. The solvent sideband is at 3530 cps.

24. Experimental and calculated spectra of the peak 11 - 13 region of $CF_2Br-CFBr_2$ at 199°K.

25. Experimental and calculated spectra of the peak 3 - 6 region of $CF_2Br-CFBr_2$ at 199°K.

26. Experimental and calculated spectra of the peak 3 - 6 region of $CF_2Br-CFBr_2$ at 210°K. Solvent sidebands are at 2852 and 2974 cps.

27. Experimental and calculated spectra of the peak 11 - 13 region of $CF_2Br-CFBr_2$ at 210°K.

28. Experimental and calculated spectra of the peak 11 - 13 region of $CF_2Br-CFBr_2$ at 217°K. Solvent sidebands are at 3549 and 3646 cps.

29. Experimental and calculated spectra of the peak 3 - 6 region of CF_2Br-$CFBr_2$ at 219°K.

30. The three rotamers of the two isomers of CFClBr-CFClBr.

31. Experimental spectrum of CFClBr-CFClBr at 177°K.

32. Experimental and calculated spectra of CFClBr-CFClBr at 194°K.

33. Experimental and calculated spectra of CFClBr-CFClBr at 207°K.

34. Experimental and calculated spectra of CFClBr-CFClBr at 233°K. The upper two spectra were calculated with E4=9.8, E5=10.5, EP4=10.1, and EP5=12.0, at the natural line width indicated on the spectrum. The other spectra were calculated at a width of 6 cps.

35. The spectrum of $CF_2BrCFBrCl$ at 150°K. The separation between peaks 1 and 24 is 1243 cps.

36. Experimental and calculated spectra of CF_2Br-CFBrCl at 154°K. The sharp peaks are sidebands of the solvent, $CFCl_3$, at 2901 and 4145 cps upfield from the solvent peak. The peak at 925 cps is off scale.

37. Experimental and calculated spectra of CF_2Br-CFBrCl at 158°K. Solvent sidebands are at 2902 and 4147 cps.

38. Experimental and calculated spectra of CF_2Br-CFBrCl at 162°K. Solvent sidebands are at 2902 and 4146 cps.

39. Experimental and calculated spectra of CF_2Br-CFBrCl at 165°K. Solvent sidebands are at 2902 and 4145 cps.

40. Experimental and calculated spectra of CF_2Br-CFBrCl at 171°K. Solvent sidebands are at 2902 and 4146 cps. The peak at 925 cps is off scale.

41. Experimental and calculated spectra of CF_2Br-CFBrCl at 175°K. Solvent sidebands are at 2997 and 4005 cps.

42. Experimental and calculated spectra of CF_2Br-CFBrCl at 186°K. Solvent sidebands are at 3084 and 4005 cps.

43. Experimental and calculated spectra of CF_2Br-CFBrCl at 196°K. Solvent sidebands are at 3084 and 4100 cps.

44. Experimental and calculated spectra of CF_2Br-CFBrCl at 205°K. Solvent sidebands are at 3084 and 4100 cps.

45. Experimental and calculated spectra of CF_2Br-CFBrCl at 220°K.

46. Experimental and calculated spectra of CF_2Br-CFBrCl at 231°K.

47. The three rotamers of CF_2Br-CFBrCl.

48. Experimental spectrum of CF_2Br-CHBrCl at 147°K.

49. Experimental and calculated spectra of CF_2Br-CHBrCl at 147°K. The sharp peaks are sidebands of the solvent, CF_2Cl_2, at 1947 and 3749 cps upfield from the solvent peak.

50. Experimental spectra of CF_2Br-CHBrCl. Solvent sidebands are at 1947 and 3748 cps at 156° and 168°, and at 2436 and 3058 cps at 210°K.

51. Experimental and calculated spectra of CF_2Br-CHBrCl at 190°K. Solvent sidebands are at 2447 and 3917 cps.

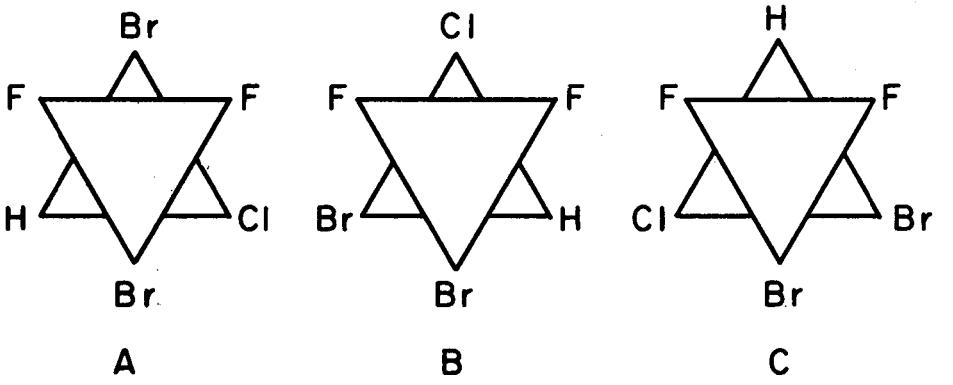

MU-34822

Fig. 1

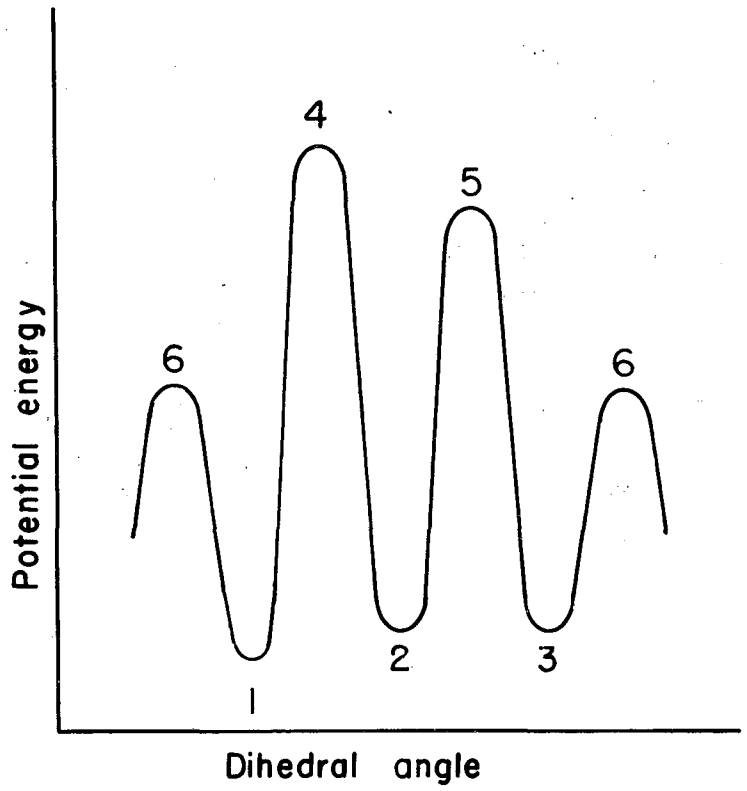

MU-34831

Fig. 2

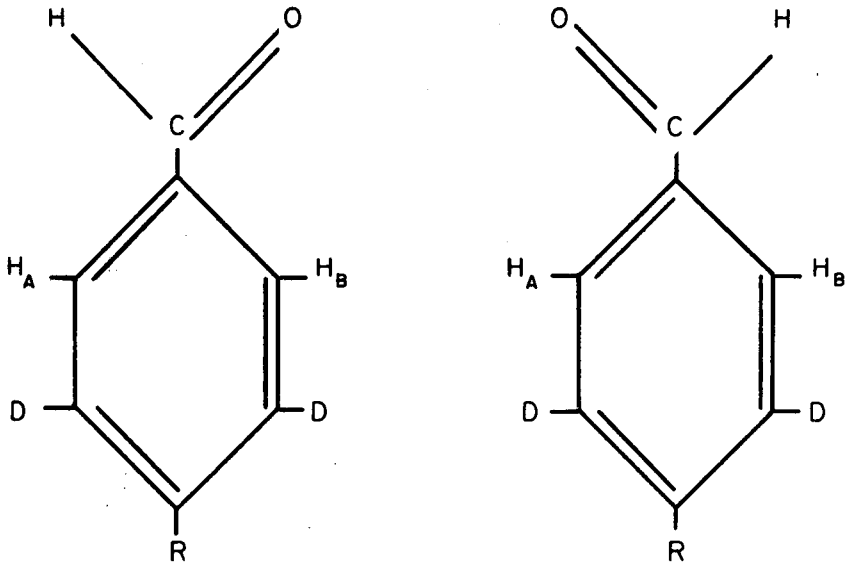

I II

MU-34834

Fig. 3

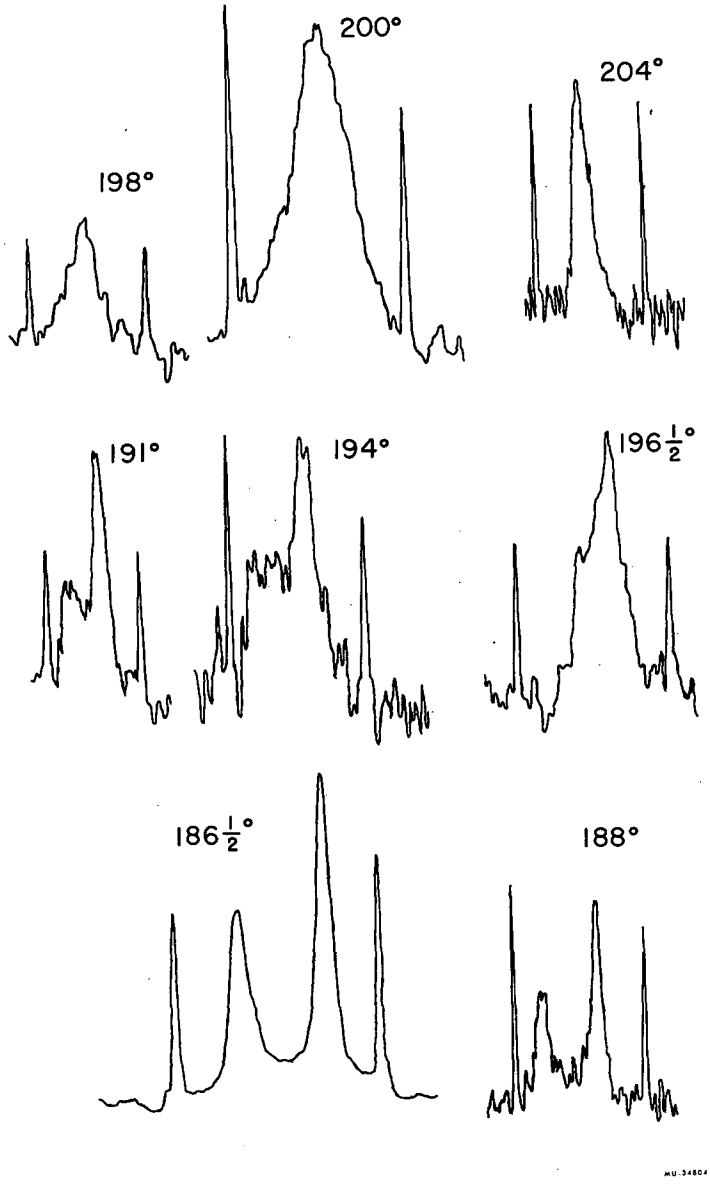

Fig. 4

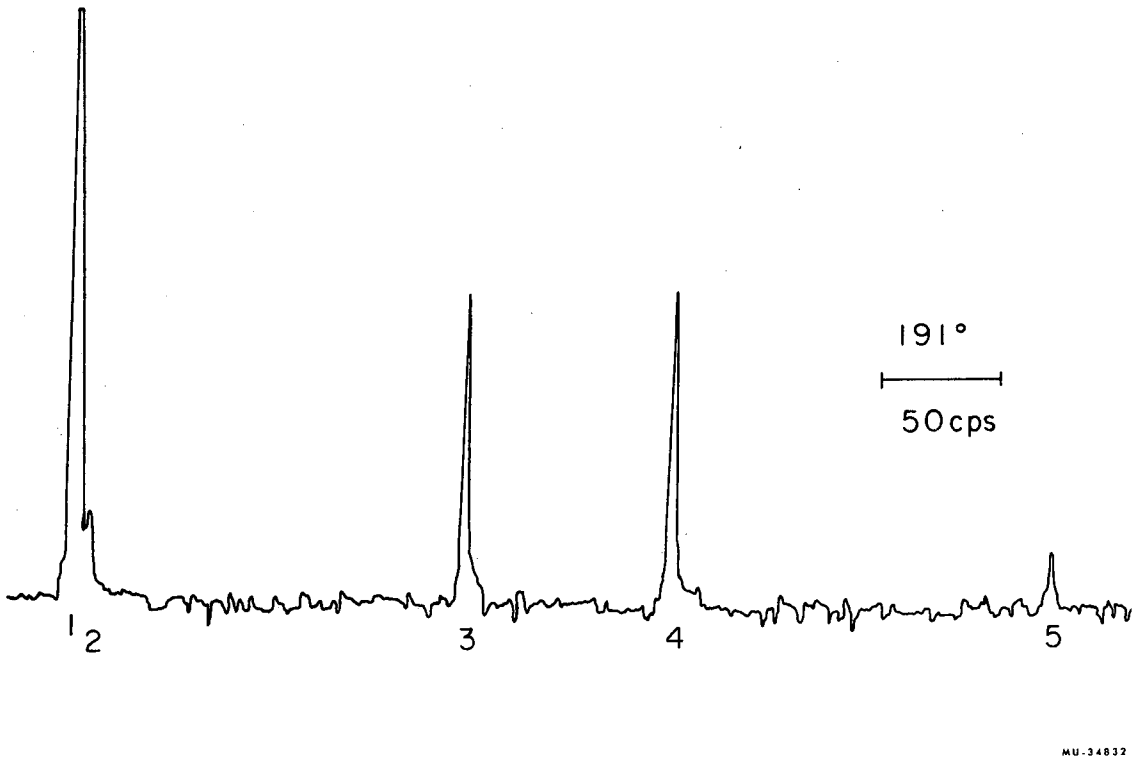

Fig. 5

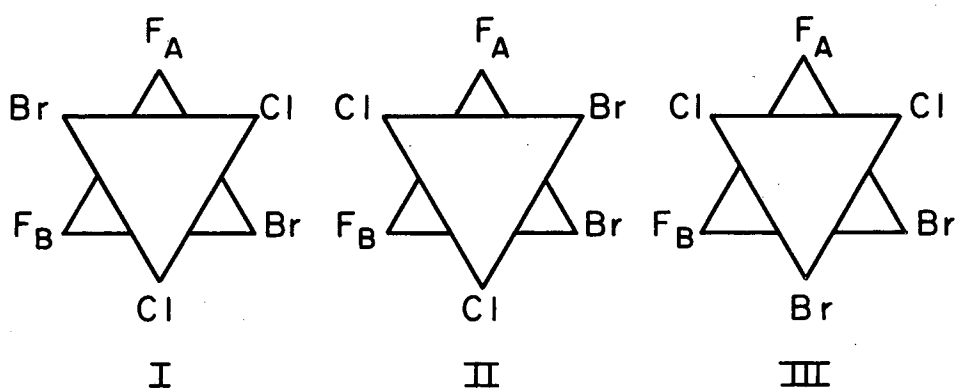

MU-34821

Fig. 6

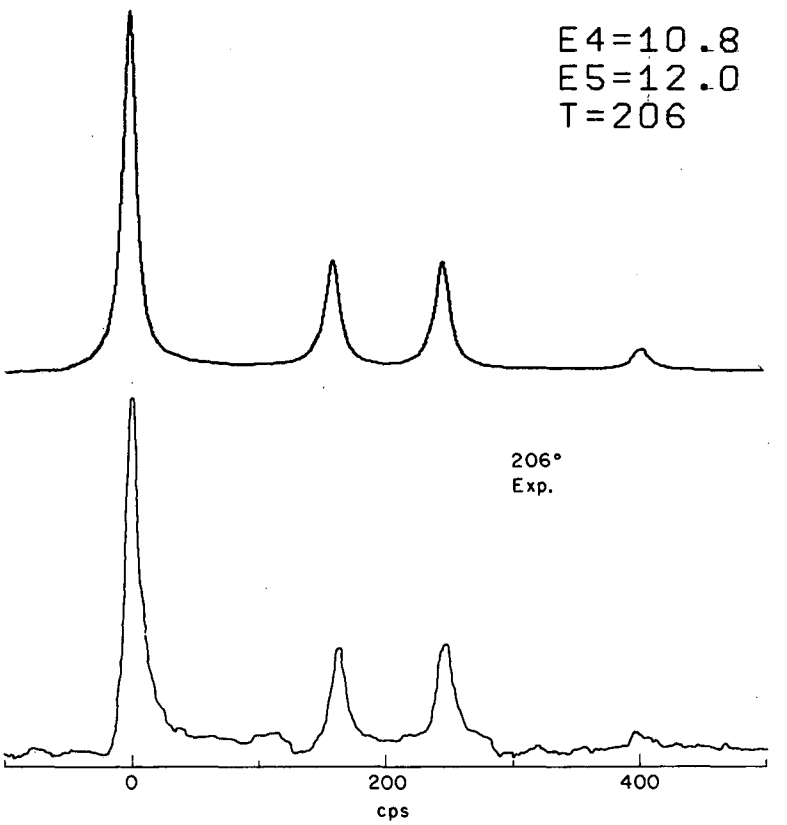

MU-34851

Fig. 7

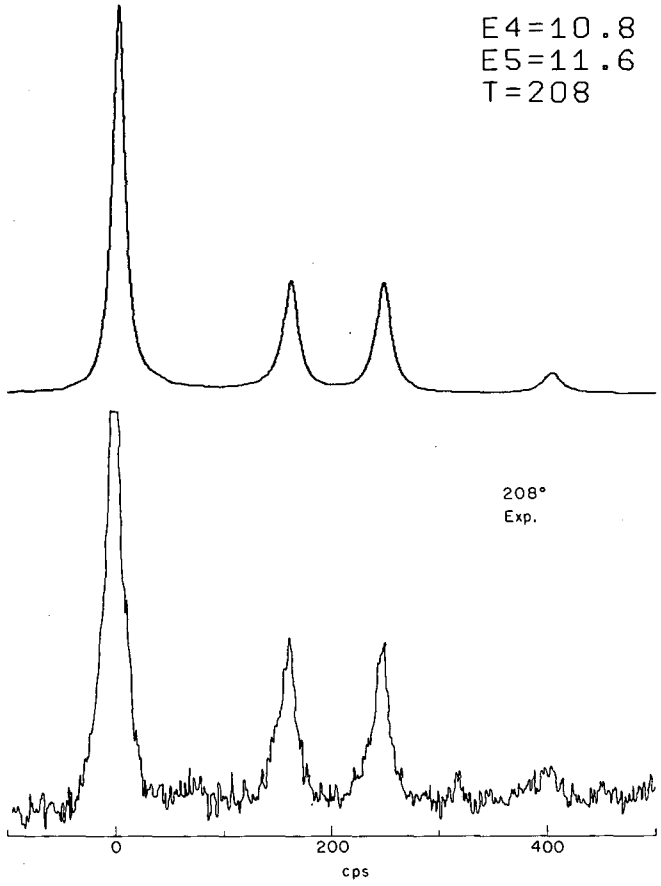

MU-34850

Fig. 8

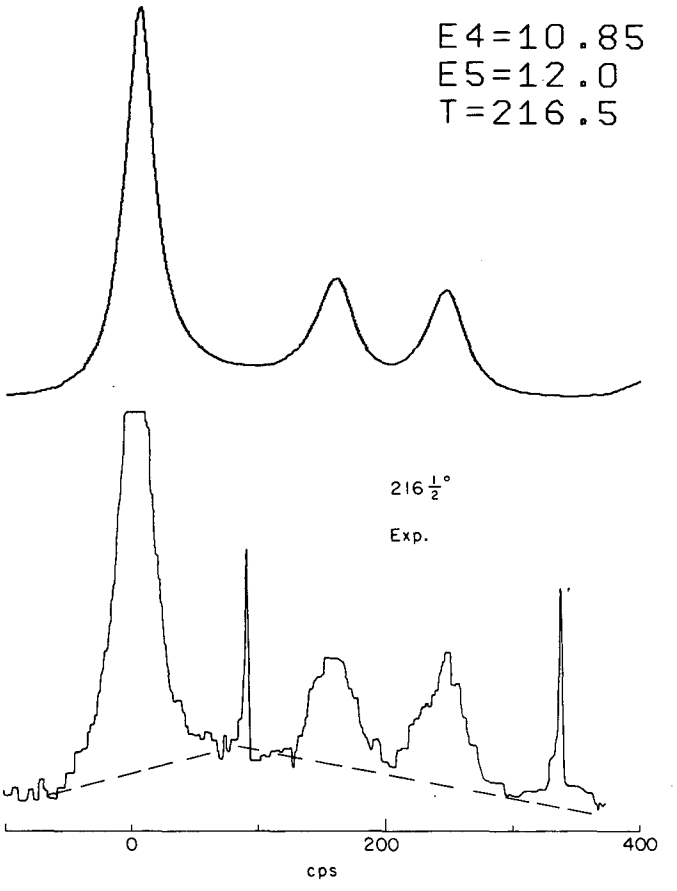

MU-34874

Fig. 9

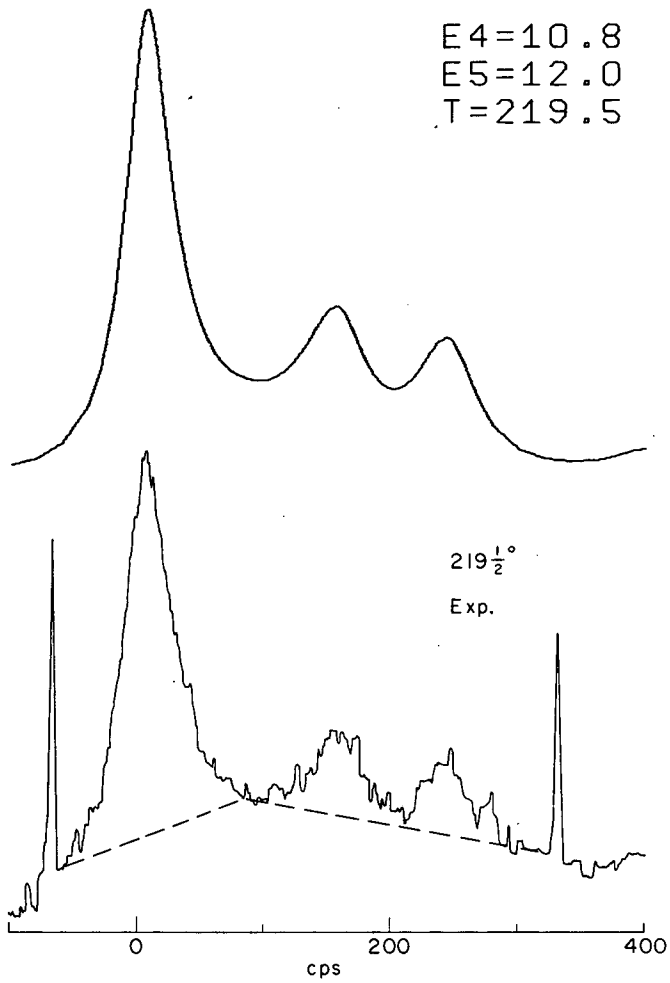

MU-34875

Fig. 10

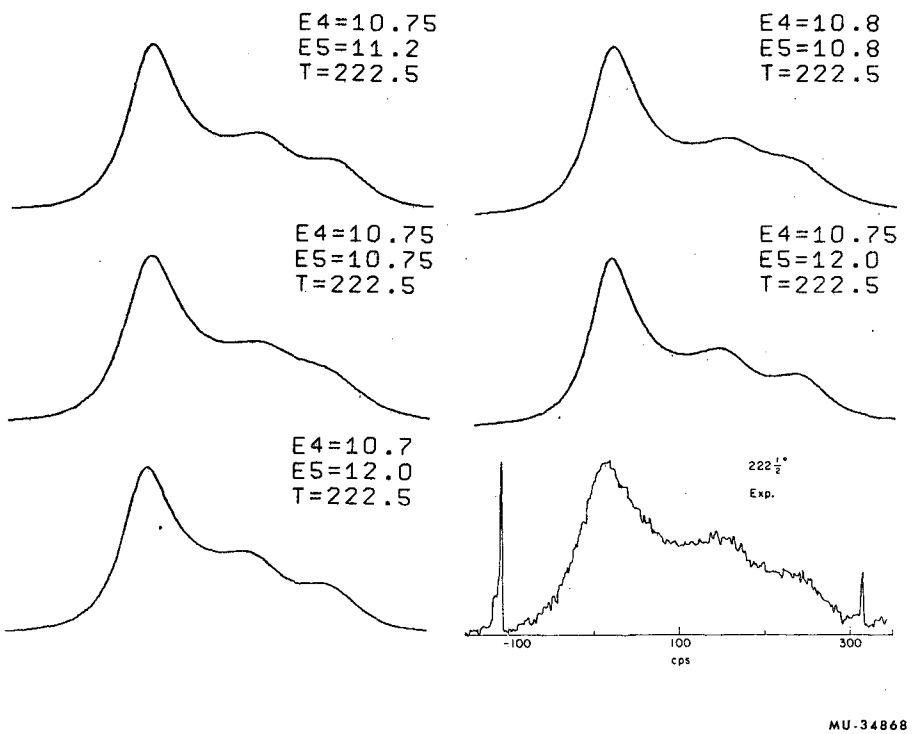
E4=10.75
E5=11.2
T=222.5
E4=10.8
E5=10.8
T=222.5
E4=10.75
E5=10.75
T=222.5
E4=10.75
E5=12.0
T=222.5
E4=10.7
E5=12.0
T=222.5
222½°
Exp.
-100
100
300
cps
MU-34868

Fig. 11

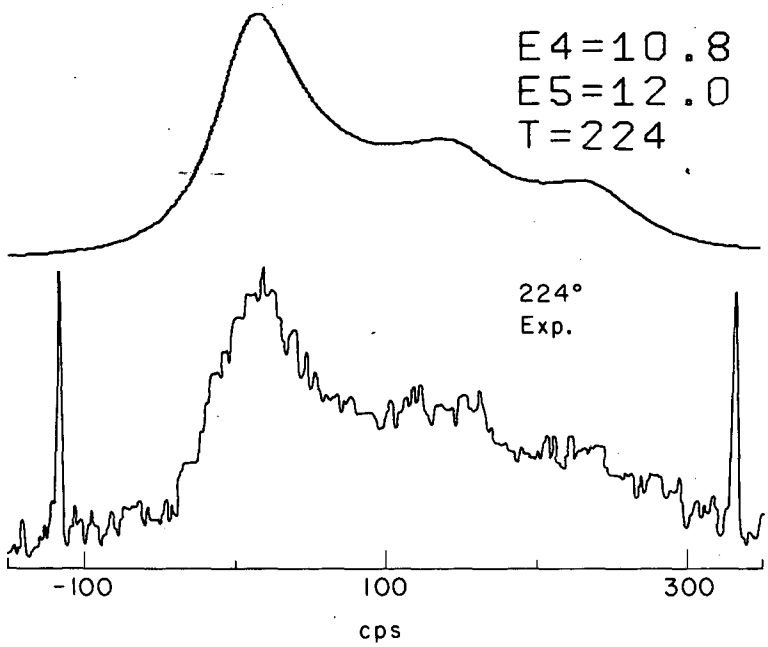

MU-34876

Fig. 12

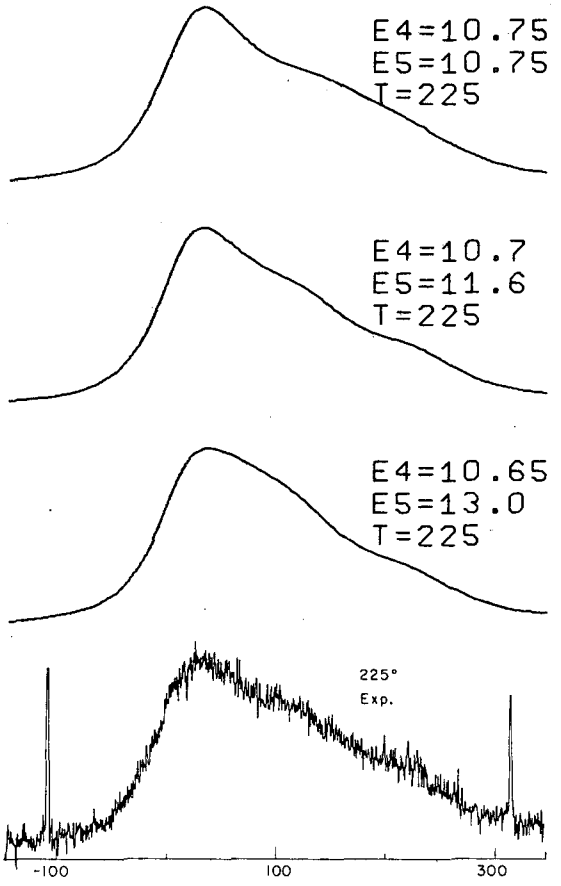

MU-34877

Fig. 13

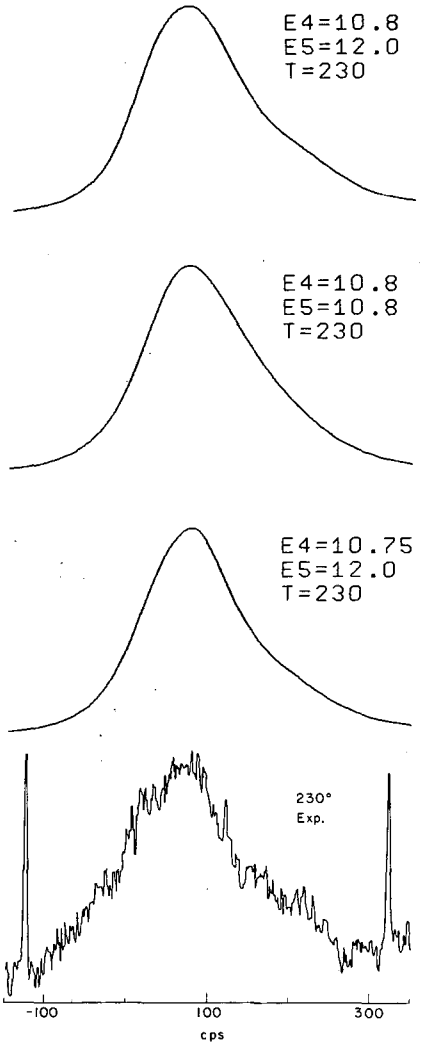

MU-34869

Fig. 14

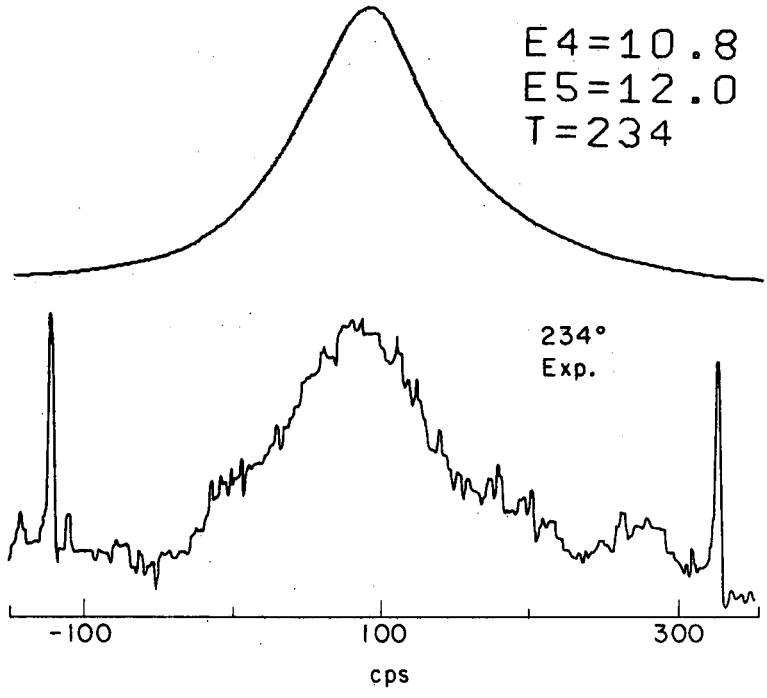

MU-34878

Fig. 15

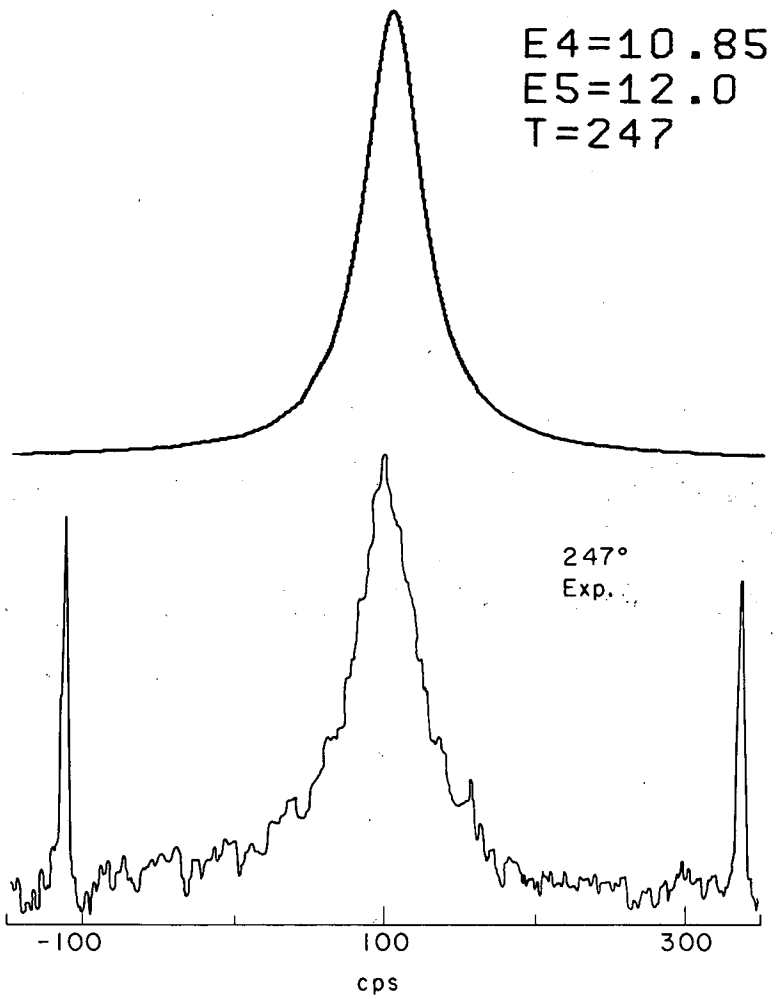

MU-34879

Fig. 16

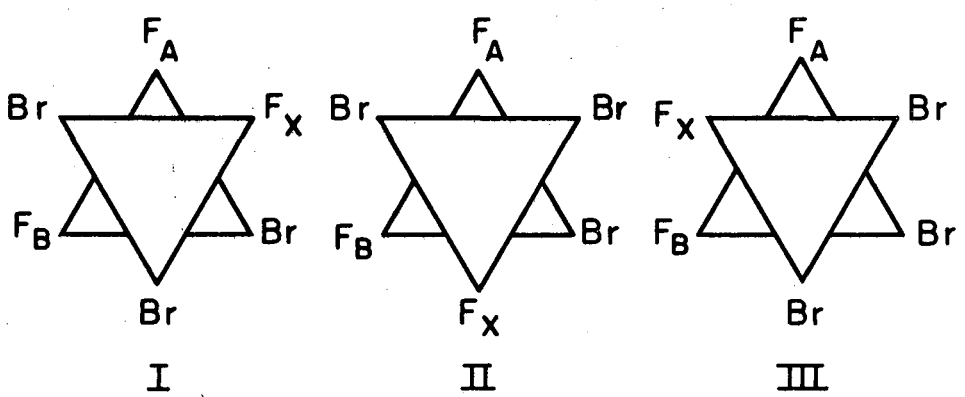

MU-34820

Fig. 17

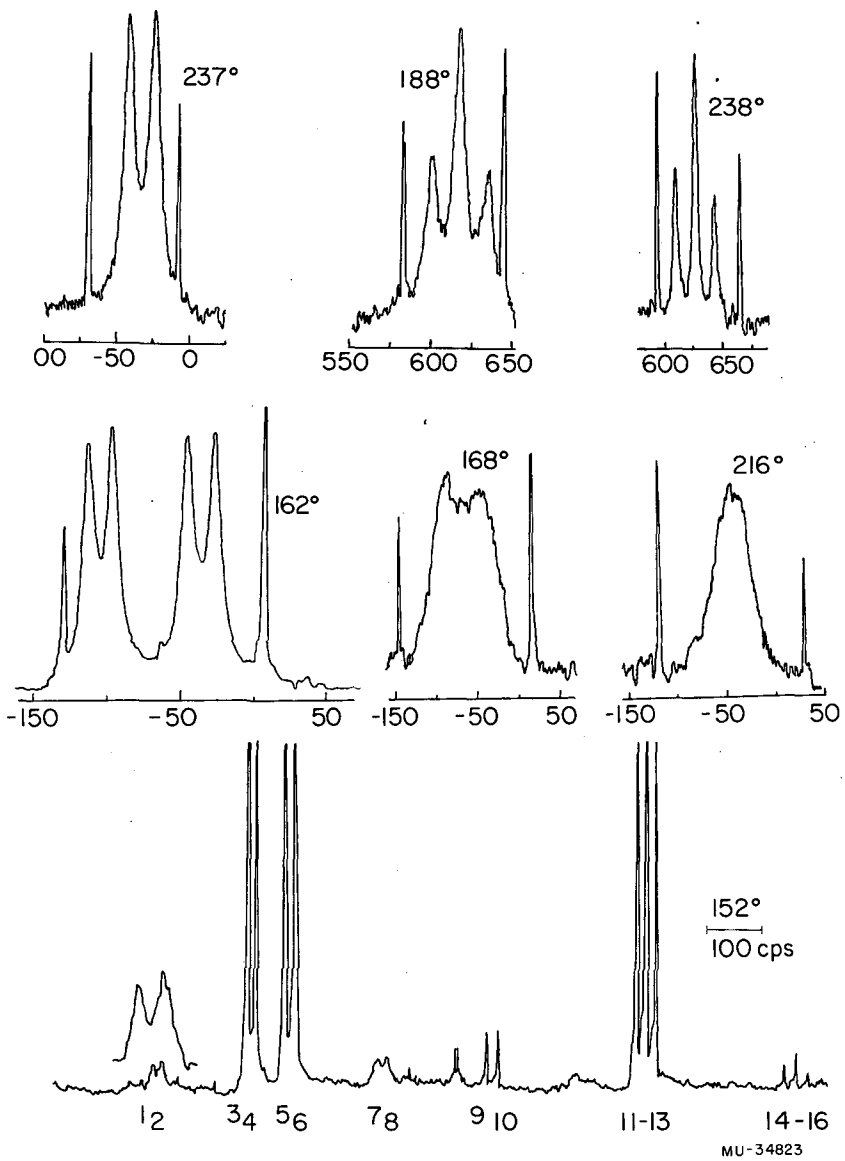
237°
00 -50 0
188°
550 600 650
238°
600 650
162°
-150 -50 50
168°
-150 -50 50
216°
-150 -50 50
152°
100 cps
1 2
3 4
5 6
7 8
9 10
11-13
14-16
MU-34823

Fig. 18

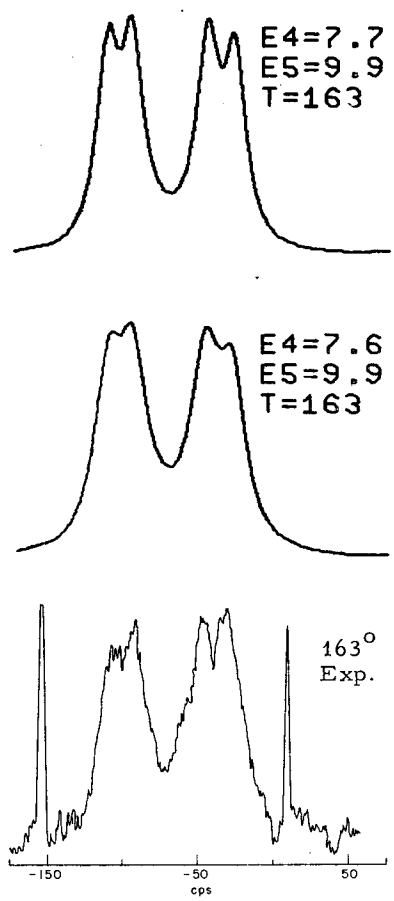

MU-34845

Fig. 19

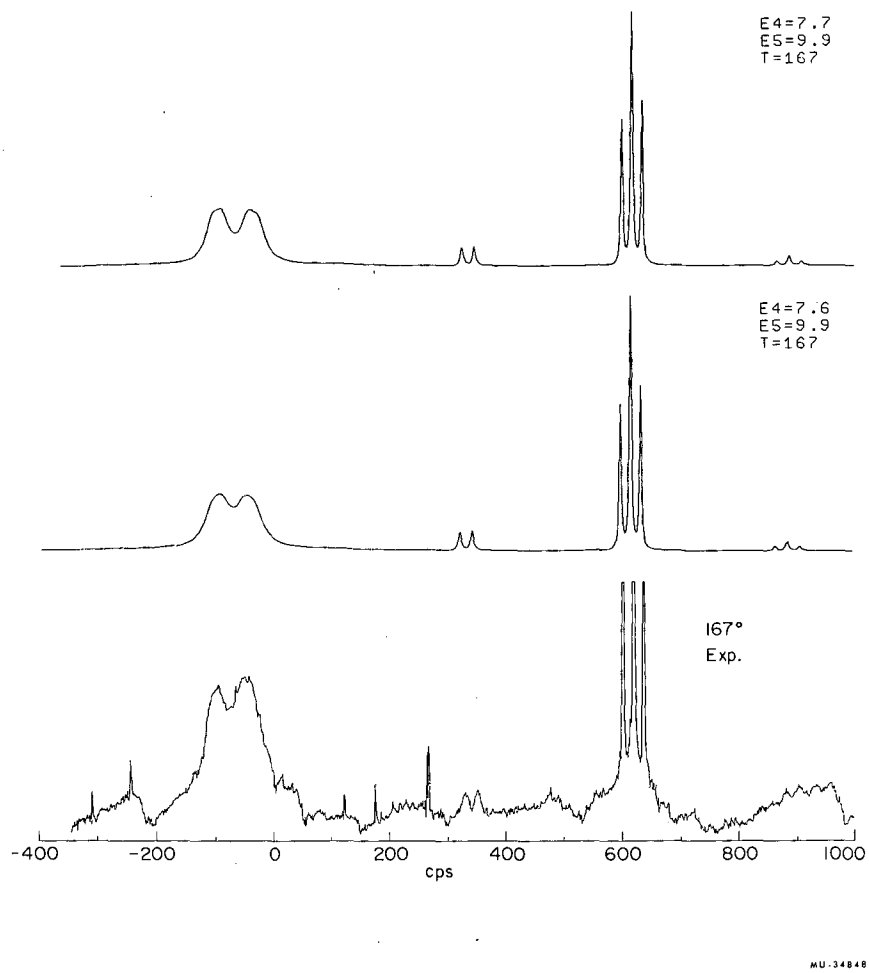
E4=7.7
E5=9.9
T=167
E4=7.6
E5=9.9
T=167
167°
Exp.
-400
-200
0
200
400
600
800
1000
cps
MU-34848

Fig. 20

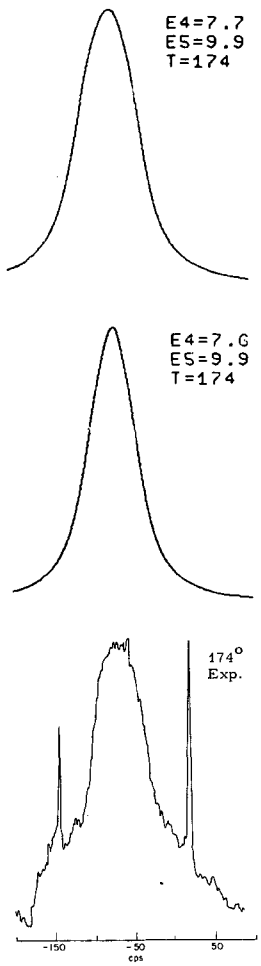

MU-34847

Fig. 21

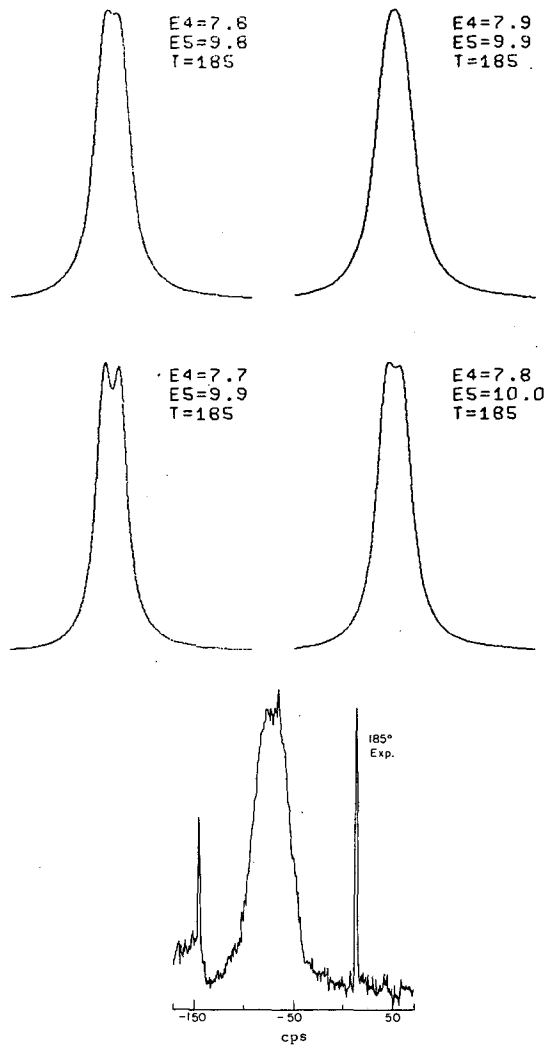

MU-34846

Fig. 22

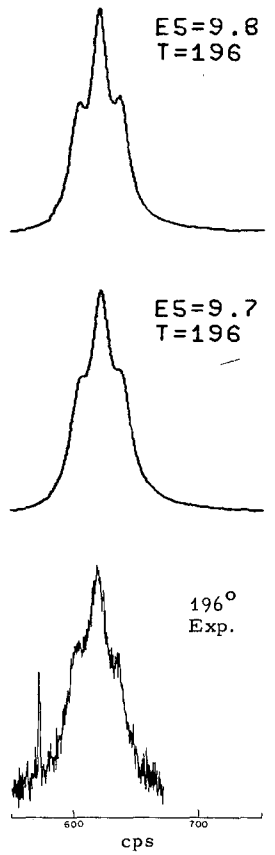

MU-34844

Fig. 23

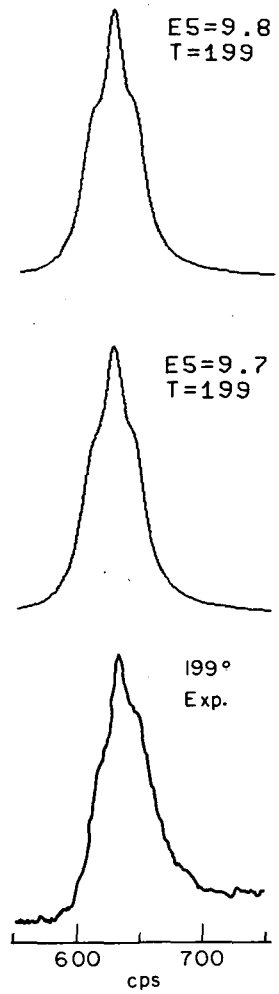

MU-34842

Fig. 24

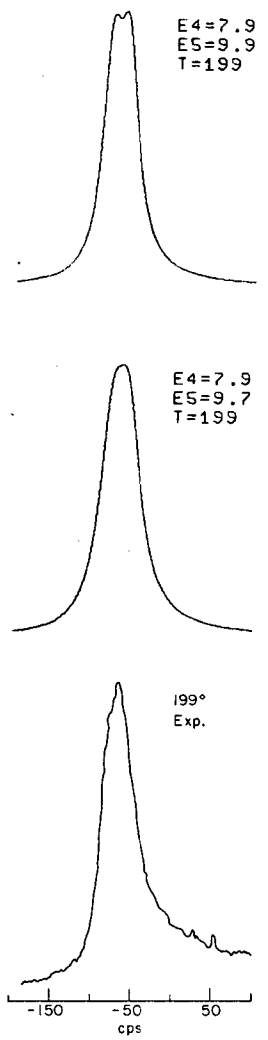

MU-34843

Fig. 25

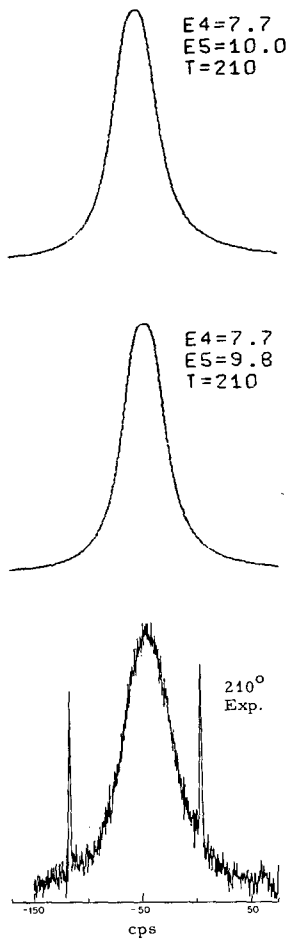

MU-34840

Fig. 26

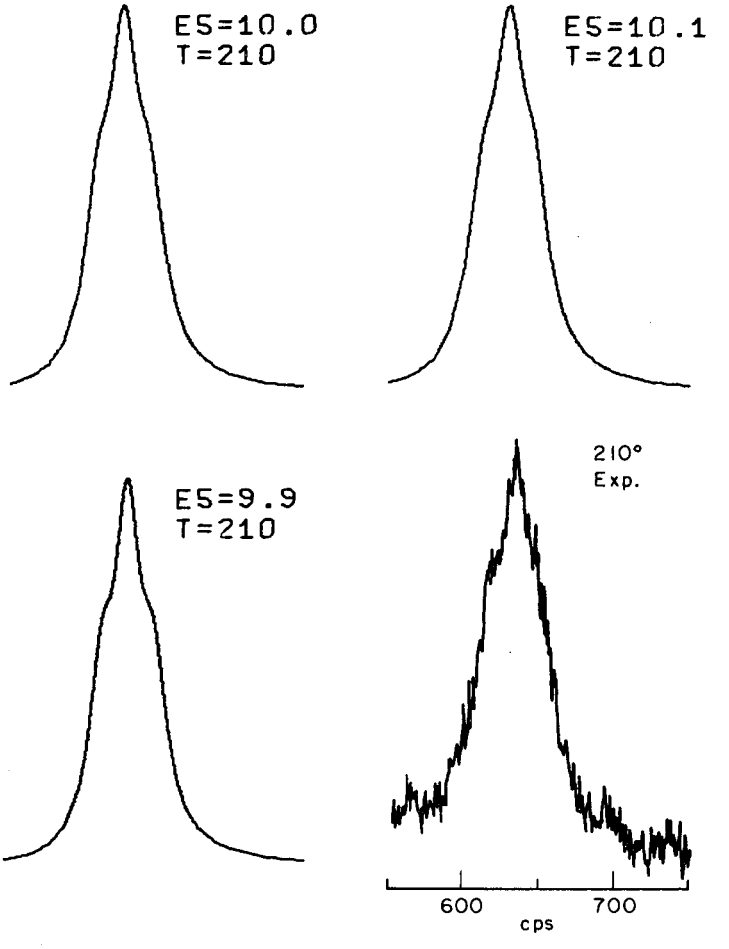

MU-34841

Fig. 27

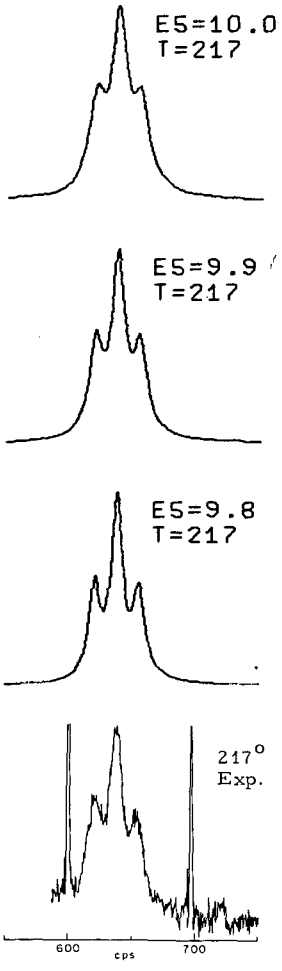

MU-34839

Fig. 28

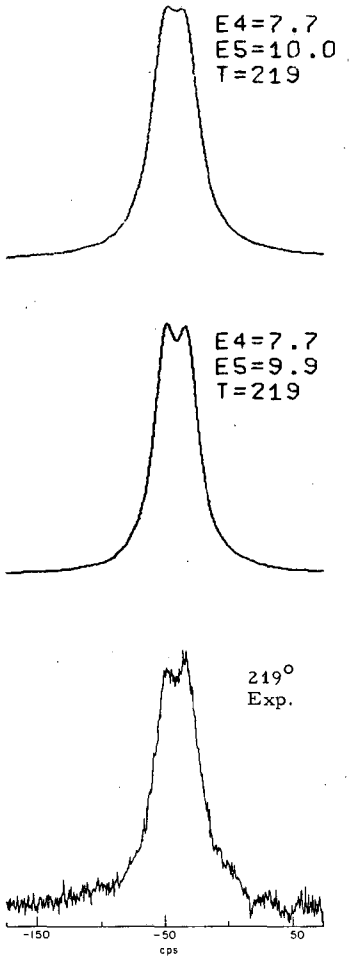

MU-34838

Fig. 29

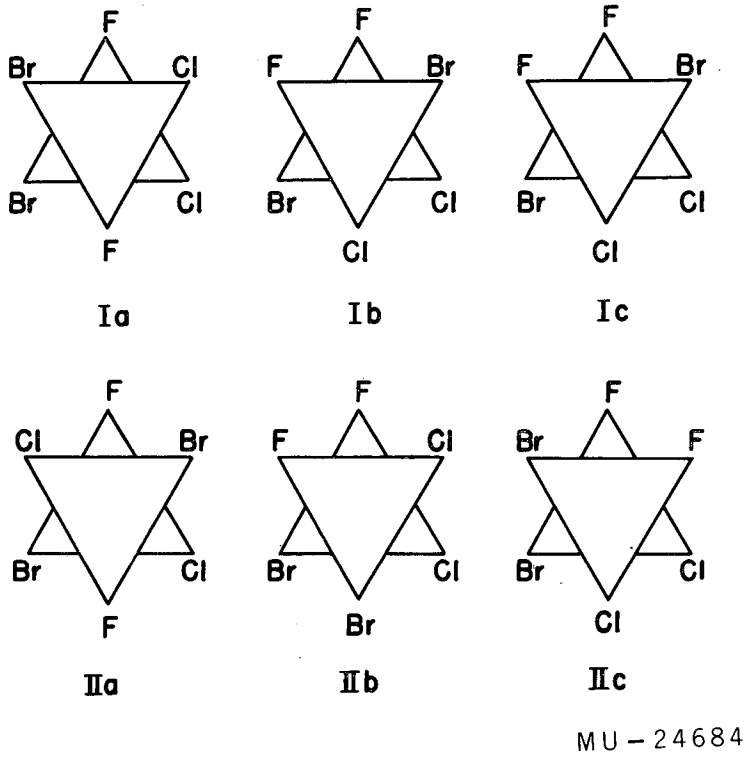
F
Br
Cl
Br
Cl
F
Ia
F
F
Br
Br
Cl
Cl
Ib
F
F
Br
Br
Cl
Cl
Ic
F
Cl
Br
Br
Cl
F
IIa
F
F
Cl
Br
Cl
Br
IIb
F
Br
F
Br
Cl
Cl
IIc
MU-24684

Fig. 30

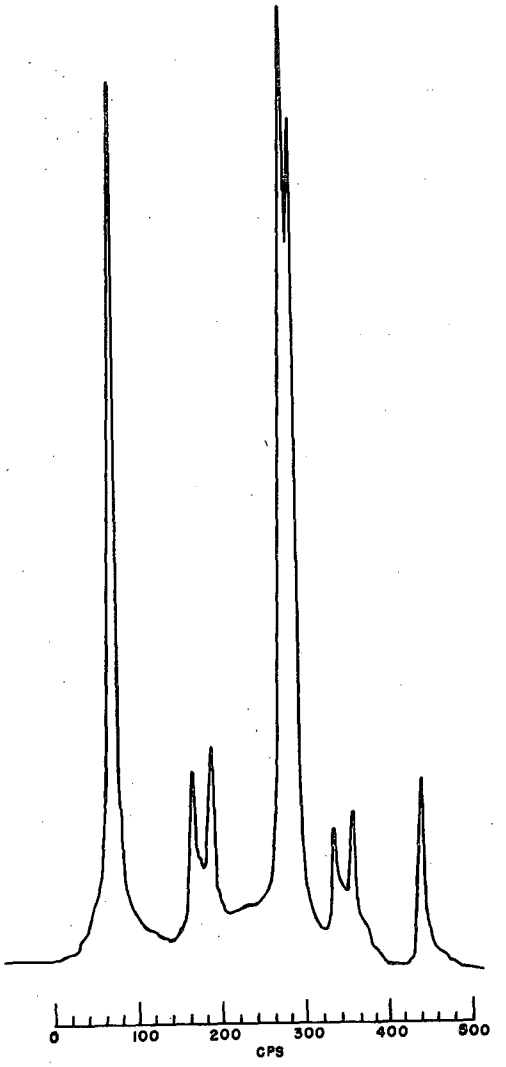

MU-24685

Fig. 31

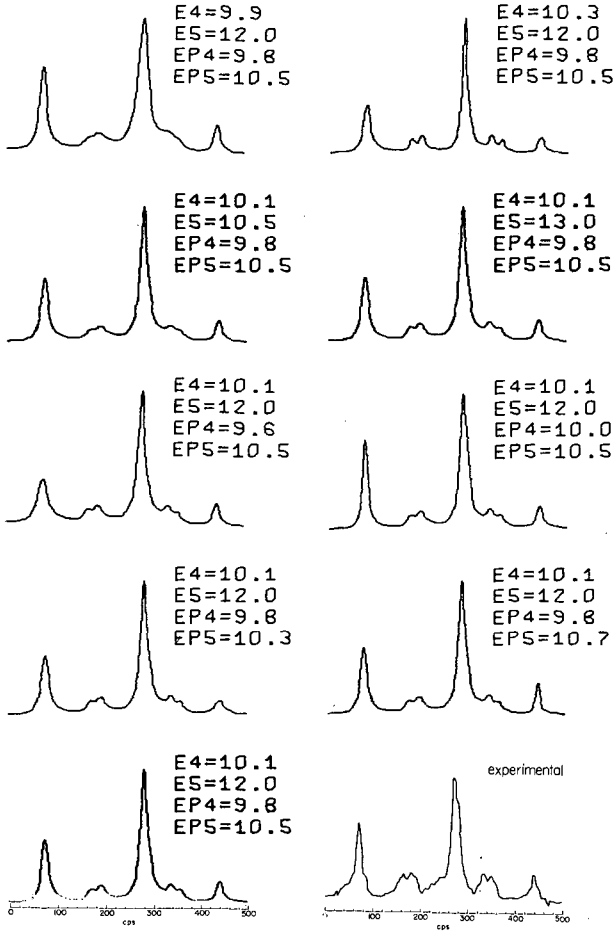

MU-34837

Fig. 32

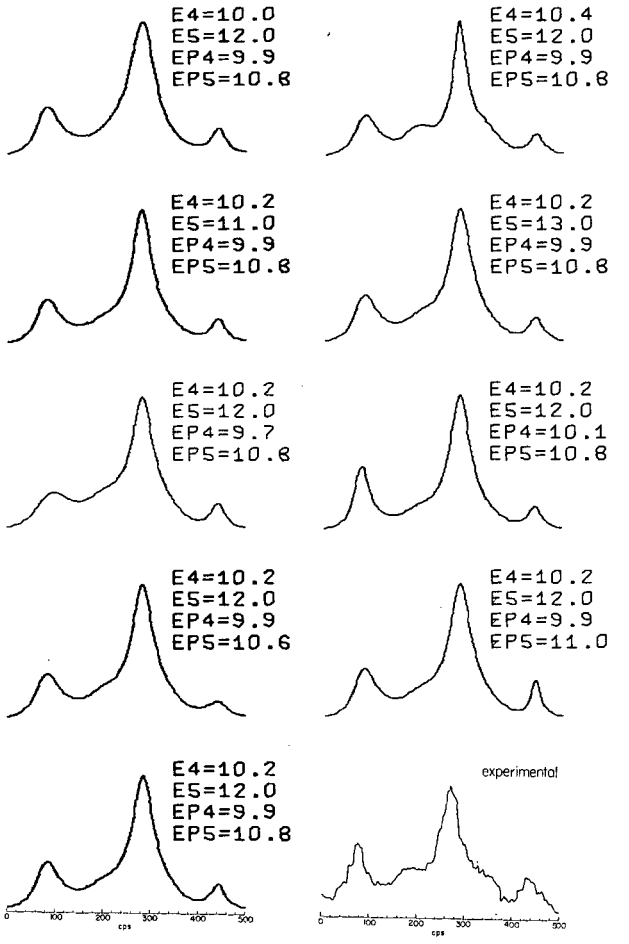

MU-34835

Fig. 33

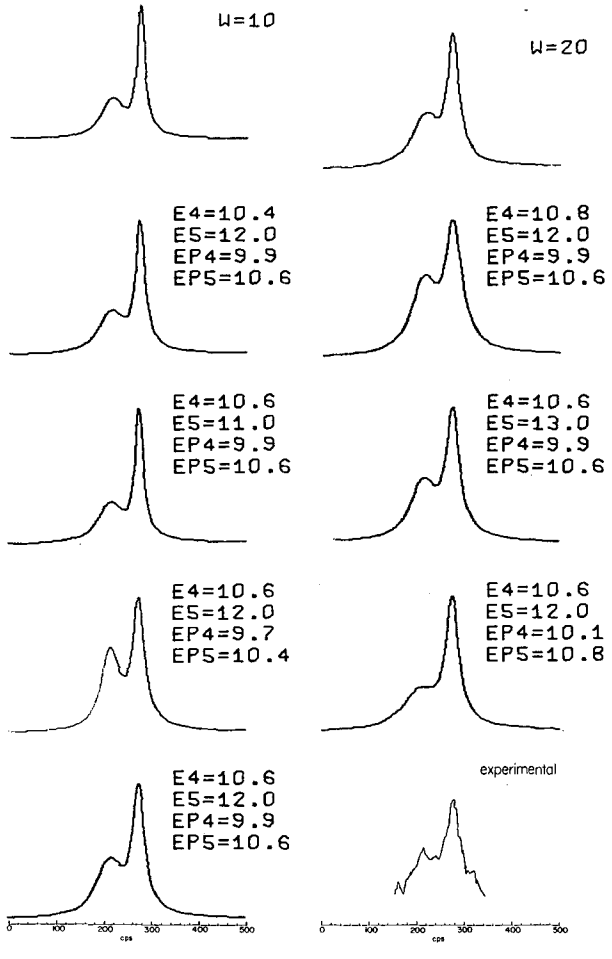

MU-34836

Fig. 34

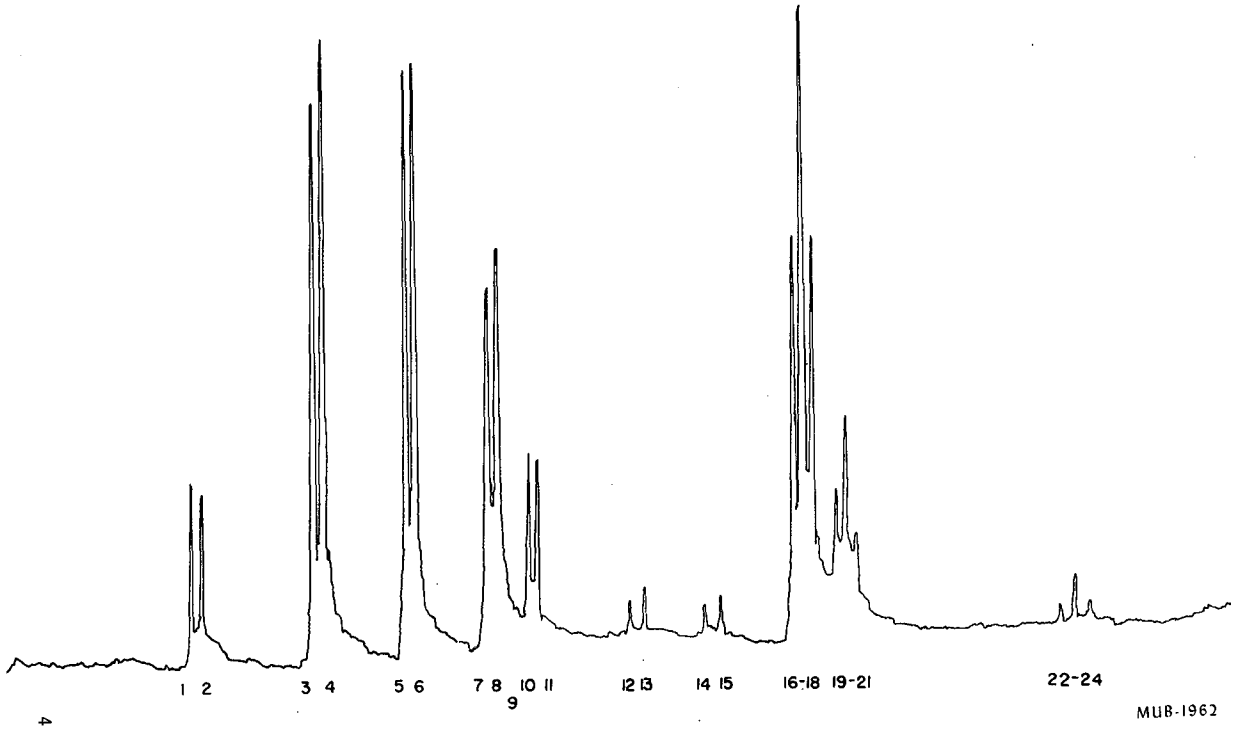

Fig. 35

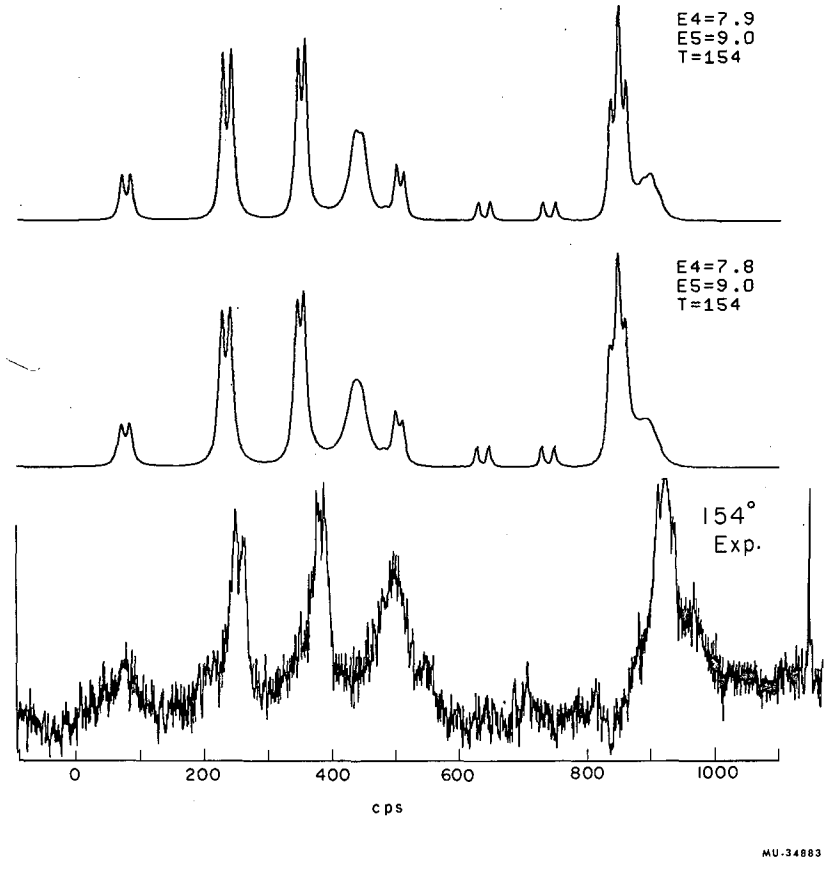
E4=7.9
E5=9.0
T=154
E4=7.8
E5=9.0
T=154
154°
Exp.
0
200
400
600
800
1000
cps
MU-34883

Fig. 36

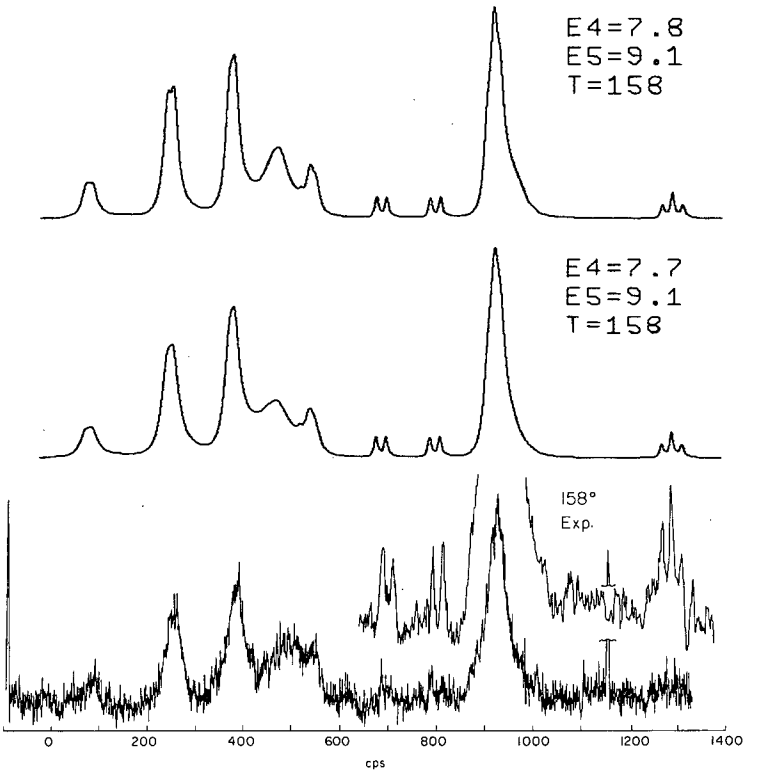

MU-34881

Fig. 37

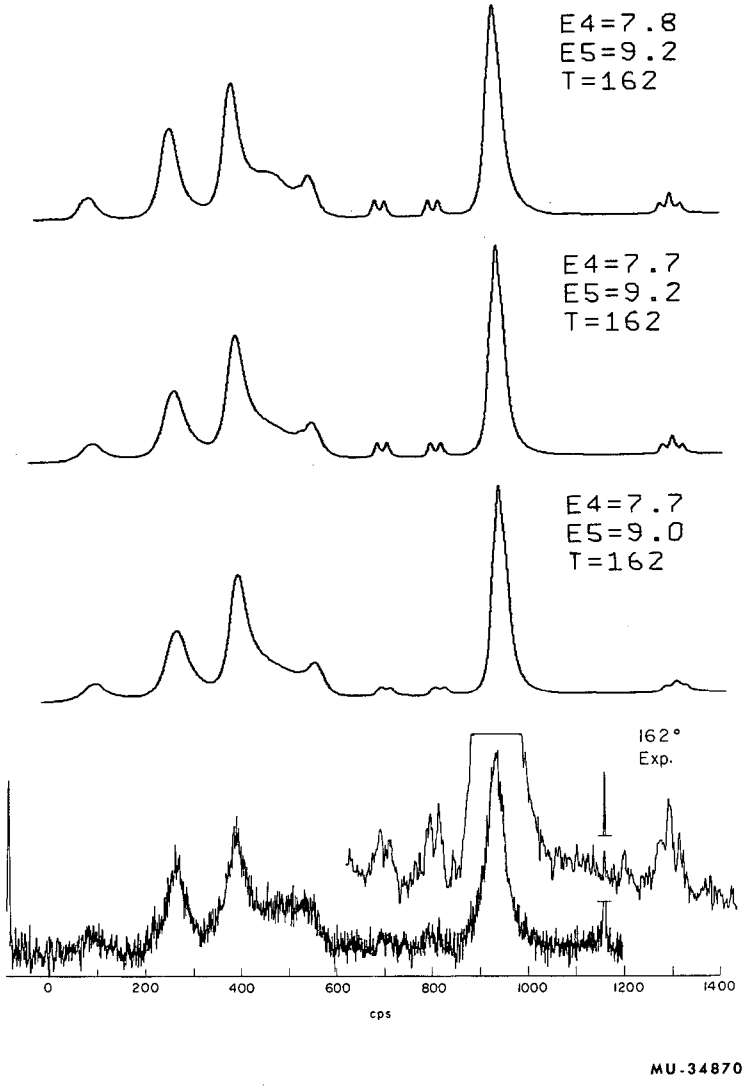
E4=7.8
E5=9.2
T=162
E4=7.7
E5=9.2
T=162
E4=7.7
E5=9.0
T=162
162°
Exp.
0
200
400
600
800
1000
1200
1400
cps
MU-34870

Fig. 38

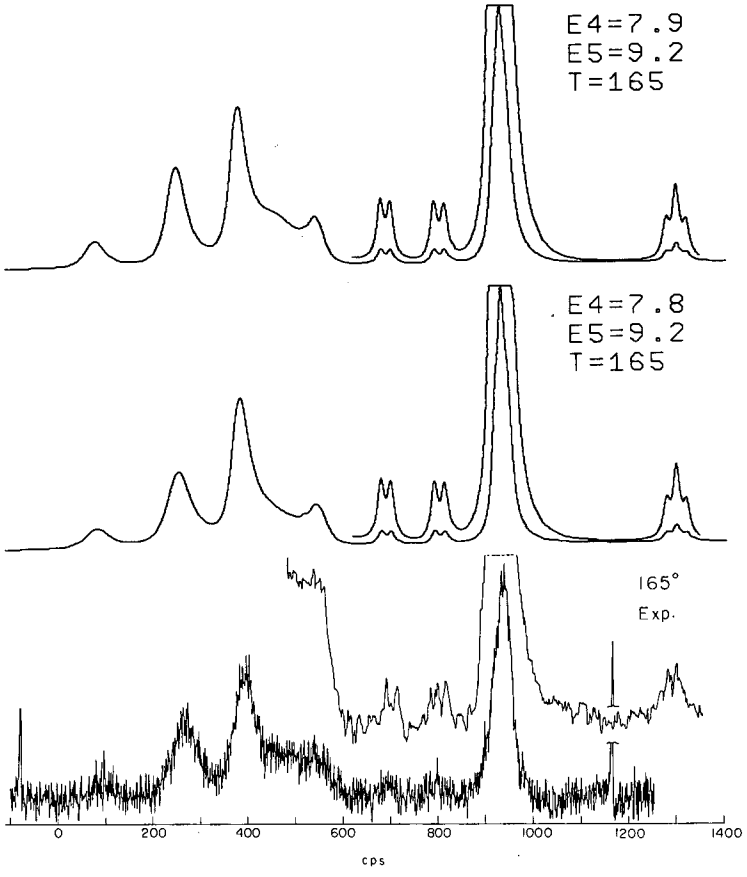

MU-34871

Fig. 39

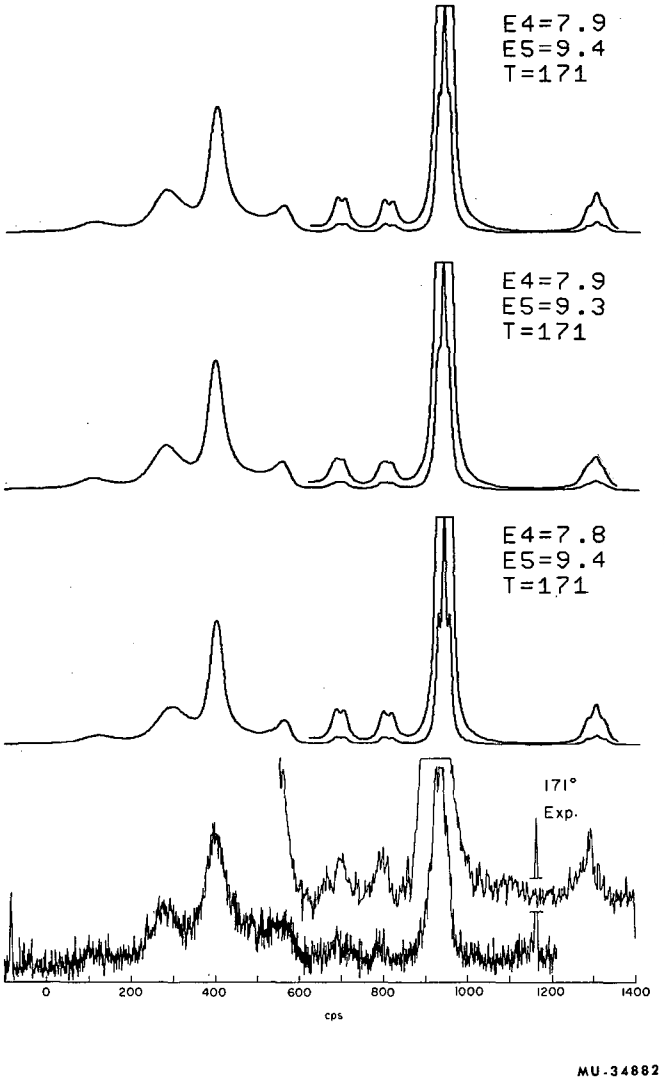
E4=7.9
E5=9.4
T=171
E4=7.9
E5=9.3
T=171
E4=7.8
E5=9.4
T=171
171°
Exp.
0
200
400
600
800
1000
1200
1400
cps
MU-34882

Fig. 40

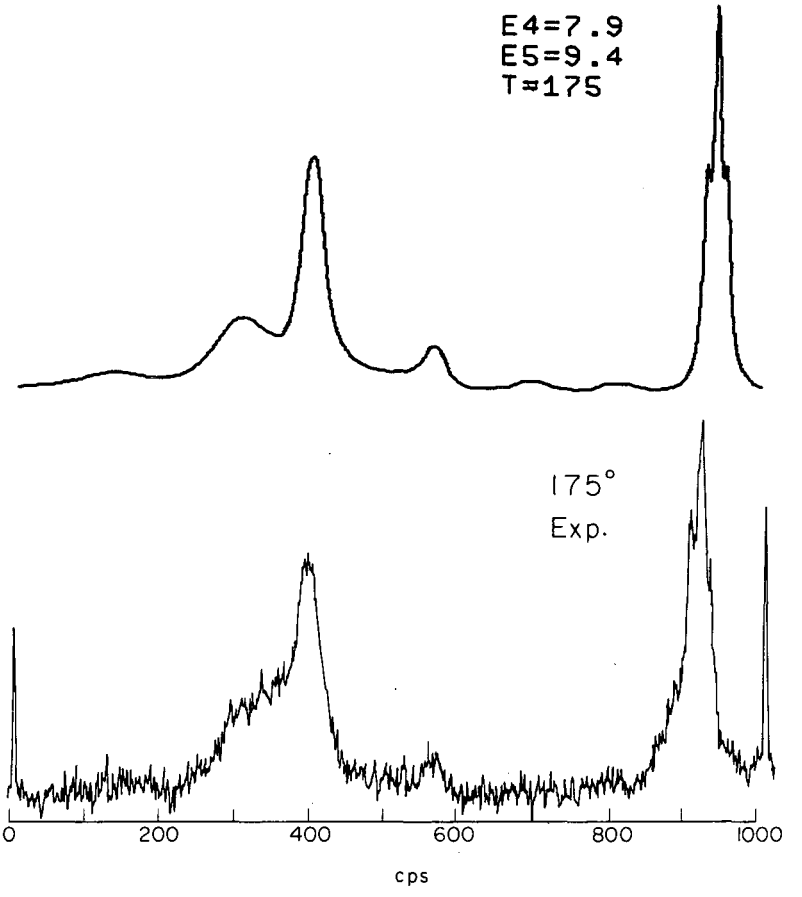

MU-34884

Fig. 41

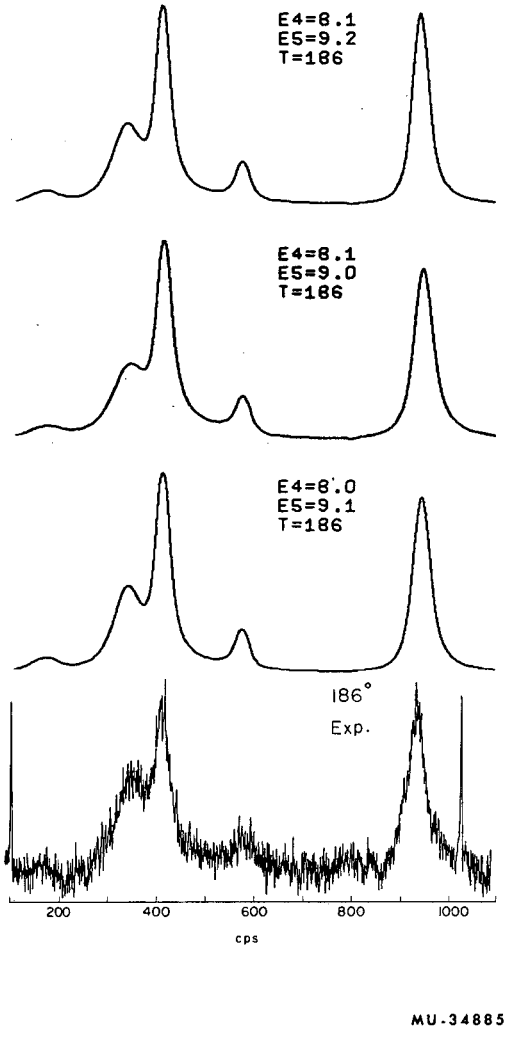
E4=8.1
E5=9.2
T=186
E4=8.1
E5=9.0
T=186
E4=8.0
E5=9.1
T=186
186°
Exp.
200
400
600
800
1000
cps
MU-34885

Fig. 42

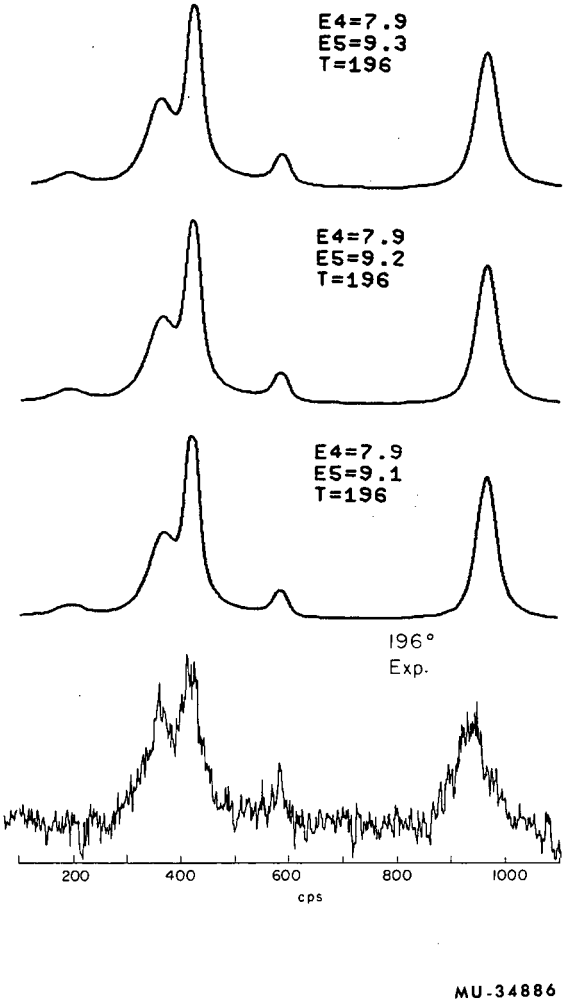
E4=7.9
E5=9.3
T=196
E4=7.9
E5=9.2
T=196
E4=7.9
E5=9.1
T=196
196°
Exp.
200
400
600
800
1000
cps
MU-34886

Fig. 43

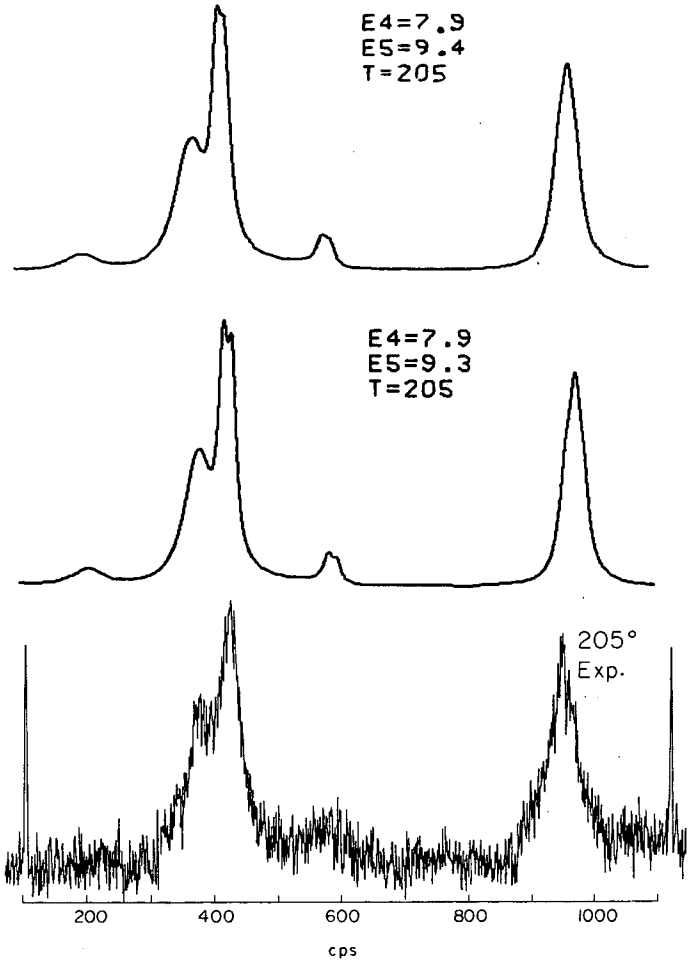

MU-34880

Fig. 44

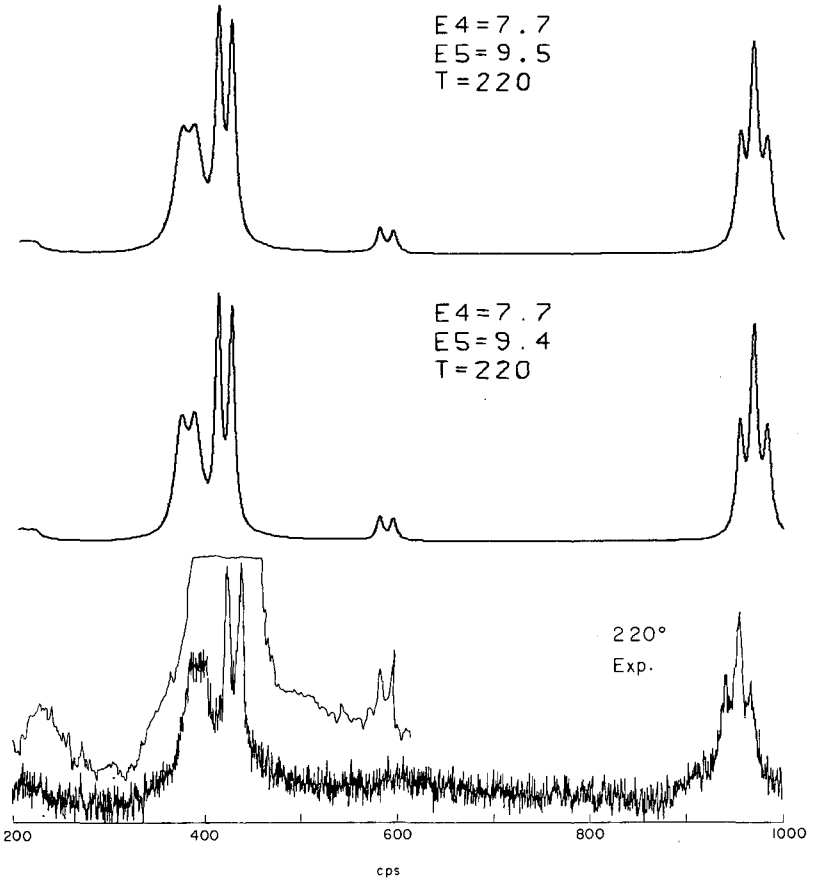

MU-34872

Fig. 45

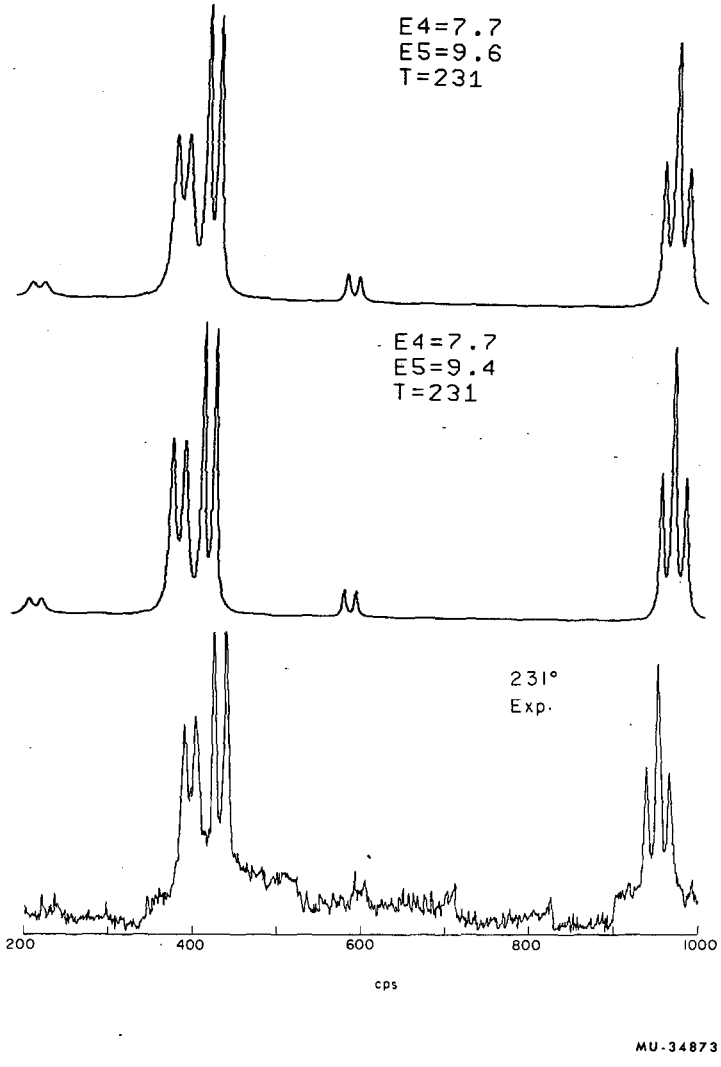
E4=7.7
E5=9.6
T=231
E4=7.7
E5=9.4
T=231
231°
Exp.
200
400
600
800
1000
cps
MU-34873

Fig. 46

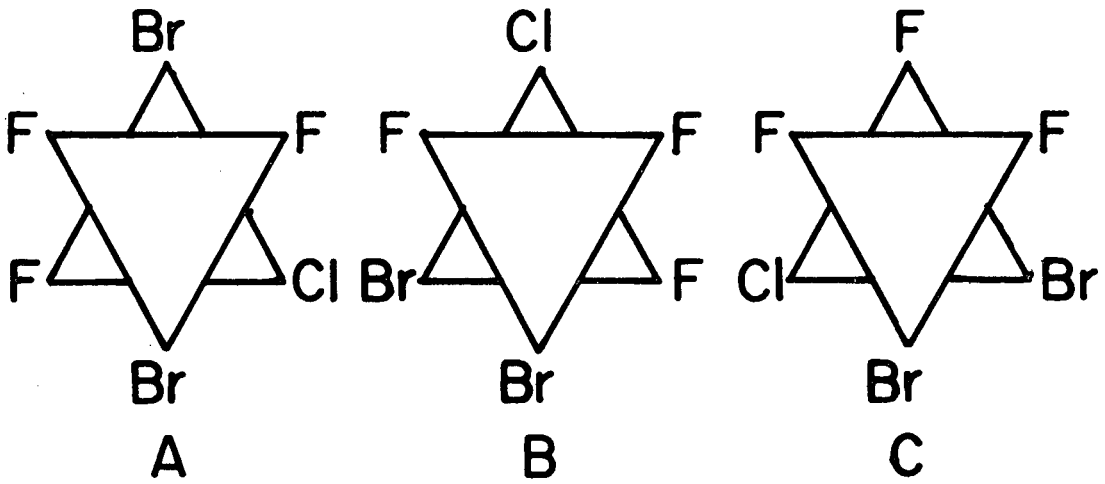

MU-31212

Fig. 47

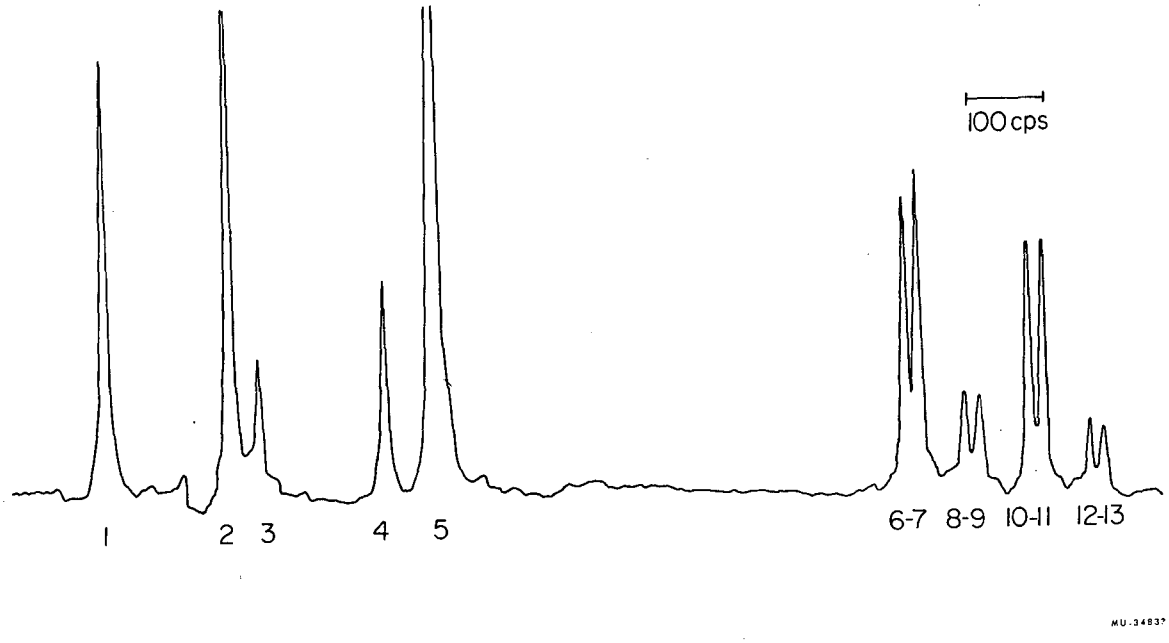

Fig. 48

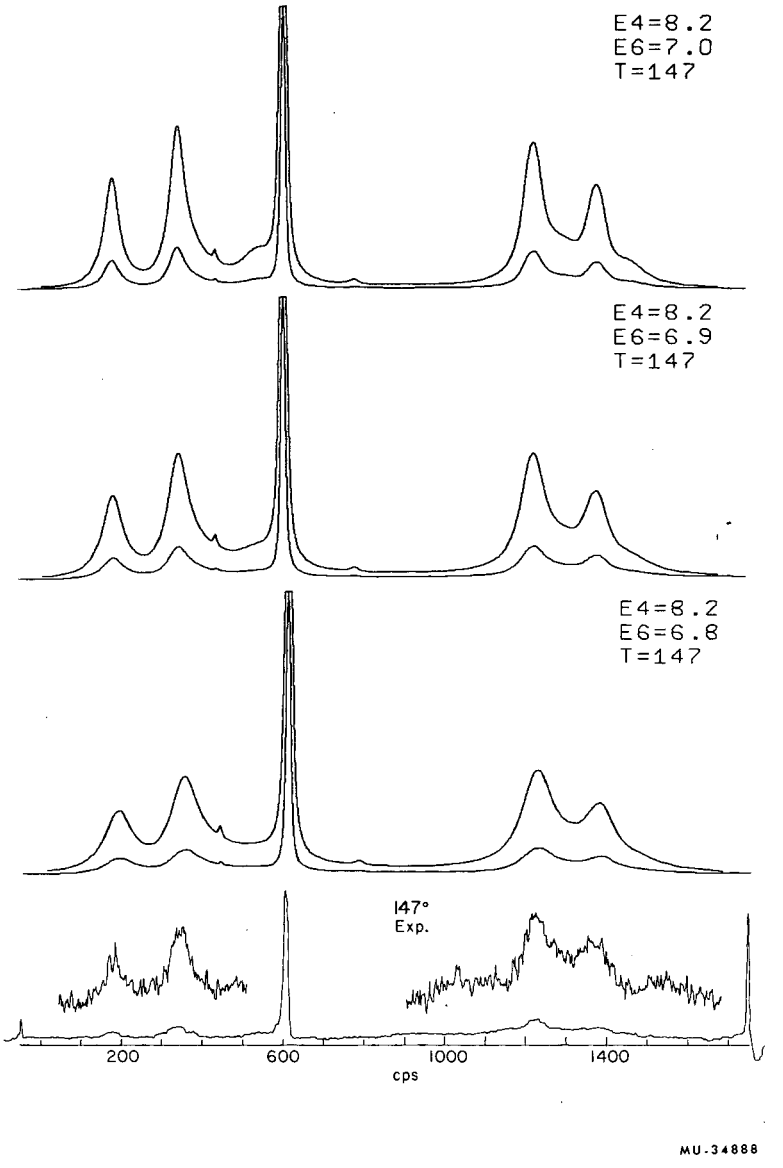
E4=8.2
E6=7.0
T=147
E4=8.2
E6=6.9
T=147
E4=8.2
E6=6.8
T=147
147°
Exp.
200
600
1000
1400
cps
MU-34888

Fig. 49

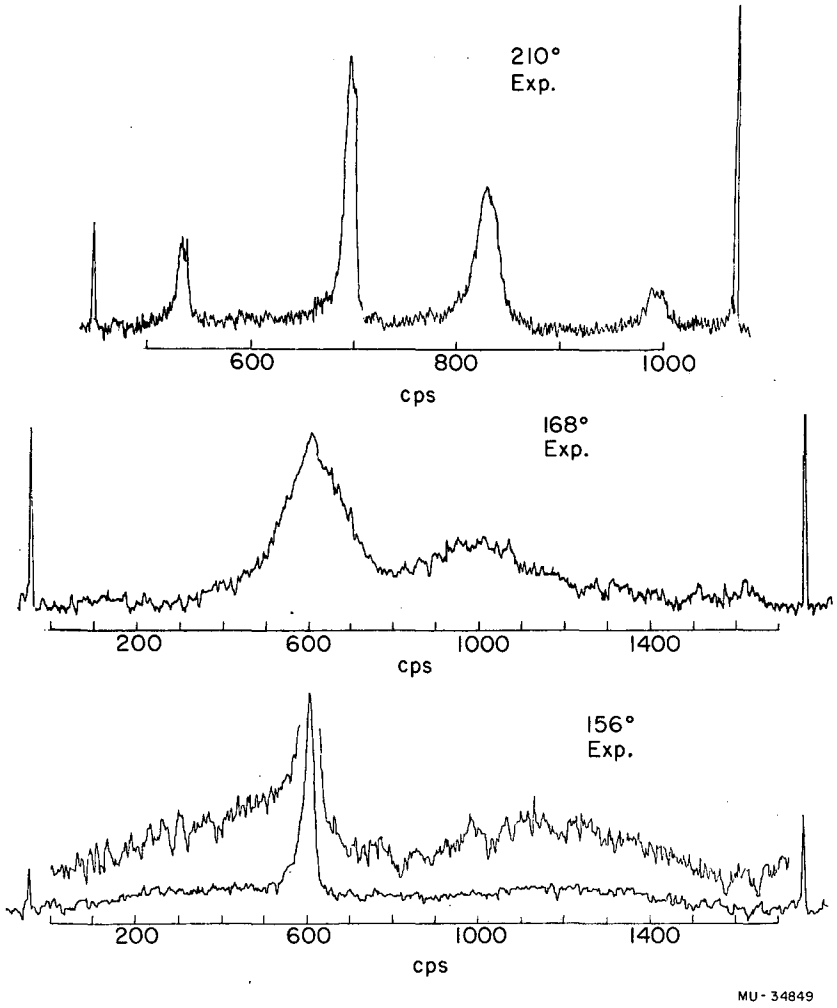
210°
Exp.
600
800
1000
cps
168°
Exp.
200
600
1000
1400
cps
156°
Exp.
200
600
1000
1400
cps
MU-34849

Fig. 50

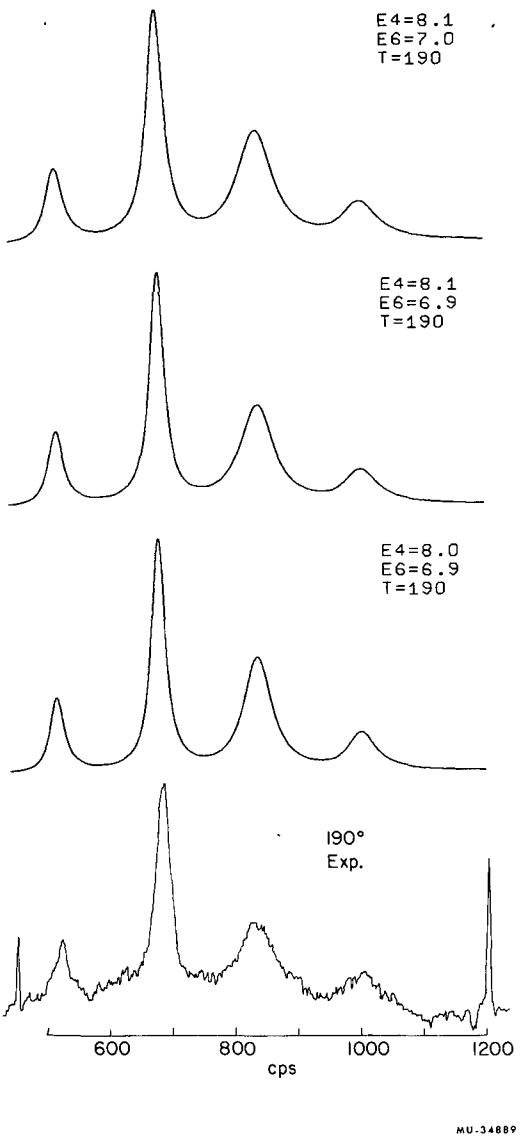
E4=8.1
E6=7.0
T=190
E4=8.1
E6=6.9
T=190
E4=8.0
E6=6.9
T=190
190°
Exp.
600
800
1000
1200
cps
MU-34889

Fig. 51

This report was prepared as an account of Government sponsored work. Neither the United States, nor the Commission, nor any person acting on behalf of the Commission:

A. Makes any warranty or representation, expressed or implied, with respect to the accuracy, completeness, or usefulness of the information contained in this report, or that the use of any information, apparatus, method, or process disclosed in this report may not infringe privately owned rights; or

B. Assumes any liabilities with respect to the use of, or for damages resulting from the use of any information, apparatus, method, or process disclosed in this report.

As used in the above, "person acting on behalf of the Commission" includes any employee or contractor of the Commission, or employee of such contractor, to the extent that such employee or contractor of the Commission, or employee of such contractor prepares, disseminates, or provides access to, any information pursuant to his employment or contract with the Commission, or his employment with such contractor.